Giardia duodenalis arginine deiminase and its role in host-parasite interplay

Dissertation

zur Erlangung des akademischen Grades

doctor rerum naturalium

(Dr. rer. nat.)

im Fach Biologie

eingereicht an der

Mathematisch-Naturwissenschaftlichen Fakultät I

der Humboldt-Universität zu Berlin

von

M.Sc. Stefanie Marek (geb. Banik)

Präsident der Humboldt-Universität zu Berlin

Prof. Dr. Jan-Hendrik Olbertz

Dekan der Mathematisch-Naturwissenschaftlichen Fakultät I

Prof. Stefan Hecht, Ph.D.

Gutachter/innen: 1. Prof. Dr. rer. nat. Richard Lucius

2. Prof. Dr. med. Ralf Ignatius

3. Prof. Dr. rer. nat. habil. Ralf Stohwasser

Tag der mündlichen Prüfung: 22.11.2013

Dedicated to Elsa

Acknowledgement

I would like to thank …

...Dr. A. Aebischer for enabling me the great opportunity to work on an interesting research topic in his group at the Robert Koch-Institute. In terms of encouragement and help he was always available with constructive advices during my PhD studies.

...Prof. Dr. R. Stohwasser, Prof. Dr. R. Ignatius and Prof. Dr. R. Lucius for kindly accepting to be my reviewer.

...all members of the research group FG16 for working in a friendly pleasant atmosphere. A special thanks to Petra Gosten-Heinrich, Elisabeth Kamal, Sandra Klein, Gudrun Kliem, Ulrike Laube, Elke Radam, Emine Temür and Petra Völkner for their help in the daily laboratory routine. A particular appreciation goes to Dr. C. Klotz, Dr. A. Lewin and Prof. Dr. Frank Seeber for always finding the time for inspiring scientific discussions. Furthermore, I thank Anna-Luise Kluge for the stimulating collaboration during her bachelor studies.

...my fellow PhD students Ina Lucas, Juliane Hahn, Nora Frohnecke and Annesha Lahiri for teaming up scientifically and amicably in the laboratory and on other occasions.

...my family and friends for their untiring support.

...last and most important my husband André.

I Table of contents

II List of tables

III List of figures

IV Abbreviations

A	Austria
ADI	Arginine deiminase
ATP	Adenosine triphosphate
BLAST	Basic local alignment search tool
bp	Base pair
CFU	Colony forming units
CDC	Centers for disease control and prevention
CD	Cluster of differentiation
CFDA-SE	Carboxyfluorescein diacetate succinimidyl ester
CFSE	Carboxyfluorescein succinimidyl ester
DC	Dendritic cells
dH_2O	Distilled water
DNA	Deoxyribonucleic acid
E. coli	*Escherichia coli*
Fig.	Figure
FPLC	Fast protein liquid chromatography
FITC	Fluorescein isothiocyanate
G	Germany
HLA	Human leukocyte antigen
Ig	Immunoglobulin
IFN	Interferon
IL	Interleukin
kb	Kilo base pairs
kDa	Kilodalton
LB	Luria-Bertani
LPS	Lipopolysaccharides
mAb	Monoclonal antibody
Mbp	Mega base pairs
MHC	Major histocompatibility complex
MOI	Multiplicity of infection
mRNA	Messenger RNA
Ni-NTA	Nickel-nitrilotriacetic acid

NL	Netherlands
OD	Optical density
ori	Origin of replication
pAb	Polyclonal antibody
PAGE	Polyacrylamide gel electrophoresis
PCR	Polymerase chain reaction
PE	Phycoerythrin
PerCP	Peridinin chlorophyll protein complex
PES	Polyethersulfone
Pfu	*Pyrococcus furiosus*
PSI-BLAST	Position specific iterated - BLAST
RKI	Robert Koch-Institute
RNA	Ribonucleic acid
rpm	Round per minute
rRNA	Ribosomal RNA
RT	Room temperature
SOB	Super optimal broth
SOC	Super Optimal broth with catabolite repression
Tab.	Table
Taq	*Thermus aquaticus*
TAE	Tris-acetate-EDTA
Tet	Tetracycline
TNF	Tumor necrosis factor
U	Unit
USA	United States of America
v/v	Volume per volume
WHO	World Health Organization
w/v	Weight per volume
x *g*	X times acceleration of gravity

V Zusammenfassung

Giardiasis, verursacht durch Infektionen mit dem einzelligen, intestinalen Parasiten *Giardia duodenalis* (*G. duodenalis*), ist weltweit eine der häufigsten humanen Parasitosen. Die Symptomatik ist dabei vielseitig und reicht von akuten Durchfällen bis hin zu schwer behandelbaren chronischen Diarrhöen und Malabsorption. Darüber hinaus gibt es auch Patienten bei denen eine Infektion völlig asymptomatisch verläuft. Bislang konnte nicht geklärt werden, wodurch die Diversität im klinischen Krankheitsbild hervorgerufen wird. Es gibt keine eindeutig beschriebenen Virulenz- oder Pathogenitätsmarker. Es wird vermutet, dass potentielle *G. duodenalis* Virulenzfaktoren Enzyme sind, die während des Kontaktes des Erregers mit den Dünndarmepithelzellen sezerniert werden. Eines dieser Enzyme ist die Arginin Deiminase (ADI), die Arginin zu Citrullin umwandelt.

Ziel der Arbeit war es die Bedeutung der Arginin Deiminase für die Wirt-Pathogen-Interaktion zu untersuchen um herauszufinden, ob es sich bei dem Enzym um einen ersten molekular definierten Virulenz- und Pathogenitätsfaktor für *G. duodenalis* handelt. Der Fokus lag dabei zum einen auf der Untersuchung des Einflusses des Enzyms auf die Wirtsimmunzellen und zum anderen auf der Bestimmung der Sequenz- und funktionellen Variabilität des Enzyms in Parasitenisolaten.

Da in der Maus gezeigt werden konnte, dass Dendritische Zellen (DC) in der Wirtsimmunantwort gegen *Giardia* Infektionen beteiligt sind, wurde die immunologische Wirkung der Parasiten ADI auf humane monozytäre DC (moDC) untersucht. Dabei zeigten die mit rekombinantem, katalytisch aktivem Enzym (Assemblage A) behandelten LPS-stimulierten moDC eine Zunahme in der Tumornekrosefaktor-alpha (TNF-α)-Sekretion und eine Abnahme in der Freisetzung von Interleukin (IL)-10 und IL-12p40. Weiterhin war eine Abnahme des DC Reifungsmarker CD83 und des kostimulatorischen Liganden CD86 nach ADI Behandlung ersichtlich. Diese Veränderungen im Phänotyp als auch in der Cytokinsekretion der moDC ließen sich auf die durch das Enzym hervorgerufene Arginindepletion und/oder auf die Bildung der Metabolite, also Citrullin und NH_4^+, zurückführen. Weiterhin konnte gezeigt werden, dass Parasitenisolate verschiedener *G. duodenalis* Assemblage A-Subtypen, vermutlich durch die katalytische Aktivität der ADI, die Stickstoffmonoxid-Bildung einer intestinalen Epithelzelllinie inhibiert. Diese beiden immunmodulatorischem Effekte deuten daraufhin, dass die ADI vom Parasiten genutzt wird um der Immunantwort des Wirts zu entgehen.

Um weitere Hinweise dafür zu finden, dass es sich bei der *G. duodenalis* ADI um einen Virulenzfaktor handelt, wurde die Variabilität in der kodierenden Sequenz des Enzyms in verschiedenen Parasitenisolaten analysiert. Anschließend erfolgte die funktionelle Charakterisierung des nativen (verschiedene Assemblage A-Subtypen) als auch des rekombinant aufgereinigten Enzyms (Assemblage A, B und E). Dabei zeigten sich Unterschiede in der Substrataffinität der ADI für Arginin, sowohl zwischen unterschiedlichen Assemblage A-Subtypen als auch unterschiedlichen Assemblage-Klassen. Erste Hinweise auf eine Korrelation zwischen Variation in der Primärstruktur und Enzymfunktion konnten beobachtet werden.

In dieser Arbeit konnte gezeigt werden, dass die *G. duodenalis* Arginin Deiminase als potentieller Virulenzfaktor die Wirtsimmunität beeinflusst und somit als Target für die Entwicklung neuer Medikamente und Impfstrategien in Frage kommen könnte.

VI Summary

Giardia duodenalis (*G. duodenalis*) is an intestinal protozoan parasite that infects humans and other mammals as well. It causes giardiasis, one of the most prevalent parasitic diseases worldwide with symptoms ranging from asymptomatic carrier stage to chronic diarrhea. So far, little is known concerning host-parasite interaction, in particular what determines the parasite's pathogenicity. Several potential virulence factors, among them the arginine deiminase (ADI) that hydrolyzes arginine into citrulline and NH_4^+, are discussed. The ADI was identified to be released upon contact with intestinal epithelium by *Giardia* trophozoites and was recognized as an immunoreactive protein during acute human giardiasis. Aim of the study was to identify potential roles of *G. duodenalis* ADI in the host-parasite interplay by analyzing the enzyme's impact on host immune cells and to functionally characterize its genotypic variation.

As dendritic cells (DC) are known to be involved in controlling giardial infection in mice, the influence of *G. duodenalis* ADI on human monocyte-derived DC (moDC) was investigated. Treatment of LPS-stimulated cells with recombinant ADI of assemblage A significantly increased tumor necrosis factor alpha (TNF-α) as well as decreased interleukin-10 (IL-10) and IL-12p40 secretion. It also reduced the upregulation of surface CD83 and CD86 molecules, which are involved in cell-cell interactions. These immunomodulatory changes in DC response were due to arginine depletion and the formation of reaction products, in particular, ammonium ions. Furthermore, trophozoites of different assemblage subtypes were shown, probably due to consumption of arginine by ADI, to reduce nitric oxide formation by intestinal epithelial cells *in vitro*. These observations underlined the presumption that ADI, like other arginine-depleting pathogen enzymes, is used by *Giardia* to evade host immune effector mechanisms.

By sequencing, variation in the ADI coding sequence of different *G. duodenalis* isolates being collected in a *Giardia* biobank was analyzed. Subsequently, functional genetics were performed with native ADI of different assemblage A subtypes expressed by these strains as well as with purified, recombinant ADI of assemblage A, B and E. First indications of a correlation between enzyme function and variation of the protein primary structure were noticed.

In this report, *G. duodenalis* ADI was identified to have a direct impact on host immunity and thus the enzyme might be a new target for future drug or vaccine design against giardial infection.

1 Introduction

1.1 *Giardia* - a smiling parasite

Giardia is a genus of intestinal protozoan parasites that was first observed by van Leeuwenhoek in 1681 (Boreham et al, 1990). They belong to the phylogenetic group of Diplomonadida that are characteristically binucleated and lack aerobic mitochondria and stacked Golgi. *Giardia* is an aerotolerant anaerobe that contains mitochondrial relicts, the mitosomes (Adam, 2001; Regoes et al., 2005). The parasite exists in two forms: the dormant, infective cysts and the vegetative, disease-causing trophozoites. Cysts are egg-shaped and approximately 8-12 µm long and 5-9 µm wide. They are enclosed by a 0.3-0.6 µm thick cyst wall, that has a fibrillous structure and is composed of β(1-3)-*N*-acetyl-D-galactosamine, at least three cyst wall proteins and a subjacent double inner membrane (Erlandsen et al., 1996; Gerwig et al., 2002; Sun et al., 2003; Ankarklev et al., 2010). In contrast, trophozoites are bilaterally symmetrical with a teardrop shape and are approximately 15 µm in length, 5 µm in width and 5 µm thick (Dawson, 2010) (Fig. 1). The ventral side is flat whereas the dorsal side is convex.

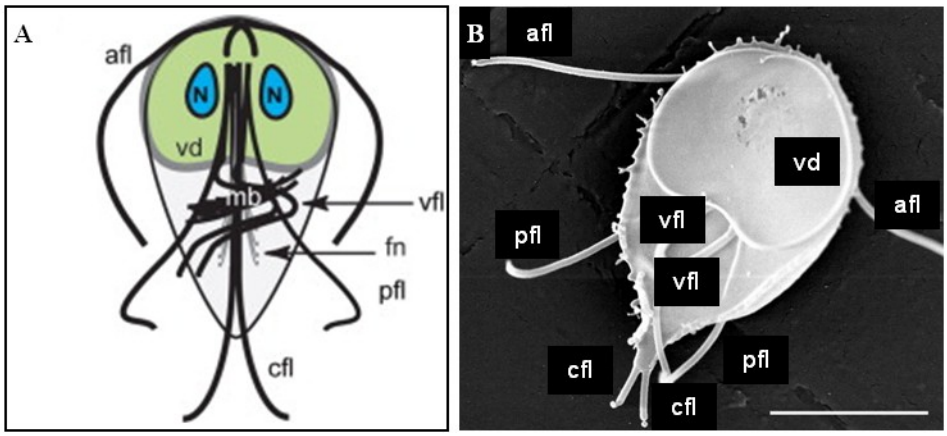

Figure 1: Morphology of *Giardia* trophozoites
(A) Schematic and (B) Scanning electron micrograph (SEM) of *Giardia* trophozoite structure. A ventral view of a *Giardia* trophozoite shows its teardrop shape with nucleus (N), median body (mb), funis (fn), ventral disc (vd) and four flagellar pairs (afl = anterior flagella, pfl = posteriorlateral flagella, vfl = ventral flagella, cfl = caudal flagella). Scale bar = 5 µm. (modified, Dawson and House 2010)

Giardia has a complex cytoskeleton. Striking microtubule-based structures are the eight flagella organized in four bilaterally symmetrical pairs (anterior, caudal, posteriolateral, ventral) that provide motility to the parasite, the ventral adhesive disc that allows attachment

to the intestinal villi as well as the median body and the funis with currently unknown function (Elmendorf et al., 2003). Characteristically, the location of the median body let the parasite "smile" when visualized by Giemsa staining.

1.2 Epidemiology of giardiasis

Giardia is distributed globally and infects a broad range of vertebrates. The species *Giardia duodenalis* (*G. duodenalis*) is the causative agent of giardiasis, one of the most prevalent parasitic diseases in humans worldwide. Due to its ill-influence on health, the parasite is included in the WHO Neglected Disease Initiative (Saviolo et al., 2006). It is estimated that worldwide 280 million people suffer giardiasis annually (Lane and Lloyd, 2002). Thereby, its regional prevalence varies. According to the CDC (2013), in developed countries nearly 2% of the adults and 6%-8% of children are affected by the disease. In developing countries, where giardial infections are very common in children (Nkrumah and Nguah, 2011), approximately 33% of people have had suffered from giardiasis.

In Germany, giardiasis is a notifiable disease. The average incidence between 2001 and 2010 was 4.7 cases per 100000 populations (RKI-Infektionsepidemiologisches Jahrbuch, 2011). In 2011, 4258 cases of giardiasis were reported with an incidence of 5.2 cases per 100000 populations. The infections were acquired autochthonous, but also travelling into foreign countries (e.g. India, Turkey) was noticed as a source of infection (RKI-Infektionsepidemiologisches Jahrbuch, 2012). In 2010 and 2011, reported giardiasis cases were constant over the whole year and did not rise in late summer (Infektionsepidemiologisches Jahrbuch, 2011 and 2012). This is in contrast to the United States, where in 2006-2008 giardiasis cases were two times higher between June to October than between January to March (CDC, 2010). In Germany, the disease had the highest incidence rates among young children (age 1-4) followed by a group of adults between 20-49 years in 2011 (RKI-Infektionsepidemiologisches Jahrbuch, 2012).

1.2.1 Classification and molecular characterization of *Giardia*

G. duodenalis is found in many mammals, including humans (Thompson, 2000). Its phylogenic investigation based on the nucleotide sequence analysis of several housekeeping genes (e.g. β-giardin, glutamate dehydrogenase, triosephosphate isomerase) and the small-subunit rRNA gene, revealed the existence of eight major genetic groups, termed assemblages A-H (Monis et al., 2003; Cacciò and Ryan, 2008; Lasek-Nesselquist et al., 2010). Some of them can be further classified into subtypes (e.g. AI, AII, AIII, AIV) (Amar et al., 2002; Cacciò et al., 2002). Each assemblage is known to infect certain host species, but among them only assemblage A and B are found in humans (Tab. 1). Globally, assemblage B is identified to be prevalent in human patients, except certain regions of South America and Mexico (Cacciò and Ryan, 2008; Jerlström-Hultqvist et al., 2010). However, a mixture of genotypes within a host can be observed from time to time, e.g. due to ingestion of genetically different *Giardia* cysts or re-infection with *Giardia* species carrying another genotype (Geurden et al., 2009; Levecke et al., 2009; Sprong et al., 2009). An additional explanation for this phenomenon is the occurrence of allelic sequence heterogeneity and/or genetic recombination that was observed to be more common in assemblage B then A (Jerlström-Hultqvist et al., 2010).

Table 1: Molecular characterization of *G. duodenalis*

Assemblage	Some species commonly infected
AI	humans and animals (cats, dogs, livestock, deer, muskrats, beavers, voles, guinea pigs, ferrets)
AII	humans (more common than A-I)
AIII, AIV	exclusively animals
B	humans and animals (livestock, chinchillas, beavers, marmosets, rodents)
C, D	dogs, coyotes
E	alpacas, cattle, goats, pigs, sheep
F	Cats
G	Rodents
H	Seals

(modified CDC, 2013)

Already in 1979, the WHO considered giardial infection a zoonosis (WHO, 1979). Nevertheless, the role of animals as reservoir for the transmission of human giardiasis remains subject of current studies. Thereby, especially domestic pets, farm animals, and wild

mammals that are commonly infected with the parasite, could be a serious source to cause infection in humans. First hints of zoonotic transmission of assemblage A and B between certain animals (e.g. cats, dogs) and humans were observed (Sprong et al., 2009; Ballweber et al., 2010; Lebbad et al., 2010; Lebbad et al., 2011; McDowall et al., 2011) confirming the potential of *G. duodenalis* to be a zoonotic organism.

So far, three distinct *G. duodenalis* isolates were analyzed on their molecular level in detail. In 2007, the 11.7 Mbp WB-assemblage A *G. duodenalis* genome with approximately 4800 predicted protein encoding genes was published (Morrison et al., 2007), followed in 2009 with those of GS-assemblage B (Franzén et al., 2009). The sequenced genomes of these both major human assemblages showed an average nucleotide identity of 77% and an amino acid identity in 4300 orthologous proteins of only 78%. Due to these genetic differences, both genotypes were discussed to be two separate species (Nash et al., 1985; Franzén et al., 2009; Monis et al., 2009). This aspect was strengthened in 2010 with the sequencing of the P15-assemblage E *G. duodenalis* genome isolated from pig. The comparison of all three isolates identified a highly conserved set of core genes (4557 genes, 91% of genome). Genomic differences were found in *Giardia*-specific gene families, e.g. variant-specific surface proteins (VSPs). The average amino acid identity between assemblage E and B was 81% and, surprisingly, between E and A was 90 % revealing a closer relationship of assemblage A and E (Franzén et al., 2009; Jerlström-Hultqvist et al., 2010).

1.3 Life cycle of *G. duodenalis*

G. duodenalis is transmitted by ingestion of cysts found on surfaces, in soil, food, and (drinking and recreational) water that have been contaminated with feces from infected humans/animals or by the fecal-oral route (hands or fomites) (Fig. 2). The infectious dose with 10 to 100 parasites is low (Farthing, 1997). After swallowing, the giardial cysts pass the stomach of the host and become exposed to low pH due to gastric acids that are thought to initiate a cell differentiation process termed excystation (Gillin et al., 1996). An infective, metabolically inactive cyst is transformed into a short-lived excyzoite stage. During this division process, metabolism within the cell is activated, gene expression is upregulated and the adhesive disc starts to assemble. The excyzoite undergoes cytokinesis twice (without intervening S phases) and finally liberates four motile trophozoites containing two diploid nuclei (Bernander et al., 2001). Once arrived in the lumen of the duodenum, trophozoites start

to reproduce. The generation time of the parasite is 6-12 hours *in vitro* (Ankarklev et al., 2010). Both diploid nuclei divide into four diploid nuclei and are separated by longitudinal binary fission (Yu et al., 2002). Earlier, the two nuclei of one trophozoite were thought to be equal in size and the amount of DNA (Kabnick and Peattie, 1990; Yu et al., 2002) being organized on five major chromosomes (Adam, 2001). However, studies revealed differences in chromosome size and number in both nuclei (Tůmová et al., 2007).

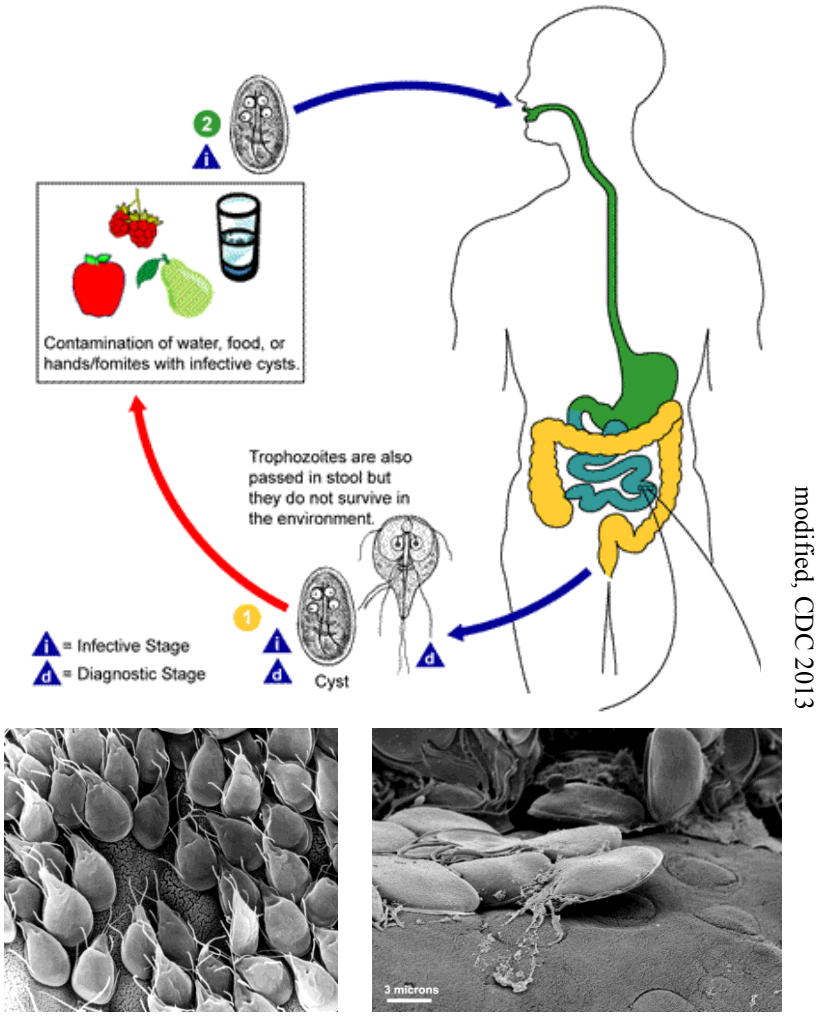

CDC/Dr. Stan Erlandsen (1988) CDC/Dr. Stan Erlandsen (1999)

Figure 2: Life cycle of *G. duodenalis*
(A) represents a schematic overview about the life stages of *G. duodenalis*. (B) and (C) shows in SEM *Giardia* trophozoites that are grouped on the intestinal mucosal surface after infection. In (C) circular lesions on the intestinal epithelial surface resulting from the strong attachment of the parasite's ventral adhesive disk are noticeable.

In the small intestine, trophozoites can attach to the mucosa without invading epithelial cells and can cause outbreak of the disease with its characteristic clinical symptoms. The entire excystation process is very fast and takes no longer than 15 minutes *in vitro* (Hetsko et al., 1998). The second developmental transition is initiated when the parasite passes toward the colon and is exposed to host specific factors e.g. high levels of bile or basic pH (Gillin et al., 1996). During this process, named encystations, replicating trophozoites are converted into nonmotile, metabolically inactive cysts. In the early phase trophozoite's flagella reform and shape rounds up, cyst wall proteins are enclosed into vesicles and transported to the developing cyst wall, the adhesive disc disassembles, and metabolism activity becomes downregulated (Ankarklev et al., 2010). After DNA replication, the cell cycle is exit in the G2 stage and the developed excyzoite contains two tetraploid nuclei that subsequently divide into four diploid nuclei during the late phase of the encystation process (Bernander et al., 2001; Svärd et al., 2003; Reiner, 2008; Ankarklev et al., 2010). After additional DNA replication, a robust, infectious cyst enclosed by a thick cell wall is formed that contains four tetraploid nuclei (and a cyst ploidy of 16*n*) and ribbon-like microtubule structures (Bernander et al., 2001). Most commonly in nondiarrheal feces, these cysts are then released into the environment in where they can survive.

1.4 Pathology of a giardial infection

Giardiasis causes a broad range of intestinal symptoms. In its acute phase occurring approximately one to three weeks post-infection (Gardner and Hill, 2001), patient can suffer from flatulence, stomach or abdominal cramps, nausea, greasy stool and diarrhea. Chronic (or recurrent) infections can lead to dehydration, weight loss and malabsorption (e.g. failure to absorb vitamin B12) (Olivares et al., 2002). It was reported that in a *G. duodenalis* hyperendemic area, 98% of the drug-cured children became reinfected within a half year (Gilman et al., 1988). This is dramatic because giardiasis effects physical and mental growth of infected children (Berkman et al., 2002; Botero-Garcés et al., 2009). Furthermore, giardial infections are discussed to be related to arthritis (Carlson and Finger, 2004), allergies (Bayraktar et al., 2005), chronic fatigue (Hanevik et al., 2012) and irritable bowel syndrome (Hanevik et al., 2009; Wood, 2011).

The duration of infection and characteristic symptoms are highly variable. Giardiasis is often self-limiting with duration of two to four weeks (Flanagan, 1992). Currently, the reasons for

half of the infected people never developing any symptoms and for the variance of the period of symptoms from two to six weeks to the point of chronic infections are still unclear.
Several drugs are available for the treatment of giardial infection. Metronidazole (MTZ), a nitroimidazole drug, that cures patient with an efficacy of 80-95% is most widely used (Gardner and Hill, 2001). Treatment success depends on medical history, nutritional and immune status of the patient (Upcroft and Upcroft, 1993; Müller et al., 2008; Solaymani-Mohammadi et al., 2010). Thus, it is sometimes necessary to increase the doses, extend the duration of treatment, or to give an alternative drug or a combination of drugs. For example, patients that have medical intolerance, or patients that are infected with resistant strains, can be treated with quinacrine, alone or in combination with nitroimidazole (Escobedo and Cimerman, 2007; The Medical Letter, 2010).

1.5 Immunology of giardial infection

The variability in clinical outcome in giardiasis is less understood. Factors being linked to disease outbreak are host´s clinical and nutritional status, age and immune response (Roxström-Lindquist et al., 2006). Thereby, especially host immune response and parasite defense mechanism interact in close relation. After introducing the mucosal immune response, host and parasitic factors influencing the pathology of giardial infections shall be explained in the following chapter.

1.5.1 The mucosal immune system

The mucosal immune system (MIS) is a unique part of the human immune system that protects mucous membranes covering i.a. the respiratory, gastrointestinal and urogenital tract from colonization and invasion of pathogens. It prevents the uptake of undegraded antigens and the development of a potentially harmful immune response against these antigens when they enter the body interior inadvertently (Holmgren and Czerkinsky, 2005).
Within this study, it is focused on the MIS of the gastrointestinal tract, especially in the small intestine. The intestinal mucosa consists of a single-layer epithelium that is arranged in villi, underlined by the lamina propria and covered by mucus and antimicrobial products (McGhee and Fujihashi, 2012). The mucosal epithelium is important for the host defense machinery by

providing a natural barrier and innate immunity. It is formed by columnar epithelial cells termed enterocytes absorbing nutrients and secreting immunoglobulins, goblet cells secreting mucin and Paneth cells secreting chemokines, cytokines, and anti-microbial peptides named α-defensins (Nagler-Anderson; 2001; Porter et al., 2002; McGuckin et al., 2011).

The MIS is a complex network that is composed of immune-inductive sites including the gut-associated lymphoid tissues (GALT) as well as immune-effector sites including the lamina propria lymphocyte compartments. The GALT include i.a. the Peyer's patches (PPs) and the Mesenteric lymph nodes (MLNs). The PPs are covered by microfold cells that sample antigens from the gut lumen and deliver them to underlying antigen-presenting cells (APC), including dendritic cells (DC) (McGhee and Fujihashi, 2012). DC were also shown to directly capture antigens by projecting dendritic extensions between epithelial cells into the lumen of the gut (Rescigno et al., 2001; Chieppa et al., 2006**)**.

Through a combination of signals such as the recognition of microbe-associated molecular patterns by pattern recognition receptors and cytokine signals, DC become stimulated to mature and migrate to peripheral lymph nodes to initiate antigen-specific immunity (Pulendran et al., 2001; Münz et al., 2005). Maturing DC upregulate cell surface markers (e.g. MHC, CD83, CD86) and release cytokines (e.g. IL-12, IL-10, TNF-α) to enable communication with and activation of T- and other immune cells (Banchereau et al., 2000). After initiation of the adaptive immune response, stimulated B and T cells pass the MLNs and are further transported *via* the blood stream to the mucosal effector sites of the gut where they are differentiated into memory or effector cells. Among others, in consequence of the adaptive mucosal immune response, CD4+ T cells support the development of IgA-producing plasma cells. Secretory IgA antibodies are transported across ECs by a process of transcytosis (McGhee and Fujihashi, 2012).

1.5.2 Host defense mechanisms

The host defense mechanism against infection with *Giardia* includes nonimmunological as well as immunological characteristics. In the beginning of the infection the parasite has to overcome natural barriers. For example, a permanent attachment of the parasite to the intestinal surface is hindered by constantly regeneration of the intestinal cells. To prevent elimination by peristalsis, *Giardia* has to move and re-attach continuously (Roxström-Lindquist et al., 2006). It was also shown that mucin, as component of the mucus produced by

the epithelial tissue, may inhibit *Giardia* trophozoite attachment *in vitro* (Roskens and Erlandsen, 2002). Furthermore, probiotic bacteria of the natural gut flora (e.g. *Lactobacillus johnsonii*, *Enterococcus faecium, Lactobacillus rhamnosus*) were identified to positively affect the anti-*Giardia* immune response *in vivo* (Benyacoub et al., 2005; Humen et al., 2005; Goyal and Shukla, 2013).

Typically, an infection with enteric pathogens induces a mucosal immune response. Beside epithelial cells, also other cells of the innate immunity like Mast cells and DC as well as cells of the adaptive immune response like B and T cells were investigated concerning their function in giardial infection control.

As a part of the innate immunity, intestinal epithelial cells (IEC) secrete antimicrobial peptides like defensin or lactoferrin that have anti-giardial activity *in vitro* (Aley et al., 1994; Turchany et al., 1995), and form nitric oxide (NO) that inhibits growth and differentiation processes, but do not affect variability of *G. duodenalis in vitro* (Eckmann et al., 2000). Ordinary, in host immune response inflammation processes are caused by secretion of several chemokines and cytokines. During giardial infection only mild inflammation is observed (Oberhuber et al., 1997). IL-8 is one of the most important cytokines secreted during inflammatory response by host epithelial cells in the gut (Yomogida et al., 2008). Its level does not rise after *G. duodenalis* infection of human intestinal epithelial cell lines *in vitro*. Other proinflammatory cytokines like IL-6, TNF-α and the immunoregulatory cytokines IFN-γ are not upregulated as well (Roxström-Lindquist et al., 2005). However, IL-6 and IFN-γ were noticed to be involved in parasite clearance mechanism in mice (Venkatesan et al., 1997; Bienz et al., 2003; Zhou et al., 2003). Thus, other cells of the innate immune system like APC might be involved in this cytokine response. The impact of APC on giardial infection is less understood. In gerbils, mast cells were identified to accumulate in the small intestine during giardial infection (Leitch et al., 1993; Hardin et al., 1997). In mice, the IL-6 production by these cells was suggested to be important for controlling giardial infection (Li et al., 2004). In contrast, a recent study in mice suggested IL-6 production by DC to be important for anti-*Giardia* immune response (Kamda et al., 2012).

Furthermore, the adaptive immunity was noticed to play a role in defense against *Giardia*. It was shown that T-cell-deficient mice infected with *G. duodenalis* could not eliminate the infection and that depletion of CD4+ T cells results in development of chronic giardiasis (Singer and Nash, 2000). Recent studies confirmed CD4+ T cells to be required for controlling giardial infection (Solaymani-Mohammadi and Singer, 2011). Furthermore, T cells were identified to be involved in causing mucosal alterations in murine giardiasis

(Gillon et al., 1982; Ferreira et al., 1990; Farthing, 1993; Scott et al., 2000). Therefore, both, CD4+ and CD8+ T cells, were responsible for increased numbers of intraepithelial lymphocytes whereas CD8+ alone caused microvillous shortening (Scott et al., 2004). It is known that humoral immune response plays a crucial role in parasite clearance mechanism. While the early phase of giardial infection is characterized by the above explained B-cell-independent mechanisms, the later phase, starting two weeks post-infection, is antibody-dependent in mice (Eckmann, 2003). Infection of humans with *G. duodenalis* leads to secretion of anti-*Giardia* secretory IgA in serum (Nash et al., 1987; Palm et al., 2003), mother´s milk and saliva (Téllez et al., 2005). It was shown that IgA-deficient, but not IgM-deficient, mice were not able to eradicate *Giardia spp.* infections (Langford et al., 2002). Furthermore, children born to mothers lacking anti-*Giardia* antibodies in their breast milk had a higher risk to contract giardial infection (Téllez et al., 2003).

To sum up, natural barriers like mucus, intestinal microbiota and peristalsis, innate immunity with defensin secretion and NO formation by IEC, cytokine production of mast cells and DC as well as the adaptive immunity including T cells response and antibody production are involved in the host defense machinery against *Giardia* (Roxström-Lindquist et al., 2006).

1.5.3 Parasite defense strategies

The mechanisms by which *G. duodenalis* causes clinical symptoms are still unclear. The parasite is not invasive and secretes no known toxins. Giardial infections were shown to affect the activity of gut enzymes like disaccharidases in gerbils (Belosevic et al., 1989; Buret et al., 1991). Furthermore, giardial infections cause damage of the mucosal surface, by shortening of crypts and microvilli, in the small intestine that result in malabsorption of electrolytes, nutrients, and water (Buret et al., 1992; Farthing, 1997; Scott et al., 2000; Scott et al., 2004). Furthermore, strain-dependent *G. duodenalis*-induced apoptosis of human IEC that leads to disruption of tight junctions and increased intestinal permeability was shown *in vitro* (Chin et al., 2002; Koh et al., 2013). Thereby, apoptosis was recognized to be induced by the parasite *via* the intrinsic and the extrinsic apoptotic pathways in IEC (Panaro et al., 2007). *In vivo* studies investigating duodenal biopsy from chronically infected patients confirmed epithelial barrier dysfunction due to changes in tight junctions and increased apoptosis (Troeger et al., 2007). Furthermore, *in vitro* studies investigating the interaction of murine bone marrow-derived DC with *Giardia* trophozoites or *Giardia* extracts suggest interferences of the parasite

with the host innate immunity due to changing cytokine secretion and surface marker expression (Kamda and Singer, 2009).

Studies from the last decades give first hints in parasite defense that implicate the existence of virulence factors. Virulence factors are defined as features (e.g. toxins, enzymes, metabolites, cell surface molecules) of a certain pathogen that are directly disease-causing or indirectly involved in the establishment of an infection. This includes especially properties of the microbe to enter, replicate and persist within the host, e.g. due to strategies for attachment to the host and/or evasion and suppression of the host immune response (Cross, 2008). Molecularly, virulence factors can have genotypic variation among different environmental isolates.

For *G. duodenalis* several virulence factors are discussed. For example, the ventral disc ensures motility to *Giardia*. It allows the parasite to attach to the intestinal surface and to differentiate into cysts to survive within and outside the host. One strategy of *G. duodenalis* is to evade the host humoral immunity by antigenic variation of its surface proteins (Aggarwal and Nash, 1988; Nash et al., 1988). The major antigens covering the outer surface of the parasite are VSPs that were targeted by the host's antibodies. They are cysteine-rich and vary in size from 20 to 200 kDa (Rópolo et al., 2005). A VSP consist of a variable amino terminus and a conserved, cytoplasmatic carboxyl terminus with a CRGKA motif (Ankarklev et al., 2010). VSPs are encoded by approximately 200 different genes, but only one VSP is expressed per trophozoites and this usually dominates within a population (Prucca et al., 2011). The changing of VSP expression that leads to antigenic variation (Nash, 2002) is, *in vivo* (von Allmen et al., 2004) and *in vitro* (Svärd et al., 1998; Carranza et al., 2002), partly initiated by cell differentiation. Beside the function of escaping the host immune system, VSPs are also known to protect the parasite against proteases *in vitro* (Nash et al., 1991). Furthermore, they were identified to be immunoreactive in milk samples from lactating women living in an endemic region. In these samples and in serum samples from patients with acute giardiasis living in a nonendemic area further immunoreactive proteins like the arginine deiminase (ADI), ornithine carbamoyl transferase (OCT) and enolase were noticed (Palm et el., 2003; Téllez et al., 2003). These three enzymes were shown to be released by the parasite upon contact with IEC *in vitro*. Studies with *G. duodenalis*-infected mice could only confirm the release of ADI and enolase in intestinal luminal fluid *in vivo* (Ringqvist et al., 2008).

1.5.3.1 *G. duodenalis* ADI and its function

The ADI (EC 3.5.3.6) is encoded by the *ArcA* gene that is located on chromosome 3 of *G. duodenalis* strain WB-C6 and contains no introns. Expression of the 1743 bp open reading frame leads to the synthesis of the 64 kDa enzyme that forms in its native form a homodimer (Knodler et al., 1998). *In vitro*, ADI is localized in the cytoplasm of the trophozoites whereas during co-incubation with IEC the enzyme is accumulated to the most anterior part of the parasite (Ringqvist et al., 2008). The ADI is involved in the energy metabolism of the parasite. It converts free L-arginine into L-citrulline and ammonia during the first step of the arginine dihydrolase (ADH) pathway. The formed L-citrulline is then further metabolized by the OCT into L-ornithine and carbamoyl phosphate that is used to generate ATP by the carbamate kinase (Schofield et al., 1990; Schofield et al., 1992). Beside its function in the metabolic pathway, *G. duodenalis* ADI was suggested to play a role in controlling antigenic variation *via* VSP citrullination. Touz et al. (2008) identified the enzyme to have a peptidyl-arginine deiminase (PAD) activity that leads to conversion of the arginine residue within the CRGKA motif of VSPs into citrulline. Additionally, they showed an impact of the enzyme in the encystation process. Interaction studies revealed an early upregulation of ADI gene expression, but a later downregulation in *Giardia* trophozoites after contact with IEC *in vitro* (Ringqvist et al., 2011). Furthermore, *in vitro* studies showed that *G. duodenalis* (Eckmann et al., 2000) as well as recombinant *G. duodenalis* ADI (Ringqvist et al., 2008) inhibits NO formation of human IEC by consumption of free arginine, the substrate of the epithelial NO synthase (NOS) to form NO. Arginine depletion by the parasite's ADI was also shown to reduce proliferation of human IEC lines *in vitro* (Stadelmann et al., 2012).

1.6 Aim of the study

Giardiasis, caused by the parasite *G. duodenalis*, is a global public health problem, especially due to common occurrence of chronic infections. Currently, less is known about virulence and pathogenicity mechanisms of *G. duodenalis* and their role in disease outcome. Certain antigens were indentified to be immunodominant in human body fluids and several were additionally found to be released after host-pathogen contact *in vitro*. These immunoreactive proteins, such as ADI, are considered to be potential virulence factors and therefore might play an important role in host-pathogen interaction. To examine the function of *G. duodenalis* ADI in human giardiasis, the following report was divided into two major parts:

1. Role of *G. duodenalis* ADI in host immune response and parasite defense mechanism

To explore the role of ADI in host-pathogen interaction, the enzyme's impact on different cell types important in mucosal immunity and on host protein modification was studied.

Thus, human monocyte-derived DC (moDC) were treated with recombinant ADI (assemblage A) to analyze host immunological features like cytokine expression and cell surface markers. Furthermore, a human intestinal cell line was treated with different human *G. duodenalis* patient isolates to investigate a strain-dependent impact on host NO production. Possible posttranslational modification of host proteins by ADI's previously described PAD activity, i.e. citrullination of intrapeptidic arginine, was analyzed.

2. Identification of *G. duodenalis* ADI sequence and functional variability in human clinical isolates

To support the hypothesis of ADI being a virulence factor, its sequence-variation in the natural human *G. duodenalis* population was analyzed. Sequence variability of the enzyme was functionally characterized to identify a potential correlation between primary structure and function. Thus, the substrate affinity for arginine was determined in enzyme kinetics for native ADI (assemblage A-subtypes) from human patients suffering giardiasis and the recombinant enzyme (assemblage A, B and E).

2 Material

2.1 Chemicals

Acetic acid	Merck, Darmstadt, G
Acetone	Roth, Karlsruhe, G
Agarose	Biozym, Hessisch Oldendorf, G
Ammonium chloride	Sigma, Steinheim, G
Ammonium ferric citrate	Sigma, Steinheim, G
Ammonium persulfate (APS)	Sigma, Steinheim, G
Ampicillin	Roth, Karlsruhe, G
L-Arginine	Merck, Darmstadt, G
L-Ascorbic acid	Sigma, Steinheim, G
Bacto agar	Oxoid, Wesel, G
Bacto™ tryptone	BD, Heidelberg, G
Bacto™ yeast extract	BD, Heidelberg, G
Bile from bovine	Sigma, Steinheim, G
Bisbenzimide	Sigma, Steinheim, G
Bovine serum albumin (BSA)	Roth, Karlsruhe, G
Bromophenol blue	Sigma, Steinheim, G
Calcium chloride ($CaCl_2$)	Sigma, Steinheim, G
L-Citrulline	Sigma, Steinheim, G
L-Cysteine	Sigma, Steinheim, G
Coomassie Brilliant Blue R-250	Roth, Karlsruhe, G
Deoxynucleoside triphosphates (dNTP)	Roth, Karlsruhe, G
Diacetyl monoxime	Sigma, Steinheim, G
Dimethyl sulfoxide (DMSO)	Sigma, Steinheim, G
Dipotassium phosphate (K_2HPO_4)	Sigma, Steinheim, G
Disodium hydrogen phosphate (Na_2HPO_4)	Sigma, Steinheim, G
Dithiothreitol (DTT)	Roth, Karlsruhe, G
Ethylenediaminetetraacetic acid (EDTA)	Roth, Karlsruhe, G
EDTA-free protease inhibitor cocktail	Roche, Mannheim, G
Entellan®	Merck, Darmstadt, G
Fetal calf serum (FCS); dialyzed	Biochrom, Berlin, G
FCS (for DC/Caco-2 cultivation)	Biochrom, Berlin, G
FCS (for *Giardia* cultivation)	Sigma, Steinheim, G
Ferric chloride ($FeCl_3$)	Sigma, Steinheim, G
Ficoll-Paque™ Plus	GE Healthcare, Munich, G
GelGreen™	Biotium, Hayward, USA
Glucose	Sigma, Steinheim, G
L-Glutamine	Biochrom, Berlin, G
Glycerol	Roth, Karlsruhe, G
Glycine	Roth, Karlsruhe, G
Granulocyte-macrophage colony-stimulating factor (GM-CSF), human	Bayer, Seattle, USA
Hepes (4-(2-Hydroxyethyl)piperazine-1-ethanesulfonic acid)	Sigma, Steinheim, G
Hepes (for cell culture)	Biochrom, Berlin, G
H_6-CRGKA	Genscript, Piscataway, USA
Imidazole	Merck, Darmstadt, G

IFN-γ, human	eBioscience, Frankfurt, G
IL-1β, human	ImmunoTools, Friesoythe, G
IL-4, human	R&D Systems, Wiesbaden-Nordenstadt, G
Kanamycin	Sigma, Steinheim, G
LPS (*E. coli* 026:B6)	Sigma, Steinheim, G
Methanol	Roth, Karlsruhe, G
Milk powder	Roth, Karlsruhe, G
Minimum essential medium (MEM) with Earle's Salts	PAA, Pasching, A
Mowiol 4-88	Roth, Karlsruhe, G
Nonessential Amino Acid Solution (NEAA)	Life technologies, Darmstadt, G
L-Ornithine	Sigma, Steinheim, G
Paraformaldehyde (PFA)	Roth, Karlsruhe, G
Penicillin/Streptomycin (for cell culture)	PAA, Pasching, A
Peptone from casein	Merck, Darmstadt, G
Phosphoric acid (H_3PO_4)	Sigma, Steinheim, G
Potassium chloride (KCl)	Merck, Darmstadt, G
Potassium dihydrogen phosphate (KH_2PO_4)	Sigma, Steinheim, G
Rapamycin	Sigma, Steinheim, G
Roswell Park Memorial Institute (RPMI) medium 1640	Sigma, Steinheim, G
Rotiphorese® Gel 30 (37.5:1)	Roth, Karlsruhe, G
RPMI 1640 medium (arginine-free)	PAN-Biotech, Aidenbach, G
Sodium chloride (NaCl)	Sigma, Steinheim, G
Sodium deoxycholate	Sigma, Steinheim, G
Sodium dodecyl sulfate (SDS)	Sigma, Steinheim, G
Spectinomycin	Sigma, Steinheim, G
Sulfuric acid	Merck, Darmstadt, G
Tetracycline	Merck, Darmstadt, G
Tetramethylethylenediamine (TEMED)	Roth, Karlsruhe, G
TNF-α, human	ImmunoTools, Friesoythe, G
Thiosemicarbazide	Sigma, Steinheim, G
Trichloroactetic acid	Merck, Darmstadt, G
Tris(hydroxymethyl)aminomethane (Tris)	Roth, Karlsruhe, G
Tris-HCl	Roth, Karlsruhe, G
Triton X-100	Sigma, Steinheim, G
Trypsin-EDTA (for cell cultue)	Life technologies, Darmstadt, G
Tween20	Roth, Karlsruhe, G
2-mercaptoethanol	Roth, Karlsruhe, G
3,3',5,5'-Tetramethylbenzidine (TMB)	KPL, Maryland, USA

2.2 Buffers and solutions

Phosphate buffered saline (PBS)	13.7 mM NaCl, 8.0 mM Na_2HPO_4, 2.7 mM KCl, 1.5 mM KH_2PO_4 (pH 7.4)
Tris buffered saline (TBS)	20 mM Tris, 137 mM NaCl (pH 7.6)

Cell lysis

Lysis buffer	10 mM Tris-HCl pH 7.2, 150 mM NaCl, 1% Triton X-100, 1% sodium deoxycholate, EDTA-free protease inhibitor cocktail

Cell staining

Fixation solution	PBS plus 2% PFA
Blocking solution	PBS plus 1.5% BSA, 1.5% goat normal serum
Bisbenzimide solution	PBS plus 0.25 µg/ml bisbenzimide

ELISA/Western blot

PBS-T	PBS plus 0.05% Tween20
TBS-T	TBS plus 0.1% Tween20
Towbin transfer buffer	25 mM Tris, 192 mM Glycin, 20% Methanol (pH 8.3)

ADI activity

Reagent 1	25% (v/v) 98% H_2SO_4, 20% (v/v) 85% H_3PO_4, 0.025% (w/v) $FeCl_3$
Reagent 2	0.5% (w/v) diacetyl monoxime, 1.2 mM thiosemicarbazide
Reagent 3	2 parts reagent 1 : 1 part reagent 2

Flow cytometry

Wash buffer	PBS plus 1% (v/v) FCS
Fixation buffer	PBS plus 4% (v/v) PFA

Gel electrophoresis

TAE electrophoresis buffer	40 mM Tris, 0.11% (v/v) acetic acid, 0.2% (v/v) 0.5 M EDTA
GelGreen™ solution	150 ml dH_2O plus 45 µl GelGreen™

Generation of moDC

MACS buffer	PBS plus 0.5% BSA and 2 mM EDTA → sterile filtration

PAD activity

Deamination buffer	40 mM Tris-HCl (pH 7.5), 5 mM $CaCl_2$, 1mM DTT

Protein purification

Buffer A	25 mM Hepes, 150 mM NaCl, 5 mM imidazole (pH 7.5)
Buffer B	25 mM Hepes, 150 mM NaCl, 1 M imidazole (pH 7.5)

SDS-PAGE

Coomassie staining solution	0.25% (v/v) Coomassie Brilliant Blue R-250, 45% (v/v) methanol, 10% (v/v) acetic acid
Coomassie destaining solution	20% (v/v) methanol, 7% (v/v) acetic acid
10% SDS gel consist of:	
SDS-PAGE separation gel (10%)	3.3 ml Rotiphorese® Gel 30 (37.5:1), 2.5 ml 1.5 M Tris (pH 8.8), 0.1 ml 10% SDS, 4 µl TEMED, 0.1 ml 10% APS, 4.0 ml dH_2O
SDS-PAGE stacking gel (5%)	0.5 ml Rotiphorese® Gel 30 (37.5:1), 0.38 ml 1.0 M Tris (pH 6.8), 30 µl 10% SDS, 3 µl TEMED, 30 µl 10% APS, 2.1 ml dH_2O
SDS running buffer	25 mM Tris, 192 mM glycin, 0.4% (w/v) SDS
Tris-Hepes-SDS running buffer	100 mM Tris, 100 mM Hepes, 0.1% (w/v) SDS
1 x SDS reducing loading buffer	50 mM Tris-HCl (pH 6.8), 2% SDS, 0.01% bromophenol blue, 10% glycerol, 100 mM 2-mercaptoethanol

3 x SDS reducing loading buffer	3.5 ml 4 x SDS/Tris-HCl buffer (pH 6.8), 1.5 ml glycerol (87%), 175 mM SDS, 302 mM DTT
5 x SDS reducing loading buffer	250 mM Tris-HCl (pH 6.8), 10% SDS, 0.05% bromophenol blue, 50% glycerol, 500 mM 2-mercaptoethanol
4 x SDS/Tris-HCl buffer (pH6.8)	5% SDS, 0.5 M Tris-HCl pH 7.4, 0.125 M EDTA

2.3 Antibodies (for Western blot analysis)

Antibodies used for Western blot analysis are summarized in Tab. 2 and 3.

Table 2: Primary antibodies

Antigen	Source	Dilution	Type	Manufacturer	Catalog number
anti-Histidine-tag	mouse	1:2500	mAb, purified	Linaris, Dossenheim, G	MAK 1396 (clone AD1.1.10)
anti-p70 S6 Kinase	rabbit	1:1000	pAb, purified	Cell signaling, Danvers, USA	#9202
anti-Phospho-p70 S6 Kinase (Thr389)	rabbit	1:1000	pAb, purified	Cell signaling, Danvers, USA	#9205
anti-E4-BP1	rabbit	1:1000	pAb, purified	Cell signaling, Danvers, USA	#9452
anti-Phospho-4E-BP1 (Thr70)	rabbit	1:1000	pAb, purified	Cell signaling, Danvers, USA	#9455
anti-β-Actin	rabbit	1:1000	pAb, purified	Cell signaling, Danvers, USA	#4967
anti-*G. duodenalis* ADI	llama	1:2500	pAb, antiserum	Preclinics, Potsdam, G	individual order

Table 3: Secondary antibodies

Antigen	Source	Dilution	Type	Manufacturer	Catalog number
anti-rabbit IgG-HRP	goat	1:2000	pAb, purified	Cell signaling, Danvers, USA	#7074
anti-mouse IgG-HRP	rabbit	1:5000	pAb, purified	Jackson ImmunoResearch, West Grove, USA	315-035-003
anti-llama IgG-HRP	goat	1:10000	pAb, purified	Bethyl Laboratories, Montgomery, USA	A160-100P

2.4 Oligonucleotides

All primers used in this study are summarized in Tab. 4. Primer design, except for ENTRY-FW/BW, was based on sequence information from *Giardia*DB (www.giardiadb.org), carried out with Geneious Pro 5.4.3 (Biomatters Ltd.) and ordered from Eurofins MWG (Ebersberg, G).

Table 4: List of primers used in this study

Name	Sequence (5' – 3')	Application
gd-3_s	AATGACTGACTTCTCCAAGGATAAAGA	cloning
gd-5_as	TCCCTCACTTGATATCGACGCAGATGTCA	cloning
gd-11_as	CGGCGGGGGCCGGTGCTTTG	ADI amplification/ sequencing
gd-12_s	GTCCGCAACACGGCTCTCGTTAC	sequencing
gd-15_as	CCGAGGCGCTTCCAGAAGAT	sequencing
gd-20_s	CTGACAAGCACTTCATTTACTG	ADI amplification/ sequencing
gd-6_a	TGCGTGACCAGCAGATAACC	sequencing
ENTRY-FW_s	GCGAAACGATCCTCGAAGC	sequencing
ENTRY-BW_as	CCCCTGATTCTGTGGATAACCG	sequencing
C424A-FW_s	GTACGGCTCTCTGCACGCCGCATCTCAGGTTGTT	mutagenesis
C424A-BW_as	AACAACCTGAGATGCGGCGTGCAGAGAGCCGTAC	mutagenesis
pASG-IBA35-FW_s	GAGTTATTTTACCACTCCCT	sequencing
pASG-IBA35-BW_as	CGCAGTAGCGGTAAACG	sequencing
pASG-IBA35-tet-FW_s	GGGGGCGGAGCCTATGGAAA	sequencing
pASG-IBA35-tet-BW_as	GGTCAAGCTTGCGGGTGGCT	sequencing

2.5 Media

Caco-2 growth medium (MEM20)	80% MEM with Earle's Salts, 20% FCS, 1% glutamine, 1% 100 x NEAA, 100 U/ml penicillin/100 µg/ml streptomycin → sterile filtration
DC growth medium (R10FCS)	RPMI 1640 plus 10% FCS, 10 mM Hepes, 100 U/ml penicillin/ 100 µg/ml streptomycin, 50 µM 2-mercaptoethanol → sterile filtration
DC growth medium (-ArgR10FCS)	RMPI 1640 (arginine-free) plus 10% dialyzed FCS, 10 mM Hepes, 100 U/ml penicillin/ 100 µg/ml streptomycin, 50 µM 2-mercaptoethanol → sterile filtration

Giardia growth medium	basic medium (18 g/l peptone from casein, 9 g/l yeast extract, 56 mM glucose, 30 mM NaCl, 1 mM ascorbic acid, 6 mM K_2HPO_4, 4 mM KH_2PO_4) plus 10% (v/v) FCS, 0.05% (w/v) bile from bovine, 0.00228% (w/v) ammonium ferric citrate, 0.2% (w/v) cysteine, 100 U/ml penicillin/ 100 µg/ml streptomycin (pH 7.0) → sterile filtration
LB agar	LB medium plus 1.5% bacto agar → autoclaving
LB medium	10 g/l bacto tryptone, 5 g/l yeast extract, 10 g/l NaCl (pH 7.5) → autoclaving
SOB medium	20 g/l bacto tryptone, 5 g/l yeast extract, 10 ml/l 1 M NaCl, 2.5 ml/l 1 M KCl, → autoclaving
SOC medium	SOB medium plus 20 mM glucose → steril filtrated

2.6 Plasmids

All plasmids that were used in this study are summarized in Tab. 5.

Table 5: List of used plasmids
E. coli cells transformed with plasmids carrying a kanamycin resistance gene were cultured with 50 µg/ml and those carrying an ampicillin resistance gene with 100 µg/ml of the appropriate antibiotic. Ass: assemblage.

Plasmid	Characteristics
pENTRY-IBA10	cloning site, kanamycin resistance gene, size: ~ 1800 bp
pENTRY-IBA10+ADI (AssA)	pENTRY-IBA10 plus inserted ADI (assemblage A) gene, size: ~ 3550 bp
pMK-RQ+ADI(AssB)	kanamycin resistance gene, ColEI ori, synthetic (codon optimized) ADI (assemblage B) gene, size: ~ 4050 bp
pMK-RQ+ADI(AssE)	kanamycin resistance gene, ColEI ori, synthetic (codon optimized) ADI (assemblage E) gene, size: ~ 4050 bp
pUC19	multiple cloning site, LacZ, LacI, ampicillin resistance gene, size: ~ 2700 bp
pASG-IBA35	f1 origin, ampicillin resistance gene, Tet-repressor, ColEI ori, Tet promoter, expression cassette with hexahistidine (His_6)-tag, size: ~ 3200 bp
pASG-IBA35 (w/o His_6-tag)	pASG-IBA35 without His_6-tag, size: ~ 3200 bp
pASG-IBA35+ADI(AssA)	pASG-IBA35 plus inserted ADI (assemblage A) gene, size: ~ 4450 bp
pASG-IBA35+ADI_{C424A}(AssA)	pASG-IBA35 plus inserted mutated ADI_{C424A} (assemblage A) gene, size: ~ 4450 bp
pASG-IBA35+ADI(AssB)	pASG-IBA35 plus inserted ADI (assemblage B) gene, size: ~ 4450 bp
pASG-IBA35+ADI(AssE)	pASG-IBA35 plus inserted ADI (assemblage E) gene, size: ~ 4450 bp

2.7 Equipment

ApoTome	Zeiss, Jena, G
Atmosphere Generation System (AnaeroJar™/AnaeroGen™)	Oxoid, Wesel, G
Axioskop2	Zeiss, Jena, G
ÄktaFPLC system	GE Healthcare, Munich, G

Flow cytometer LSR II	BD, Heidelberg, G
Gel documentation system DIAS II	Serva, Heidelberg, G
Gel electrophoresis chamber	Bio-Rad, Munich, G
Helios Gamma Spectrophotometer	Thermo Scientific, Karlsruhe, G
Heracell 150i	Thermo Scientific, Karlsruhe, G
Heraeus® Multifuge® 1S-R	Thermo Scientific, Karlsruhe, G
High-pressure homogenizer EmulsiFlex	Avestin, Mannheim, G Incubator
Incubator shaker Innova®40	New Brunswick, Edison, USA
Microplate reader Infinite M200Pro	Tecan, Crailsheim, G
Nalgene® freezing container	Sigma, Steinheim, G
NanoDrop® ND-1000 Spectrophotometer	Thermo Scientific, Karlsruhe, G
Neubauer counting chamber	Marienfeld, Lauda-Königshofen, G
Power PAC3000	Bio-Rad, Munich, G
Rocking platform	VWR, Darmstadt, G
SDS electrophoresis chamber	Bio-Rad, Munich, G
Semi-Dry electro blotter	Peqlab, Erlangen, G
Sonifier Cell Disruptor W-350	Brandson ultrasonics, Danbury, USA
Sorvall RC-5B superspeed centrifuge	DuPont Instruments, Newtown, USA
Tabletop centrifuge himac	VWR, Darmstadt, G
Thermal Cycler	Bio-Rad, Munich, G
Thermomixer compact	Eppendorf, Hamburg, G

2.8 Expendable materials

HisTrap™FF column	GE Healthcare, Munich, G
Maxisorp 96-well ELISA plate	Nunc, Wiesbaden, G
Ni-NTA HisSorb Strips	Qiagen, Hilden, G
Nitrocellulose membrane	Bio-Rad, Munich, G
PD-10 column	GE Healthcare, Munich, G
Pore size filter (0.22 µm, 0.45 µm)	Sartorius, Göttingen, G
Vivaspin concentrator (5 kDa PES membrane)	Sartorius, Göttingen, G

2.9 Biologicals

2.9.1 Bacterial strains

All *E. coli* strains that were used in this study are summarized in Tab. 6.

Table 6: List of used *E. coli* strains

***E. coli* strain**	**Genotype**	**Used antibiotic(s) for cultivation**
DH5αZ1	(F-) supE ΔlacU169 ΔargF hsdR17 recA1 endA1 gyrA96 thi-1 relA1, tetR+ lacIq+ SpecR	spectinomycin (50 µg/ml)
ER2508	F- ara-14 leuB6 fhuA2 Δ(argF-lac)U169 lacY1 lon::miniTn10(TetR) glnV44 galK2 rpsL20(StrR) xyl-5 mtl-5 Δ(malB) zjc::Tn5(KanR) $\Delta(mcrC\text{-}mrr)_{HB101}$	kanamycin (25 µg/ml) tetracycline (12 µg/ml)
JWK clpX-1	BW25113:lacIq rrnB3 ΔlacZ4787 hdsR514 Δ(araBAD)567 Δ(rhaBAD)568 rph-1 FRT::ΔclpX/Kan::FRT	kanamycin (50 µg/ml)
XL1-Blue	recA1 endA1 gyrA96 thi-1 hsdR17 supE44 relA1 lac [F´ proAB lacIqZΔM15 Tn10 (TetR)]	-

2.9.2 Eukaryotic cell lines

Caco-2 cells (DSMZ Accession No. ACC 169) were established from the primary colon tumor (adenocarcinoma) of a 72-year-old Caucasian man in 1974 (Fogh et al., 1977; Rousset, 1986). These IEC have a doubling time of ~ 80 h and grow in colonies after splitting. In contrast, confluent cells grow as epithelial adherent cells and are differentiated 17-21 days post-confluence.

In 1979, *G. duodenalis* WB strain (ATCC® 30957™) was isolated from a 30-year-old white American man chronically infected since traveling to Afghanistan in 1977 (Smith et al., 1982). The 1983 established clone of this strain, *G. duodenalis* WB clone C6 (ATCC® 50803™), was used as laboratory strain in this study. Additionally, in the Aebischer research group *Giardia* cysts were isolated from human stool samples, excystated and diluted to obtain trophozoite population lines routinely. These parasitic isolates, as well as the laboratory strain WB-C6, were genotypically characterized by PCR and subsequent sequencing of the triosephosphate isomerase locus according to a published protocol from Sulaiman et al. (2003). After alignment with reference sequences filed in *Giardia*DB

(www.giardiadb.org), trophozoite population lines along with patient and genotype information were collected in a *G. duodenalis* biobank and used for this study (Tab. 7).

Table 7: List of *G. duodenalis* strains used in this study

Name	Assumed origin of acquired infection	Assem-blage	Course of disease	Clinical symptoms	Therapy-refractory (MTZ)
WB-C6	Afghanistan	AI	chronically	vomiting, abdominal cramps, flatulence, diarrhea (foul-smelling, watery stools), weight loss	yes
16-01/E1	Ghana	AII	chronically	no (or only weak) complaints	yes
11-04/E3	India	AII	chronically	severe complaints	yes
14-03/F7	Dominican Republic	AII	chronically	malabsorption	yes
115-01/H2	Belize	AII	self-limited → arguable	indeterminable → co-infection with *Clostridium difficile*	no

3 Methods

3.1 Molecular biological methods

3.1.1 Genomic DNA extraction

Genomic *G. duodenalis* DNA from each patient isolate or the laboratory strain WB-C6 was extracted from approximately 1 x 10^7 trophozoites that were harvested at 4°C for 5 min at 900 x *g* and then washed in PBS. DNA was isolated with the QIAamp DNA stool Mini Kit (Qiagen) according to the manufacturer's manual. Finally, DNA concentration was measured with NanoDrop ND-1000 Spectrophotometer. DNA was stored at 4°C.

3.1.2 Agarose gel electrophoresis

DNA samples were mixed with 6 x loading dye (Fermentas) and loaded on a 1% agarose gel. Separation took place in a horizontal gel electrophoresis chamber at 5-10 V/cm electrode distance using TAE electrophoresis buffer. To visualize DNA, the gel was stained after electrophoresis in GelGreen™ solution for 15 min. GelGreen™ intercalated as a fluorescent nucleic acid dye into DNA and was excited by visible blue light with gel documentation system DIAS II. DNA size marker GeneRuler™ 1 kb Plus DNA Ladder (Fermentas) was used to determine the length of DNA fragments.

3.1.3 Preparation of chemically competent *E. coli* bacteria

To prepare chemically competent *E. coli* bacteria, an overnight pre-culture was diluted 1:50 in 200 ml LB medium containing the appropriate antibiotics. *E. coli* bacteria were incubated at 37°C under agitation at 155 rpm until an OD_{600} of 0.3-0.4 was reached. Afterwards, the culture was centrifuged at 4°C for 10 min at 3000 x *g*. Supernatant was discarded and pellet was resuspended in pre-chilled 8 ml 100 mM $CaCl_2$. After resting on ice for 20 min, culture was centrifuged and resuspended again in pre-chilled 8 ml 100 mM $CaCl_2$. After incubation overnight at 4°C, 4 ml of pre-chilled 60% glycerol was added, bacteria were aliquoted and

stored until usage at -80°C. A transformation efficiency of 0.1-1.0 x 10^8 cfu/µg pUC19 DNA was calculated.

3.1.4 Transformation

For transformation, 200 µl chemically competent bacteria were thawed for 30 min on ice. Plasmid DNA of 50-100 ng was added and bacteria were rested on ice for further 10 min. Bacteria were heat shocked for 90 sec at 42°C and immediately transferred on ice. After 2 min, 1 ml SOC medium was added and bacteria were incubated for 1 h at 37°C. To concentrate bacterial inoculum, culture was centrifuged for 1 min at 10100 x *g* and 1 ml supernatant was discarded. Bacterial pellet was then resuspended in the remaining volume and plated on LB agar that contained the appropriate antibiotics. Agar plates were incubated overnight at 37°C. After separation and testing of single clones, bacterial glycerol stocks were prepared.

3.1.5 Preparation of glycerol stocks

Bacterial glycerol stocks were prepared by addition of 200 µl 80% sterile glycerol to 800 µl overnight *E. coli* culture and were frozen immediately in liquid nitrogen. Until usage bacteria were stored at -80°C.

3.1.6 Isolation of plasmid DNA

Three ml LB medium supplemented with appropriate antibiotics were inoculated with a single colony of transformed *E. coli* bacteria and incubated at 37°C overnight. Then, plasmid DNA isolation was carried out using Zyppy™ Plasmid Miniprep Kit according to manufacturer's information (ZymoResearch, Freiburg, G). Concentration of plasmid DNA was measured with NanoDrop ND-1000 Spectrophotometer and plasmid DNA was stored at 4°C.

3.1.7 Restriction digest and ligation

After isolation, plasmid DNA was controlled by restriction digest. Plasmid DNA was incubated for 15 min at 37°C with the restriction enzyme *Sac*I (FastDigest®) according to manufacturer's manual (Fermentas). DNA fragments were visualized *via* agarose gel electrophoresis.
For preparation of the control plasmid pASG-IBA35 (w/o His_6-tag), the vector pASG-IBA35+ADI was digested with the restriction enzymes *Xba*I and *Hind*III (FastDigest®) according to manufacturer's instructions (Fermantas). The complete reaction mixture was loaded on an agarose gel and DNA of the linearized vector was extracted. Resultant overhangs were filled with Klenow fragment according to manufacturer's manual (Fermantas) and DNA was extracted from gel after agarose gel electrophoresis. Blunt-end linearized vector was then ligated with T4 DNA ligase as described by the manufacturer (Fermentas). Ligation mixture was directly used for transformation into *E. coli*. Successful preparation of the control vector pASG-IBA35 (w/o His_6-tag) was verified by *Spe*I (FastDigest®) after transformation following the manufacturer's instructions (Fermentas).

3.1.8 DNA extraction from gel

After amplification of ADI from genomic *G. duodenalis* DNA, entire PCR reaction mixture was loaded on an agarose gel. The desired PCR fragment was isolated from the gel using a clean scalpel. Same procedure was also performed in case of digested pASG-IBA35+ADI plasmid. DNA was extracted with the QIAquick® Gel Extraction Kit according to manufacturer's information (Qiagen). Purified DNA was analyzed on an agarose gel and stored at until use 4°C.

3.1.9 Purification of PCR products

To remove primers, excessive dNTP's and polymerase after PCR, amplified DNA was purified using the DNA Clean and Concentratot™-25 Kit (ZymoResearch). Until sequencing purified PCR fragments were stored at 4°C.

3.1.10 Cloning of *G. duodenalis* ADI with StarGate®

The 1.8-kb ADI (assemblage A) PCR fragment obtained from the amplification of genomic *G. duodenalis* WB-C6 DNA was purified by gel extraction and cloned into the entry vector pENTRY-IBA10 to generate the donor vector pENTRY-IBA10+ADI (AssA). The donor vector was mixed with the acceptor vector pASG-IBA35 to generate the destination vector pASG-IBA35+ADI(AssA) for expression of the recombinant protein with an N-terminal His_6-tag. This cloning procedure was performed using the StarGate® system in accordance to the manufacturer's information (IBA).
For the expression of recombinant ADI of assemblage B and E, both genes were synthesized (codon optimized, flanked by *Bsm*BI restriction sites, start codon replaced to AATG, stop codon replaced to GGGA) by GeneArt® (Invitrogen, Darmstadt, G) in a plasmid lacking a *Bsm*BI cleavage site and carrying a kanamycin resistance gene. In the subsequent cloning procedure with the StarGate® system, these delivered plasmids were used as donor vector equivalents.

3.1.11 Site-directed mutagenesis

To obtain a catalytically inactive mutant form of ADI (ADI_{C424A}), cysteine was replaced with alanine at amino acid sequence position 424. Site-direct mutagenesis was carried out with the three-step procedure of the QuikChange® II Site-Directed mutagenesis kit according the manufacturer's instructions (Agilent, Böblingen, G). First, point-mutation was inserted by PCR using the mutagenic primers C424A-FW/C424A-BW and the expression vector pASG-IBA35+ADI as template. Second, parental methylated and hemimethylated DNA was digested to select for mutation-containing synthesized DNA. The principle behind is that template DNA purified from dam^+ *E. coli* strain is methylated and thus will be a substrate for *Dpn*I, a restriction enzyme that cleaves only when its recognition site is methylated. In contrast, the newly synthesized DNA is unmethylated and therefore will be not digested. Thus, in a third step, the mutated vector could be transformed. After transformation, plasmid DNA was prepared and gene of interest (GOI) sequence checked by DNA sequencing to verify nucleotide exchange.

3.1.12 PCR for amplification of ADI from genomic *G. duodenalis* DNA

For expression of recombinant ADI of assemblage A, its coding sequence was amplified from genomic DNA of *G. duodenalis* strain WB-C6 by PCR. This was carried out with the proofreading *Pfu* DNA Polymerase (Tab. 8) according to manufacturer's information (Promega, Mannheim, G) under conditions that are summarized in Tab. 9.

Table 8: Reaction mixture for amplification of *G. duodenalis* WB-C6 ADI

Reaction mixture (50 µl)	1x
genomic DNA (20 ng/µl)	10 µl
Pfu DNA Polymerase 10x Reaction Buffer with $MgSO_4$	5 µl
40 mM dNTP	1 µl
10 mM Primer-gd3	1 µl
10 mM Primer-gd5	1 µl
Pfu DNA Polymerase (2–3 U/µl)	0.5 µl
dH_2O	31.5 µl

Table 9: Thermocycler conditions for amplification of *G. duodenalis* WB-C6 ADI

1x	denaturation	2 min	95°C
35x	denaturation	30 sec	95°C
	primer-annealing	30 sec	60°C
	elongation	3 min 40 sec	72°C
1x	polishing	5 min	72°C
	storage		4°C

To identify sequence variants, ADI was amplified from genomic DNA of *G. duodenalis* patient isolates or the laboratory strain WB-C6 with Mango*Taq*™ DNA Polymerase (Tab. 10) as described by the manufacturer (Bioline, Luckenwalde, G). The PCR conditions are shown in Tab. 11.

Table 10: Reaction mixture for amplification of genomic *G. duodenalis* ADI

Reaction mixture (25 µl)	1x
DNA sample (20-50 ng/µl)	1 µl
5 x Mango*Taq*™ reaction buffer	5 µl
40 mM dNTP	0.5 µl
50 mM $MgCl_2$	0.75 µl
10 mM Primer-gd11	0.5 µl
10 mM Primer-gd20	0.5 µl
Mango*Taq*™ DNA Polymerase (5 U/µl)	0.25 µl
dH_2O	16.5 µl

Table 11: Thermocycler conditions for amplification of genomic *G. duodenalis* ADI

1x	denaturation	3 min	96°C
35x	denaturation	30 sec	96°C
	primer-annealing	30 sec	58°C
	elongation	2 min 30 sec	72°C
1x	polishing	7 min	72°C
	storage		4°C

3.1.13 DNA sequencing

Purified PCR fragments (10-20 ng/reaction) or plasmid DNA (150-300 ng/reaction) were used as templates for DNA sequencing (Tab. 12) that was carried out with the BigDye® Terminator v 3.1 Cycle Sequencing Kit as recommended by the manufacturer (Life technologies). Primers ENTRY-FW, ENTRY-BW and gd-6 were used to prove whether cloned (mutagenized) ADI sequence was correctly inserted into the vector pENTRY-IBA10. Furthermore, to evaluate the insertion into the vector pASG-IBA35, primer pASG-IBA35-FW, pASG-IBA35-BW and gd-6 were used. For sequencing of genomic ADI from different *G. duodenalis* patient isolates and the laboratory strain WB-C6 the primer gd-11, gd-12, gd-15 and gd-20 were applied. Amplification was carried out as described in Tab. 13. Remaining working steps were performed by the internal sequencing service of the RKI. Sequence files of each primer were finally analyzed with SeqMan Pro™ software (DNASTAR®, Inc.) to obtain contig-sequences. Those were aligned using ClustalW (EMBL-EBI). For translation of nucleic acid into peptide sequences EMBOSS Transeq (EMBL-EBI) was used.

Table 12: Reaction mixture for DNA sequencing

Reaction mixture (10 µl)	1x
DNA sample	1.5 µl
5 x buffer	1.5 µl
10 mM Primer	0.5 µl
Sequencing mix (BigDye 3.1)	1.0 µl
dH_2O	5.5 µl

Table 13: Thermocycler conditions for DNA sequencing

1x	denaturation	2 min	96°C
25x	denaturation	10 sec	96°C
	primer-annealing	5 sec	60°C
	elongation	4 min	60°C
	storage		4°C

3.2 Biochemical methods

3.2.1 Protein characterization

3.2.1.1 Determination of protein concentration

The protein concentration was determined with the Pierce® BCA Protein Assay Kit according to the manufacturer's manual (Thermo Scientific). BSA standard, that was included in the kit, was diluted for a linear working range in PBS. Absorbance was measured at 562 nm with the microplate reader Infinite M200Pro.

To investigate the ADI expression of various transformed *E. coli* strains, similar protein amounts in SDS-PAGE and Western blot analysis were compared. Therefore, the harvested bacterial pellets were resuspended in 3 x SDS loading buffer after thawing and were then diluted with PBS to a final SDS concentration less than 5%. To have an equivalent standard, to BSA samples diluted in PBS 3 x SDS loading buffer was added in corresponding amounts.

3.2.1.2 Enzymatic activity assay

The enzymatic activity of recombinant ADI and ADI_{C424A} was measured by colorimetric determination of citrulline formation as described previously (Knodler et al., 1995) and was found to be stable for the duration of the study.

The verification of citrulline is based on a two-step reaction that runs under acidic conditions (Fig. 3). In a condensation reaction of citrulline with diacetyl monoxime a glycolurile derivate is formed. In presence of heat, concentrated acid, Fe^{3+} and oxygen, this derivate converts into a dye that can be measured photometrically (Lorentz and Koch, 1971). In the first reaction step, hydroxylamine is formed as side product. This reducing agent disturbs the color development and therefore is necessary to be removed by the addition of thiosemicarbazide (Knipp and Vasák, 2000). The reaction conditions are achieved by usage of freshly prepared reagent 3, that is a mixture of reagent 1 (including acids and Fe^{3+}) and reagent 2 (including diacetyl monoxime and thiosemicarbazide).

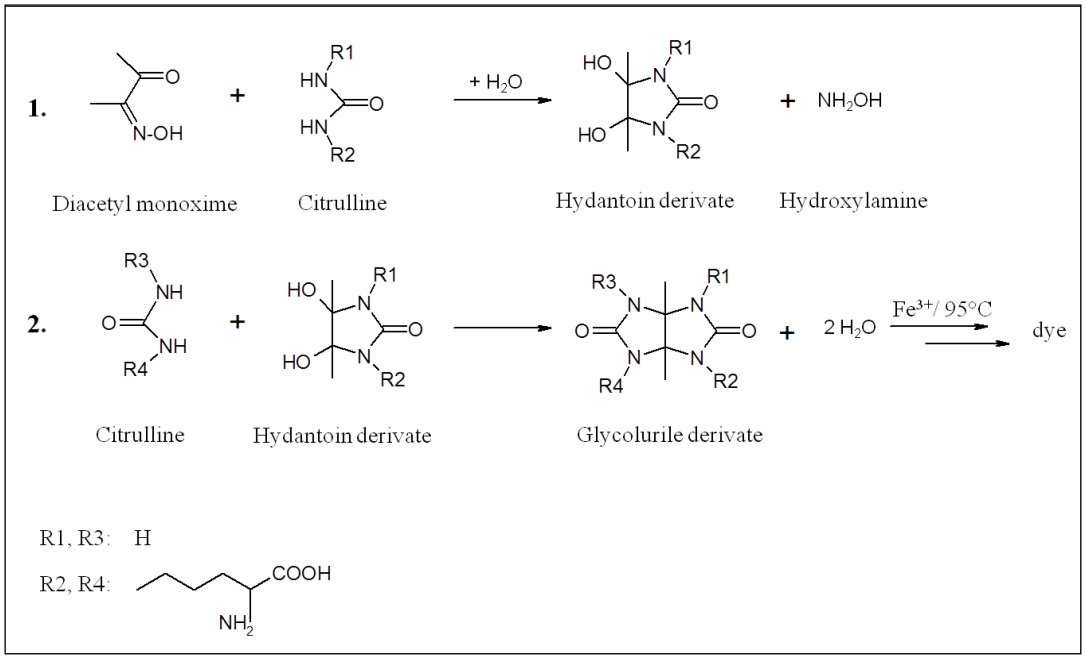

Figure 3: Chemical reaction for the verification of citrulline

To determine the enzymatic activity, 10 µl of (thawed) purified recombinant enzyme (0.5-2 µg/ml) was added to 30 µl 40 mM Hepes buffer (pH 7.0) and 10 µl 100 mM arginine (prepared in dH_2O). As negative control 10 µl recombinant enzyme was replaced by PBS. The reaction mixture was incubated for 10 min at 37°C. Deimination of arginine was stopped by addition of 10 µl 6% trichloroactetic acid. To determine the enzyme activity, citrulline

concentration was measured. Therefore, 200 µl reagent 3 was added and the sample was heated to 96°C for 6 min. Finally, the OD at 540 nm was measured in a 96-well microtiter plate. To quantify the formed citrulline, a standard curve with citrulline ranging from 0-625 µM was prepared in parallel. To determine formed citrulline after treatment of moDC with recombinant ADI, 10 µl or 20 µl of cell culture supernatants were refilled with dH_2O up to 50 µl. Ten to twenty µl of DC growth medium was used as negative control. Finally, 200 µl of reagent 3 were added and it was proceeded as above described.

3.2.1.3 Enzyme kinetics of *G. duodenalis* ADI

As a characteristic parameter to describe an enzyme kinetic, the K_m value of recombinant and native ADI was determined. Therefore, lysates as well as final purified enzymes from the DH5αZ1 strain expressing the recombinant ADIs (assemblage A, B and E) were used. For preparation of *E. coli* lysates, 45 ml bacterial cultures were grown to an OD_{600} between 2.4-3.0 without induction and pellets were harvested at 4°C with 12000 x *g*. Bacterial pellets were washed in PBS and stored at -80°C. Thawed pellets were resuspended in 10 ml ice-cold PBS and disrupted using a French Press. After centrifugation (15000 x *g*, 30 min, 4°C), substrate affinity of ADI for arginine was determined in the supernatants.
To determine the K_m value of native ADI from *G. duodenalis* trophozoites, lysates were prepared. Three cultivation flasks of confluent trophozoites per strain were washed with ice-cold PBS and placed for 30 min on ice. Cultures were harvested, combined and centrifuged (900 x *g*, 5 min, 4°C). After additional washing with PBS, cell pellet was resuspended in 500 µl PBS, trophozoites were counted in a Neubauer counting chamber and frozen at -70°C. Subsequently, frozen trophozoites were thawed, exposed to a second freeze/thaw-cycle and finally disrupted by ultrasound (duty cycle 60%, output 6, 4°C) in six 30 sec periods with 30 sec resting in between. Cell debris was removed by centrifugation for 20 min at 12000 x *g* at 4°C. Supernatant was collected and 10 µl lysate was directly [or in appropriate dilution with 40 mM Hepes buffer (pH 7.0)] used for the enzyme activity assay. To determine the K_m value the substrate concentration was varied. Ten µl of different arginine concentrations [diluting 100 mM arginine stock solution with 40 mM Hepes buffer (pH 7.0)] were applied to obtain final concentrations ranging from 0-15 mM in the assay. As negative control 10 µl lysate was replaced by 40 mM Hepes buffer (pH 7.0) for each arginine concentration. To calculate the correct turnover, the initial citrulline concentration in the

lysates was detect. Therefore, arginine was replaced by 40 mM Hepes buffer (pH 7.0) in the reaction mixture. The computation of the K_m value was carried out with GraphPAD Prism5.01 (GraphPAD Software, Inc.). For determination of the specific ADI activity expressed as units (U) per trophozoites in *G. duodenalis* lysates, it was proceeded as described by using only 20 mM arginine as substrate.

3.2.2 SDS gel electrophoresis

For SDS-PAGE (Laemmli , 1970) 5 x SDS reducing loading buffer was mixed with samples and heated at 95°C for 5-10 min to completely disrupt secondary and tertiary structures and to inactivate potential proteases. To investigate the protein expression after induction of various transformed *E. coli* DH5αZ1 strains, bacterial pellet was directly resuspended in 3 x SDS reducing loading buffer and was heated at 95°C for 5-10 min. For determination of the protein concentration within these samples, 3 x SDS reducing loading buffer was prepared without bromophenol blue.

Samples were then loaded on 10% SDS gels or commercial 4-20% Precise™ protein gels (Thermo Scientific) and SDS gel electrophoresis was performed in a vertical electrophoresis chamber according to manufacturer's instructions (Bio-Rad). SDS-PAGE was carried out in SDS running buffer at 10 mA for stacking and at 25 mA for separation. Commercial gels were run in Tris-Hepes-SDS running buffer at 100 mA. As molecular weight standard PageRuler™ Prestained Protein Ladder (Thermo Scientific) was used. Gels were either used for Western blot analysis or for Coomassie staining (Sambrook et al., 1989). Proteins were visualized by staining of gels with Coomassie staining solution for 2-4 h. Destaining was performed overnight at RT under agitation.

3.2.3 Western blot analysis

After separation by SDS-PAGE proteins were transferred to nitrocellulose membranes (Towbin et al., 1992). Therefore, gels were equilibrated for 15 min and nitrocellulose membranes (pore size: 0.45 µM) for 5 min in Towbin transfer buffer. Proteins were transferred onto the membrane at 1.2 mA/cm^2 membrane by constant current regulated by Power PAC3000 for 45 min in a Semi-Dry electro blotter. After blotting, the membrane was

washed twice in PBS and incubated for 1 h at RT or overnight at 4°C in blocking solution (PBS plus 5% milk powder) to saturate nonspecific protein binding sites. The membrane was incubated with specific primary antibody (2.3), diluted to working concentrations in blocking solution, for 2 h at RT or overnight at 4°C. The membrane was washed thrice for 10 min in PBS-T. Bound antibodies were detected with appropriate enzyme-conjugated second antibody diluted to working concentrations in blocking solution. The membrane was incubated for 2 h at RT and was then washed three times for 10 min in PBS-T. To detect (phosphorylated) proteins involved in the mammalian target of rapamycin (mTOR)-signaling pathway, a total of 50 µg protein was separated by SDS-PAGE and Western blot analysis were performed as described except that membranes were blocked with 5% milk powder-0.1% Tween20-TBS, washed with TBS-T and antibodies were diluted in 5% BSA-0.1% Tween20-TBS. TBS was preferred to use because anti-phosphate antibodies can interfere with the phosphate groups in PBS. Protein detection was carried out either with the BM Chemiluminescence Western blot Kit (Roche) or ECL™ Plus Western Blotting Detection reagent (GE Healthcare). In presence of hydrogen peroxide (H_2O_2) the horseradish peroxidase-labeled secondary antibody catalyzes the oxidation of luminol (BM kit) or Lumigen PS-3 Acridan (ECL™ Plus kit). As a result, an activated intermediate reaction product is formed which decays to the ground state by emitting light. Thereby, oxidation of the Lumigen substrate produces a more intense light emission of longer duration. Both chemiluminescence signals were visualized on autoradiography films (Kodak, Stuttgart, G; GE Healthcare). Quantification of Western blot signals was performed with ImageJ 1.42q software (NIH, USA).

3.2.4 Protein expression

To verify ADI expression, pre-cultures of various transformed *E. coli* strains were used as inoculum for 25 ml LB medium with the appropriate antibiotics. At an OD_{600} between 1.4-1.6, bacteria were induced (for 20 min) or not with 200 ng/ml anhydrotetracycline (AHT) and further incubated. One ml bacterial culture was collected and centrifuged for 5 min at 12000 x *g*. Pellet was stored at -80°C.

E. coli DH5αZ1 strains transformed with the expression vectors pASG-IBA35+ADI(AssA), pASG-IBA35+ADI_{C424A}(AssA), pASG-IBA35+ADI(AssB) or pASG-IBA35+ADI(AssE) were used as inoculum for 5 ml LB liquid cultures supplemented with 100 µg/ml ampicillin and 50 µg/ml spectinomycin. After cultivation overnight at 37°C and 180 rpm, 4 ml pre-

culture were used to inoculate 4 l LB medium supplemented with the same antibiotics. Bacteria were grown at 37°C, 180 rpm until an OD_{600} of 1.5-1.8 was reached. For purification of ADI of assemblage B and E, bacteria were induced with 200 ng/ml AHT. Bacterial cells were harvested by centrifugation (8200 x *g*, 10 min, 4°C) and then washed twice in ice-cold PBS. Until protein purification, the pellets were stored at -80°C.

3.2.5 Purification of recombinant proteins

To purify mutated or wild-type enzyme, frozen pellets were thawed and each was resuspended in 25 ml of buffer A plus a half tablet complete EDTA-free protease inhibitor cocktail. Bacterial cells were disrupted with a high-pressure homogenizer. After centrifugation (15000 x *g*, 30 min, 4°C), the supernatants were passed through a 0.45-µm-pore-size filter and loaded onto a HisTrap^{TM}FF column pre-equilibrated with buffer A on an ÄktaFPLC system. Purification was carried out in two steps: first, unbound proteins were washed off with 7% buffer B (equal to ~ 70 mM imidazole), second, proteins were eluted in 20% buffer B (equal to ~ 200 mM imidazole). After affinity chromatography imidazole was removed by desalting with a PD-10 column, and residual LPS was removed with an EndoTrap® kit according to the manufacturer's manuals (Hyglos, Bernried am Starnberger See, G). Recombinant proteins in PBS were concentrated with a Vivaspin concentrator (5-kDa PES membrane). The purified enzymes were stored in aliquots at -70°C.

3.3 Cell biological methods

3.3.1 Cultivation of parasites

G. duodenalis strain WB-C6 as well as the different patient isolate strain trophozoites were propagated in *Giardia* growth medium (modified TYI-S-33 medium; Keister, 1983) at 37°C under anaerobic conditions in flat-sided culture tubes. Twice a week, confluent grown cultures were placed on ice for 30 min for detachment of trophozoites and split 1:100 or 1:1000 with fresh *Giardia* growth medium.

3.3.2 Cryopreservation of parasites

Giardia culture with 0.5-1.0 x 10^7 trophozoites was centrifuged (900 x *g*, 4°C, 5 min), supernatant discarded and pellet resuspended in 1 ml *Giardia* growth medium supplemented with 10% DMSO. Trophozoites were transferred into a cryo tube that was slowly frozen within a freezing container to -70°C. For long term storage cryo tubes were placed in liquid nitrogen. Frozen aliquots were thawed and transferred into 10 ml pre-warmed *Giardia* growth medium. After centrifugation (900 x *g*, 5 min, 4°C), pellet was resuspended in 10 ml *Giardia* growth medium and transferred into a flat-sided culture tube.

3.3.3 Cultivation of eukaryotic cell line

Caco-2 cells were cultivated under 5% CO_2 at 37°C in T-25 (25 cm^2) culture flask until a confluence of 50-80% was reached. For subcultivation, cell layer was rinsed with PBS and incubated with 2 ml 0.05% trypsin-EDTA solution twice a week. After detachment 6 ml Caco-2 growth medium (MEM20) was added and cells were split 1:6 with 6 ml fresh Caco-2 growth medium (MEM20). For cell culture experiments, 100-300 µl of the Caco-2 cell suspension was seeded into 12-well tissue culture plates containing 1.5 ml Caco-2 growth medium (MEM20) to obtain a confluent cell layer with 8 x 10^5 cells/well within 3-5 days. The cells Caco-2 growth medium (MEM20) m was renewed once a week. For cell staining 12-well tissue culture plates were additionally equipped with cover glasses.

3.3.4 Cryopreservation of Caco-2

For long term storage approximately 2.0 x 10^6 Caco-2 cells were harvested, centrifuged (900 x *g*, 10 min, RT) and resuspended in 1 ml freezing medium (70% Caco-2 growth medium (MEM20), 20% FCS, 10% DMSO). Cell suspension was then transferred into a cryo tube that was slowly frozen within a freezing container to -70°C. For long term storage cryo tubes were placed in liquid nitrogen.
Cells were thawed at 37°C and transferred into 10 ml Caco-2 growth medium (MEM20). Cell were centrifuged (900 x *g*, 10 min, RT), supernatant discarded and pellet used as inoculum for 6 ml Caco-2 growth medium (MEM20) in a T-25 (25 cm^2) flask.

3.3.5 Generation of human moDC

The first step in the generation of human moDC was the isolation of peripheral blood mononuclear cells (PBMC) from buffy coats of healthy volunteers (German Red Cross, Berlin, G) by density gradient centrifugation. Therefore, two 50 ml-falcon tubes containing 10 ml Ficoll were overlaid with the entire buffy coat (each with 35 ml) and were centrifuged (20 min, 830 x *g*, RT, without bracket). The resulting interphases were collected separately, diluted in a ratio 1:4 in PBS and centrifuged at 4°C for 10 min at 350 x *g*. The supernatant was discarded and the washing step repeated twice. Both pellets were resuspended, each in 20 ml MACS buffer, combined and PBMC were counted. Afterwards, cells were centrifuged and washed once in MACS buffer. Monocytes were enriched by magnetic-activated cell sorting (MACS) with CD14 MicroBeads according to the manufacturer's manual (Miltenyi Biotec, Bergisch Gladbach, G). After separation CD14-positive cells were collected in DC growth medium (R10FCS), centrifuged (350 x *g*, 10 min, 4°C) and again washed in the same medium. CD14-positive cells were resuspended in 3-4 ml DC growth medium (R10FCS) and counted. To quantify enrichment, an aliquot of cells was taken and analyzed in flow cytometry. To generate moDC, 3.0×10^6 monocytes/well were seeded into 6-well tissue culture plates. Wells contained 3 ml DC growth medium (R10FCS) supplemented with 1000 U/ml human rGM-CSF and 10 ng/ml human rIL-4. After 6 days, immature DC were harvested, centrifuged (350 x *g*, 10 min, 4°C) and washed depending on the experiment either once in DC growth medium (R10FCS) or twice in arg-free RPMI. Afterwards, cell pellet was resuspended in 3 ml DC growth medium with (R10FCS) or without arginine (-ArgR10FCS) and moDC were counted. Cell population was characterized by analyzing an aliquot by flow cytometry.

3.3.6 Treatment of human moDC

Immature DC were seeded into a 12-well tissue culture plate at 5×10^5/ml and cultured at 37°C either in DC growth medium (R10FCS) or in arginine-free DC growth medium (-ArgR10FCS) supplemented or not, alone or combined with 2 mM or 0.2 mM arginine, citrulline, ammonium chloride, urea or ornithine. Cells were exposed or not to different concentrations of recombinant ADI or $ADI_{C424A,}$ and 1 µg LPS/ml or 10 ng LPS/ml was added at the same time to trigger DC maturation. Cell culture supernatants were collected

after 24 h. An aliquot for detection of formed citrulline was taken and the remaining supernatant was frozen at -70°C until cytokine determination. DC were harvested for flow cytometry analysis.

To investigate the impact of arginine turnover by ADI on the mTOR signaling pathway, 1 x 10^6 immature DC/well were seeded into a 12-well tissue culture plate in 1 ml arginine-free DC growth medium (-ArgR10FCS) containing 1000 U/ml human rGM-CSF and 10 ng/ml human rIL-4 and further supplemented or not with 2 mM arginine, citrulline and/or ammonium chloride. After 30 min of resting, cells were treated with 2 µM rapamycin, recombinant ADI, or ADI_{C424A} and further cultured at 37°C for 90 min. The immature cells were then exposed to 1 µg/ml LPS. For flow cytometry analysis, cells were harvested after 24 h. In parallel, for citrulline detection and Western blot analysis, cells were harvested after 30 min by centrifugation (300 x *g*, 10 min, 4°C). Supernatants were collected and cell pellets were washed twice in ice-cold PBS before resuspension in 80 µl lysis buffer. After incubation for 30 min on ice, cell debris was removed by centrifugation (5 min, 14000 x *g*, 4°C) and lysates were stored at -70°C. For Western blot analysis, lysates were thawed and protein concentration was determined.

3.3.7 Detection of ADI release

To verify that ADI is released by *Giardia* trophozoites after contact with Caco-2 cells, different patient isolates as well as the laboratory strain WB-C6 were incubated with these cells. Parasites were washed with PBS, incubated on ice for 30 min and harvested by centrifugation (900 x *g*, 5 min, 4°C). After a further washing step in PBS trophozoites were resuspended in Caco-2 growth medium without FCS and counted. Differentiated Caco-2 cells that were washed with PBS were treated with the parasites (MOI of 3). After 45 min cell-culture supernatants were harvested, centrifuged (10 min, 930 x *g*, 4°C) and 450 µl cell-free supernatants were mixed with 2 volumes 100% acetone. After incubation overnight at -20°C the precipitated proteins were harvested by centrifugation (12000 x *g*, 20 min, 4°C). Supernatant was discarded and pellet dried. Proteins were resuspended in 20 µl 1 x SDS reducing loading buffer, heated for 5 min at 96°C and separated by SDS-PAGE for Western blot analysis.

3.3.8 Eukaryotic cell staining

To investigate cell morphology, differentiated (17-21 days post-confluence) Caco-2 cells grown on cover glasses were fixed with fixation solution for 30 min at 37°C. Fixation solution was exchanged with PBS. After incubation for 1 h at RT, PBS was replaced by fresh PBS and cells were washed thrice for 5 min. Differentiated Caco-2 cells were then stained with the DiffQuik® staining set (Medion Diagnostics, Gräfelfing, G). In a first step cells were again fixed for 30 sec on cover slips by incubation in a solution containing methanol. Afterwards, cells were colorized for 20 sec in a solution containing eosin, for 15 sec in a solution containing methylene blue and were then rinsed in PBS. Stained cover slips were fixed on microscope slides with Entellan® and analyzed under the microscope.

To verify formation of tight junction between Caco-2 cells, cover slips were prepared for staining procedure as described above. After the last washing step with PBS, cells were blocked for 1 h in blocking solution. Blocking solution was then removed and 2.5 µg/ml polyclonal rabbit anti-ZO-1 antibody (Life technologies) (diluted 1:100 in blocking solution) was added. After 1 h, cells were washed thrice with PBS for 5 min and 6.5 µg/ml goat anti-rabbit-Alexa Fluor®488 (Life technologies) secondary antibody (diluted 1:300 in blocking solution) was added for 30 min. After three washing steps with PBS for 5 min cells were further stained with bisbenzimide, a fluorescent stain for DNA. Therefore, bisbenzimide solution was added for 15 min and was then removed by three washing steps in PBS. Stained cover slips were fixed on microscope slides with Mowiol 4-88 and analyzed under the fluorescence microscope.

3.4 Immunological methods

3.4.1 Flow cytometry

In flow cytometry, cells in a fluid pass a laser beam within a flow cytometer where light scattering and fluorescent light can be measured. The principle of the technique is based on the nature of cells to scatter light differently. Thereby, the scattering of light correlates with size and complexity of the cell. These properties are quantified due to two parameters: the side scatter (SSC) which serves as an indicator for the granularity and the complexity of a cell (e.g. size and structure of the nucleus, amount of vesicles) and the forward scatter (FSC)

which is proportional to the volume of the cell. Fluorescent signals are only detected on cells that were stained before with fluorescent-labeled antibodies raised against special surface proteins. Due to these both parameters, the fluorescence signal and the light scattering, special cell types of a cell population can be distinguished.

To confirm the isolation and enrichment of CD14-positive cells, the generation of moDC and the change in cell surface molecules of treated moDC, flow cytometry was performed. After MACS, approximately 150000 CD14-positive cells/well were seeded in a 96-well plate. As negative control, part of the cells remained unstained to determine auto-fluorescence, others were stained with mouse mAb anti-human CD3, CD14 or CD20 as well as the respective iso-type (IgG1) control for 45 min on ice or overnight at 4°C according to the manufacturer's information (Immunotools). Cells were then washed twice with 150 µl wash buffer by centrifugation (670 x *g*, 2 min, 4°C). Pellets were resuspended in 50 µl wash buffer and cells were stained, except the negative control, with polyclonal goat anti-mouse FITC-conjugated secondary antibody (Immunotools). After an incubation time of 30 min on ice in the dark, the washing procedure was repeated as described above. Subsequently, cell pellets were resuspended in 100 µl wash buffer and the same volume of fixation buffer was added. The samples were transferred into tubes and data were acquired on an LSR II flow cytometer and analyzed by FlowJo software (Tree Star, Inc.). Dead cells were excluded by gating according to FSC/SSC characteristics.

To measure cell surface markers on moDC directly after their generation or after their treatment, the same staining procedure was followed except that the following mouse conjugated mAb were used: anti-human FITC-CD14 (Immunotools), PerCP-CD86 (Abcam), PE-HLA-DR (Immunotools), AlexaFluor488-CD83 (Biolegend, San Diego, USA), Dyomics647-CD25 (Immunotools) or iso-type control Biotin-IgG1(Immunotools) with the relevant streptavidin-conjugates PE, PERCP, FITC (eBioscience) and Alexa488 (Life technologies).

3.4.2 ELISA for cytokine detection

The enzyme-linked immunosorbent assay (ELISA) is an immunoassay used to determine concentrations of biomolecules (e.g. peptides, cytokines and hormones) in liquids. The principle is based on an antibody-antigen reaction that allows quantification. The substrate conversion by an enzyme-coupled marker causes a measurable signal. Thereby, intensity of

the signal is direct proportional to the amount of investigated biomolecule within the liquid (Engvall and Perlmann, 1971).

To determine cytokine concentrations in cell-culture supernatants, Sandwich-ELISA was performed. Therefore, frozen samples from treatment of moDC were thawed and used for human TNF-α, IL-10, IL-12p70 (eBioscience), IL-23 (U-CyTech, Utrecht, NL) or IL-12p40 ELISA (Biolegend) following manufacturer's protocols. First, the coating antibody was immobilized on the solid material of a Maxisorp 96-well ELISA plate through hydrophobic interactions. After washing with PBS-T, free protein binding sites were blocked to avoid unspecific binding of enzyme-linked antibodies or antigen molecules. Further washing steps followed. Supernatants for cytokine content determination from cell culture experiments as well as the respective cytokine standards, included in the ELISA kit, were added. If specific cytokines were present, they were bound by the coating antibody. Then, a biotin-conjugated detection antibody was added which had also a binding site different from the coating antibody for the specific cytokine to form an antibody-antigen-antibody complex. After further washing steps, the complex formation was detected by addition of a horseradish peroxidase being linked to (strept)avidin which bound the conjugated biotin of the detection antibody. Subsequently, TMB, a chromogenic substrate that yields a blue color when oxidized with H_2O_2 to its radical form by horseradish peroxidase (HRP), was added. The enzyme was denatured and inactivated by addition of 100 µl 2 M H_2SO_4 to stop substrate conversion and color development. Additionally, due to protonation of the radical, TMB turned yellow and was read photometrically at 450 nm in a plate reader.

3.4.3 Indirect ELISA for detection of PAD activity

Ni-NTA HisSorb Strips coated with Ni-NTA moieties enabled screening of His_6-tagged biomolecules. Here, 2.3 µmol H_6-CRGKA (VSP-tail) (according to Touz et al., 2008) was immobilized for 2 h at RT in 200 µl PBS-1% BSA under agitation. Afterwards, strips were washed thrice with PBS-T and finally twice with PBS. To each well 200 µl deamination buffer was added. Wells were treated with 200 mU (15 µg) recombinant ADI or similar amounts of recombinant ADI_{C424A}, 3 mU ADI of *G. duodenalis* lysate, as negative control PBS and as positive control 25 mU human PAD (MQR, Nijmegen, NL) were added. To verify PAD activity strips were incubated for 16 h at 50°C. Afterwards, wells were washed four times with PBS-T and 200 µl first antibody (diluted 1:1000 in PBS-1% BSA), a mouse

anti-deiminated arginine antibody included in the Antibody Based Assay for PAD activity (ABAP) kit (MQR), was added. Strips were incubated at RT for 2 h under agitation. Wells were washed four times with PBS-T and a secondary HRP-labelled anti-mouse Ig antibody, that was also included in the ABAP kit (MQR), was diluted 1:2000 in PBS-1% BSA and 200 µl were added. Strips were incubated again for 2h at RT under agitation. Afterwards, wells were washed four times with PBS-T and 200 µl TMB substrate was added. Reaction was stopped with 50 µl 2 M H_2SO_4. Finally, OD was measured at 450 nm.

3.4.4 Stimulation of IEC and determination of NO production

Undifferentiated Caco-2 cells were seeded for differentiation into 12-well tissue culture plates. Seventeen to twenty-one days post-confluence, 8 x 10^5 cells were washed with pre-warmed PBS and finally stimulated with 500 µl MEM20 Caco-2 growth medium supplement with a cytokine mixture containing 25 ng IL1-β/well, 50 ng TNF-α/well and 50 ng IFN-γ/well or with 500 µl Caco-2 growth medium alone. To measure NO formation over time, cell-free supernatants were collected after different time point's and stored at -70°C until further processing. Total nitrite concentration was then determined using the Nitric Oxide Colorimetric Assay Kit according to the manufacturer's manual (BioVision, Milpitas, USA). The kit was used because formed NO is unstable and oxidizes to nitrite (NO_2^-) that is further oxidized to nitrate (NO_3^-). First, in a two-step process, NO_3^- is reduced NO_2^- by a nitrate reductase. In the second step, the nitrite is then converted into a deep purple azo compound that can be measured photometrically at 540 nm. Thereby, the amount of the azochromophore reflects the NO amount within samples.

To determine the NO formation by Caco-2 cells upon contact with trophozoites, differentiated Caco-2 cells were washed with PBS. Trophozoites cultures of different patient isolates as well as the laboratory strain WB-C6 were washed with PBS, incubated on ice for 30 min and harvested by centrifugation (900 x *g*, 5 min, 4°C). After a further washing step in PBS, trophozoites were resuspended either in Caco-2 growth medium or in Caco-2 growth medium supplemented with a cytokine mixture (25 ng IL1-β/well, 50 ng TNF-α/well, 50 ng IFN-γ/well). After counting of trophozoites, 8 x 10^5 Caco-2 cells were infected with 2.7 x 10^5 parasites (MOI of 0.33) or 24 x 10^5 parasites (MOI of 3) within 500 µl of appropriate medium. After 28 h incubation, supernatants were collected and total NO_2^- was determined.

3.5 Descriptive statistics

Data are given as means ± standard deviations (SDs). Statistical significance was assessed by paired (two-tailed) *t* test. All analyses were performed with GraphPad Prism 5 software (GraphPad Software, Inc., USA) with a statistical significance level of $P < 0.05$.

4 Results

The ADI is known to be released by *G. duodenalis* upon contact with IEC *in vitro* and *in vivo* (Ringqvist et al., 2008). To address the question whether *G. duodenalis* ADI is a potential virulence factor, its enzyme characteristics and its influence on human host cells were investigated. The following experiments had focus on both: the native form occurring naturally in *G. duodenalis* lysates and the recombinant, purified form that was obtained after expression in *E. coli*.

4.1 Generation of recombinant *G. duodenalis* ADI and its catalytically inactive mutant

4.1.1 Expression of recombinant proteins

Both recombinant proteins, ADI and ADI_{C424A}, were generated with the purchasable StarGate® cloning system. Although confidential, as underlying strategy the 'Golden Gate' cloning technology described by Engler et al. (2008) is presumed. The system allows a rapid transfer of any GOI from an entry vector into an expression vector by using Type II restriction endonucleases. For this study, in a first one-tube reaction the ADI-coding sequence, that was amplified from genomic *G. duodenalis* WB-C6 DNA by PCR, was inserted into an entry vector. In a second one-tube reaction, the formed donor vector was used together with the provided acceptor vector pASG-IBA35 for the generation of the destination vector pASG-IBA35+ADI that enables the expression of the recombinant protein with an N-terminal His_6-tag in *E. coli* (Fig. 4).

A

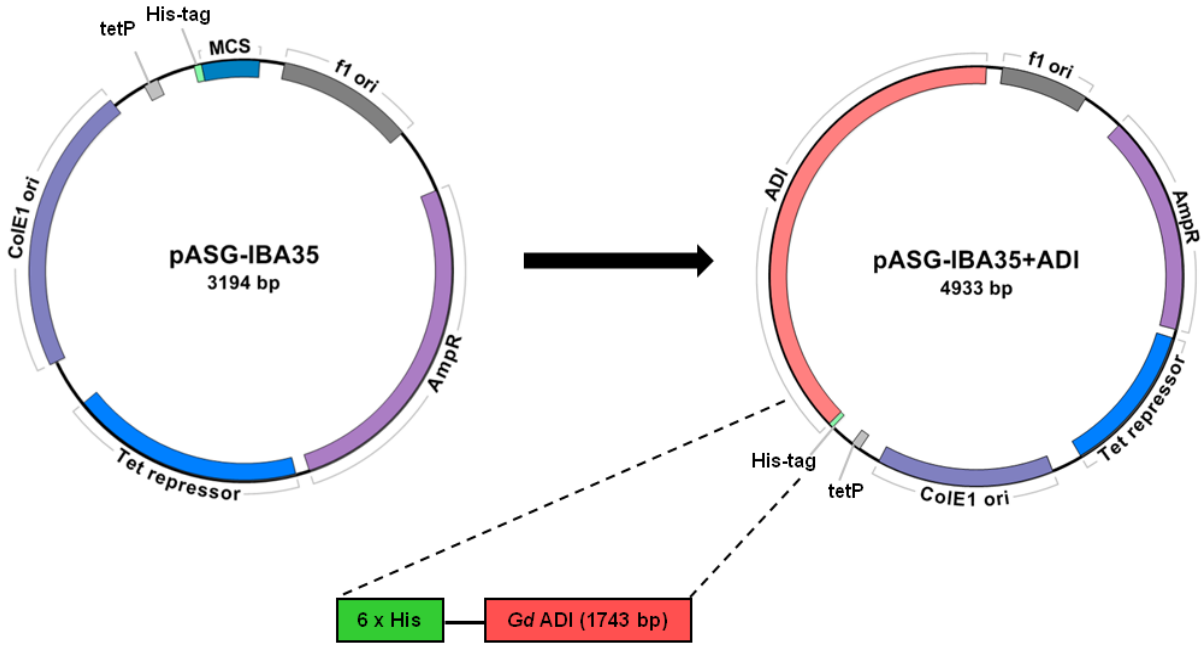

B

C

```
1          10         20         30         40         50         60         70         80         90        100
TTTTTGTTGA CACTCTATCA TTGATAGAGT TATTTTACCA CTCCCTATCA GTGATAGAGA AAAGTGAAAT GAATAGTTCG ACAAAAATCT AGAAATAATT
                                                                                                  XbaI (89)
           tetP
         110        120        130        140        150        160        170        180        190        200
TTGTTTAACT TTAAGAAGGA GATATACAAA TGGCTAGCCA TCACCATCAC CATCACTCCG GAATGACTGA CTTCTCCAAG GATAAAGAGA AGCTTGCACA
                                 M  A  S  H  H  H  H  H  H  S  G  M  T  D  F  S  K  D  K  E  K  L  A  Q
                                          His-Tag                                                 HindIII (191)
                                                                                                  ADI
         210        220        230        240        250        260        270        280        290        300
GGCAACCCAG GGGGGAGAGA ACGAGCGCGC AGAGATAGTC GTCGTGCACC TCCCTCAGGG AACGTCGTTC TTGACCTCTC TCAACCCCGA GGGGAACTTG
  A  T  Q  G  G  E  N  E  R  A  E  I  V  V  V  H  L  P  Q  G  T  S  F  L  T  S  L  N  P  E  G  N  L
ADI
         310        320        330        340        350        360        370        380        390        400
                    SacI (330)
CTTGAGGAGC CCATATGCCC CGACGAGCTC AGACGCGATC ACGAGGGCTT CCAGGCCGTT CTCAAGGAGA AGGGGTGCCG GGTTTATATG CCGTACGACG
L  E  E  P  I  C  P  D  E  L  R  R  D  H  E  G  F  Q  A  V  L  K  E  K  G  C  R  V  Y  M  P  Y  D
ADI
         410        420        430        440        450        460        470        480        490        500
                                                                  SacI (474)
TCCTCTCCGA GGCCTCTCCG GCTGAGAGGG AGGTCCTCAT GGATCAAGCA ATGGCCTCGC TGAAGTACGA GCTCCATGCC ACAGGTGCAC GCATCACCCC
V  L  S  E  A  S  P  A  E  R  E  V  L  M  D  Q  A  M  A  S  L  K  Y  E  L  H  A  T  G  A  R  I  T  P
ADI
         510        520        530        540        550        560        570        580        590        600
CAAGATGAAG TACTGTGTTT CGGACGAGTA CAAACGCAAG GTCCTTTCGG CCCTGTCGAC CAGAAACCTT GTAGACGTGA TTTTATCCGA GCCCGTCATC
K  M  K  Y  C  V  S  D  E  Y  K  R  K  V  L  S  A  L  S  T  R  N  L  V  D  V  I  L  S  E  P  V  I
ADI
         610        620        630        640        650        660        670        680        690        700
CACCTAGCTC CTGGTGTCCG CAACACGGCT CTCGTTACCA ACTCTGTGGA GATCCACGAT AGCAATAACA TGGTCTTTAT GCGTGACCAG CAGATAACCA
H  L  A  P  G  V  R  N  T  A  L  V  T  N  S  V  E  I  H  D  S  N  N  M  V  F  M  R  D  Q  Q  I  T
ADI
         710        720        730        740        750        760        770        780        790        800
CCCGGCGCGG AATAGTCATG GGCCAGTTTC AGGCGCCGCA GAGGAGGCGC GAGCAGGTCC TGGCCCTGAT CTTCTGGAAG CGCCTCGGGG CCCGCGTCGT
T  R  R  G  I  V  M  G  Q  F  Q  A  P  Q  R  R  R  E  Q  V  L  A  L  I  F  W  K  R  L  G  A  R  V  V
ADI
         810        820        830        840        850        860        870        880        890        900
GGGAGACTGC CGTGAGGGAG GACCGCACTG CATGCTCGAG GGTGGGGACT TCGTGCCTGT GTCGCCCGGG CTGGCGATGA TGGGTGTGGG CTTGCGCAGC
G  D  C  R  E  G  G  P  H  C  M  L  E  G  G  D  F  V  P  V  S  P  G  L  A  M  M  G  V  G  L  R  S
ADI
         910        920        930        940        950        960        970        980        990      1,000
ACCTATGTCG GAGCGCAGTA TCTTATGTCT AAAGATCTCC TCGGGACCCG GCGGTTTGCT GTCGTCAAGG ACTGCTTTGA TCAGCACCAG GACCGTATGC
T  Y  V  G  A  Q  Y  L  M  S  K  D  L  L  G  T  R  R  F  A  V  V  K  D  C  F  D  Q  H  Q  D  R  M
ADI
```

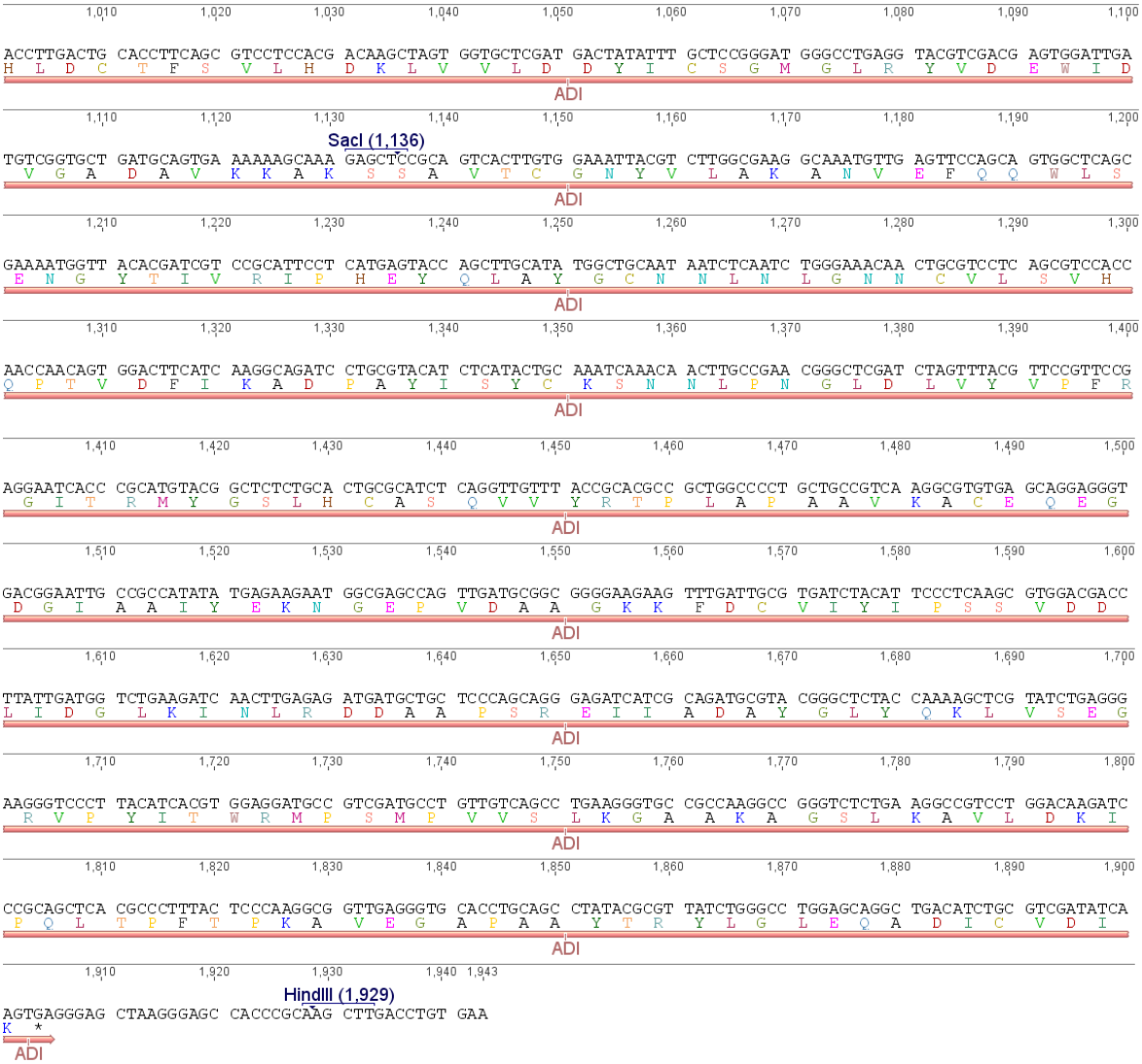

Figure 4: Cloning of *G. duodenalis arcA* gene into the expression vector pASG-IBA35
Shown is a schematic representation of the acceptor vector pASG-IBA35 before (A) and after insertion of the ADI coding sequence (B). A section of the plasmid map from the expression vector pASG-IBA35+ADI is illustrated in C. In the gene expression cassette tetP, His_6-tag, ADI and restriction sites are highlighted. tetP (tet promoter); MCS (multiple cloning site); AmpR (ampicillin resistance gene); f1 and ColE1 ori (origin).

The destination vector pASG-IBA35+ADI carried the inducible promoter/operator region of the *tetA* resistance gene (Tet-on system) to allow the regulated expression of the recombinant protein. The constitutive expression of the *tet* repressor gene, that was also encoded on the expression plasmid, ensured the repression of the promoter by binding on the operator in absence of the inducer. In contrast, addition of AHT fully induced the *tet* promoter and allowed protein expression.

Further experiments required the generation of a control plasmid. The fusion protein of the expression vector pASG-IBA35+ADI was removed by *Xba*I/*Hind*III restriction digest, the

resulting overhangs were filled with Klenow fragment and the plasmid was ligated. By removal of the inserted ADI coding sequence, the His_6-tag was deleted. The resulting plasmid was termed pASG-IBA35 (w/o His_6-tag).

Furthermore, a catalytically inactive mutant of the recombinant ADI was generated. It was previously described that the ADI of several other organisms uses an active-site cysteine for hydrolysis of arginine (Lu et al., 2004; Galkin et al., 2005; Li et al., 2009). Thus, the cysteine at amino acid sequence position 424 was exchanged to alanine by site-directed mutagenesis using the destination vector pASG-IBA35+ADI as template.

After transformation into *E. coli*, both destination vectors pASG-IBA35+ADI_{C424A} and pASG-IBA35+ADI were verified by restrictions digest and additionally by sequencing.

The aim of protein expression is to obtain an intact product with high purity in high yield. The latter can be influenced by the biological properties of the expression strain as well as the protein characteristics itself. To sufficiently generate recombinant ADI and ADI_{C424A}, different *E. coli* strains were tested for their ability to express the proteins. The genotypes of the used bacterial strains are summarized in Tab. 6. Exemplarily, *E. coli* strains transformed with the destination vectors pASG-IBA35+ADI and, as control, with pASG-IBA35 (w/o His_6-tag) were grown to OD_{600} of ~ 1.5 and were induced with AHT for 20 min. One ml of each bacterial culture was taken before and after induction and compared in Western blot analysis with each other. Obviously, the induction of *G. duodenalis* ADI expression in all *E. coli* strains led to occurrence of degradation products. The rate of degradation compared to ADI expression differed amongst the strains and is summarized in Tab. 14. The AHT-induced *E. coli* DH5αZ1 strain revealed the highest ADI expression with no or minimal degradation.

Table 14: Summary of different *E. coli* strains tested for *G. duodenalis* ADI expression
Different *E. coli* strains entailed varied rates of ADI degradation after induction of gene expression. To quantify degradation rate for each strain, the anti-His signal obtained for ADI was related to the overall anti-His signals obtained in Western blot. Degradation grade: + low (> 0.55); ++ middle (0.45-0.55); +++ high (< 0.45).

***E. coli* strain**	**Degree of degradation**
DH5αZ1	+
ER2508	+++
JWK clpX-1	+++
XL1-Blue	++

Interestingly, ADI was expressed by DH5αZ1 cells that were grown under noninduced conditions (Fig. 5), i.e. AHT was absent and in consequence the *tet* promoter blocked. Additionally, induction with AHT did not lead to remarkably increased amounts of produced recombinant protein in comparison to noninduced *E. coli* cells. These effects seemed to be independent from the activity of the ADI because same observations were made for the catalytically inactive mutant. To date, the reason for this phenomenon remained still unclear. Mistakes in the DNA sequence of the promoter, that could e.g. prevent binding of the repressor, were excluded by sequencing of the region.

It was decided to express both recombinant proteins a) under noninducing conditions to minimize the risk for degradation and therefore obtain functional proteins and b) within the DH5αZ1 strain to obtain maximum yield.

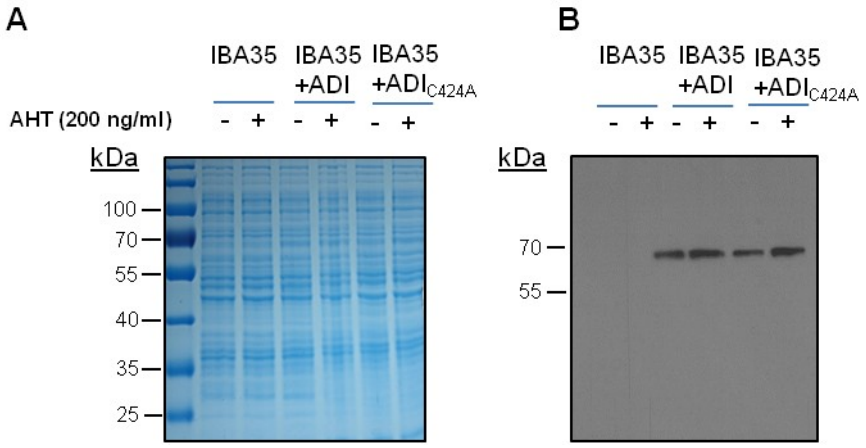

Figure 5: Induced and noninduced expression of recombinant protein

E. coli DH5αZ1 strain was transformed with expression vector pASG-IBA35+ADI, pASG-IBA35+ADI_{C424A} or the empty vector pASG-IBA35 (w/o His_6-tag) as negative control. At OD_{600} between 1.4-1.6, bacteria were either induced for 20 min with 200 ng/ml AHT (+) or not (-). Samples were taken and 40 µg cell lysate per lane were loaded for SDS-PAGE (A) and for Western blot analysis (B). Immunoblot was developed with an antibody raised against the His-tag.

4.1.2 Protein purification and characterization of recombinant proteins

Prior to purification, ADI and ADI_{C424A} were identified to be expressed as soluble proteins in the cytoplasm of *E. coli* DH5αZ1 (data not shown). Thus, it was sufficient to harvest *E. coli* culture and to directly disrupt the resuspended bacterial pellets with a High-pressure homogenizer. After centrifugation of cell debris, bacterial lysates were loaded onto columns prepacked with precharged Ni Sepharose that allowed one-step purification of the

His_6-fusion proteins with the ÄktaFPLC system. After binding of the sample, nonspecifically bound molecules were removed by washing with buffer that included 70 mM imidazole. Finally, recombinant proteins were eluted with buffer including 200 mM imidazole. To prevent influence of imidazole on ADI activity and host cells in future experiments, the substance was remove after affinity chromatography. One effective method to remove low-molecular weight compounds is dialysis. Unfortunately, most of the ADI and ADI_{C424A} protein aggregated and became insoluble during this procedure. An alternative was to use desalting columns where imidazole was removed by gel filtration. Thereby, impurities were separated and buffer exchanged to PBS. Remaining traces of LPS, that is known to be a stimulus for immune cells, were removed with EndoTrap® columns. Finally, ADI and ADI_{C424A} were concentrated with Vivaspin concentrators, aliquoted and stored at -70°C until further use.

After protein purification, both enzymes were characterized. First, success of purification procedure was verified by SDS-PAGE and Western blot. In Fig. 6, a representative analysis of a purification experiment (here shown exemplarily for ADI) is summarized.

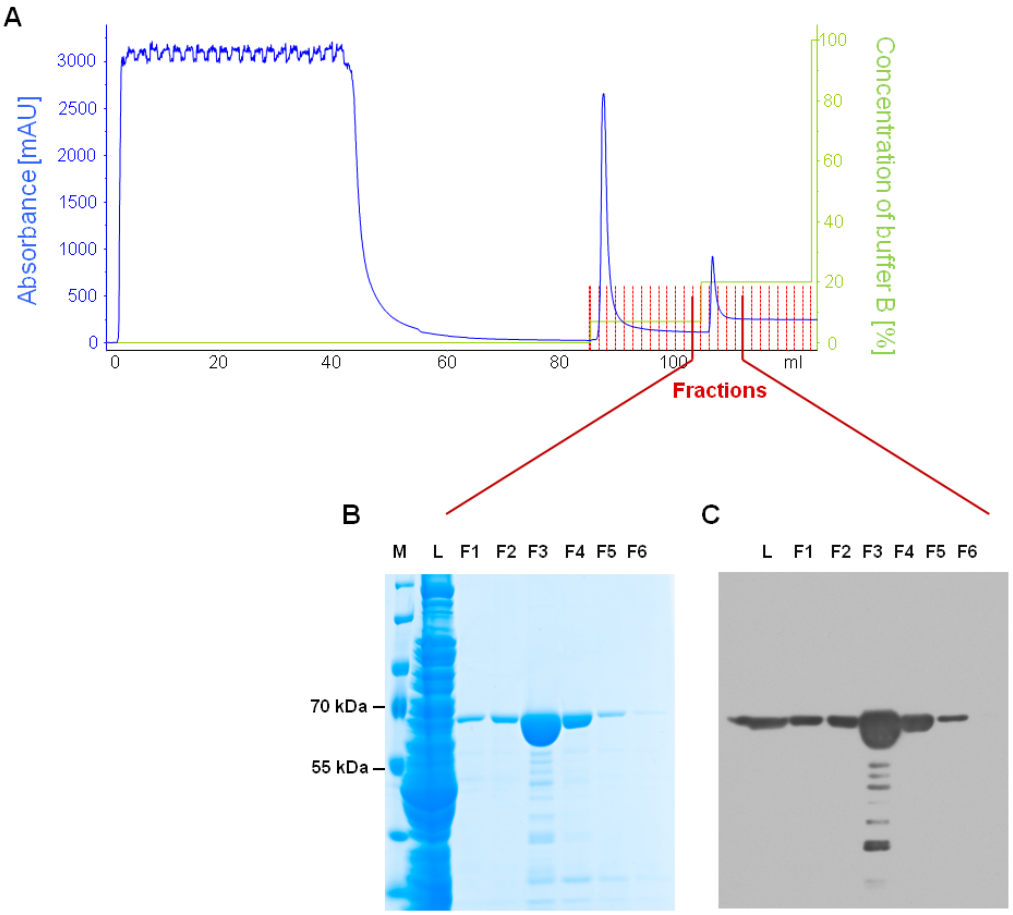

Figure 6: Purification of recombinant *G. duodenalis* ADI
(A) Shown is a representative chromatogram obtained after purification of ADI. Left y-axis reflects absorbance at 280 nm expressed in mAU. Right y-axis shows the variation in buffer B concentration (100% are equal to 1 M imidazole) that allowed a gradual purification. (B) During purification, fractions were collected and those containing the recombinant protein were analyzed in SDS-PAGE and (C) Western blot. SDS gel was stained with Coomassie and immunoblot was developed with an antibody against the His-tag. Fraction with the highest peak (F3) was used for further experiments. mAU: milli-absorbance unit; F: Fraction; M: Marker; L: Lysate.

Single fractions obtained during affinity chromatography were analyzed on SDS-PAGE (Fig. 6B) and in Western blot using an anti-His antibody (Fig. 6C) to confirm high purity and specificity of the 64 kDa recombinant protein in the main elution peak.

Second, to determine the yield of the purification process and to further characterize the recombinant enzymes, protein concentration as well as catalytic activity was measured. For determination of enzymatic activity arginine served as substrate and its conversion into citrulline was determined by a colorimetric assay. The yield of the purification procedure and the enzymatic characterization of the recombinant ADI are summarized in Tab. 15. As consequence of low expression, at least two liters of *E. coli* DH5Z1 cells carrying the plasmid pASG-IBA35+ADI were harvested to obtain recombinant protein in sufficient amounts. Activity for recombinant ADI was measured with approximately 7.7 U/ml which equals

11.6 U/mg. The specific activity of purified recombinant ADI varied between different purifications from 7 to 12 U/mg.

Recombinant ADI_{C424A} was analyzed identically. As expected, the mutated enzyme was catalytically inactive and could serve in the following experiments as negative control.

Table 15: Summary of one-step purification of recombinant *G. duodenalis* ADI

Characterization of affinity purified ADI from 2 l *E. coli* DH5αZ1 culture is shown. Protein amount was determined by BCA assay and as substrate for the enzyme activity assay arginine was used. U is defined as µmol substrate/min at 37°C in Hepes buffer.

	Protein [mg]	Volume [ml]	Volume activity [U/ml]	Total U	Specific activity [U/mg]	Enrichment (X-fold)	Yield [%]
Crude extract	218	40.0	0.5	17.8	0.08	-	100
Purified protein	1.0	1.5	7.7	11.6	11.6	145	65

The recombinant ADI was used for the generation of polyclonal antibodies. An alpaca was immunized four times (days 0, 21, 35, and 49; Preclinics, Potsdam, G) with 300 µg of purified recombinant enzyme resuspended in 100 µl PBS plus adjuvant (complete Freund's adjuvant for the first injection and incomplete Freund's adjuvant for subsequent booster injections). Pre-immune serum was collected prior to the first immunization. After the last booster injection, the antiserum was obtained. Antigenic specificity of the polyclonal antiserum was tested in Western blot analysis (Fig. 7). The anti-*G. duodenalis* ADI antiserum identified both 64 kDa recombinant proteins and revealed that both behaved similarly to the endogenous ADI parasite protein included in *G. duodenalis* lysate. Preimmune serum, used as a control, did not react with any *G. duodenalis* protein (data not shown).

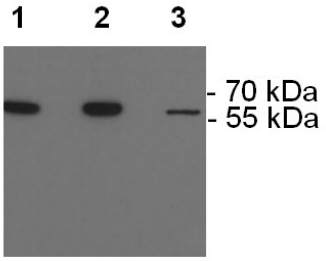

Figure 7: Western blot analysis of purified recombinant and native *G. duodenalis* ADI by polyclonal antiserum
Antigenic identification of 0.5 µg affinity-purified recombinant ADI (lane 1), 0.5 µg catalytically inactive ADI_{C424A} (lane 2) and native ADI in 2.9 µg *G. duodenalis* strain WB-C6 lysate (lane 3) by Western blotting with alpaca polyclonal antiserum raised against ADI.

4.2 Recombinant *G. duodenalis* ADI and its influence on host immune response

4.2.1 Recombinant *G. duodenalis* ADI had no PAD activity

Posttranslational modification of a protein can affect its folding and thereby can influence its function directly or indirectly. Exemplarily, such a modification is the enzymatic deimination of intrapeptidic arginine into citrulline, termed citrullination. This enzymatic reaction is catalyzed by PADs and can lead to an altered three-dimensional protein structure that in consequence result in changes of its antigenic properties. Such citrullinated proteins are not longer recognized as endogenous but instead were noticed as foreign by the human immune system. In consequence, autoantibodies are generated, an inflammatory immune response is initiated and in long term an autoimmune disease develops. One example is rheumatoid arthritis, that causes destruction of joints and adjacent tissue, where e.g. citrullinated vimentin is described to play an important role in its pathogenesis (Van Steendam et al., 2010; Sanchez-Pernaute et al., 2012; Bicker and Thompson, 2013).
In previous work, Touz et al. (2008) identified that recombinant ADI purified from *G. duodenalis* trophozoites had a PAD activity and therefore was able to deiminate arginine within the conserved CRGKA tail of VSPs. This posttranslation modification could have serious consequences for the host immune response after giardial infection. First, citrullination of free proteins by ADI could lead to the formation of noval B and T cell epitopes on host cells. Second, modification of membrane-bound receptors of immune cells that are in close surrounding to the released ADI (like DC branching between epithelial cells) could directly affect cells' immunological function.

A PAD activity-ELISA was performed to test whether the recombinant ADI purified from *E. coli* catalyzes not only the conversion of free arginine into citrulline but also deiminates intrapeptidic arginine. Therefore, same conditions and substrate described by Touz et al. (2008) were used. A synthetic peptide H_6-CRGKA was immobilized on Ni-NTA HisSorb Strips. The substrate was incubated with recombinant ADI and ADI_{C424A}, *G. duodenalis* lysate and, as positive control, with human PAD for 16 h at 50°C. The results of one experiment with three technical replicates are shown in Fig. 8.

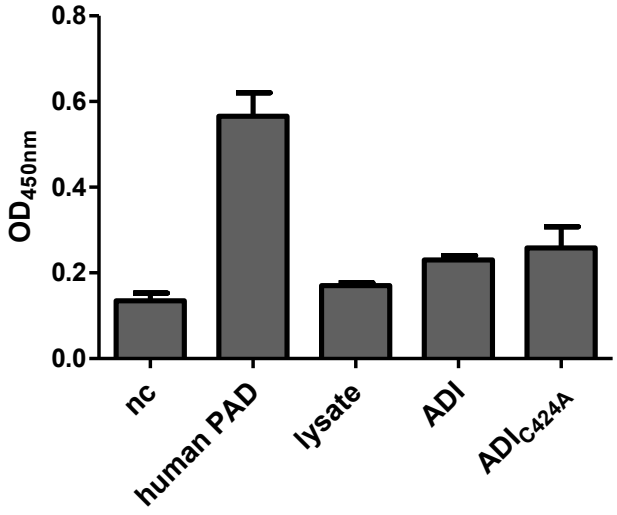

Figure 8: Investigation of *G. duodenalis* ADI for PAD activity
Recombinant ADI (200 mU) as well as native ADI (4 mU) from *G. duodenalis* WB-C6 lysates were tested for their ability to citrullinate intrapeptidic arginine in a peptide corresponding to the VSP-tail in ELISA. Recombinant human PAD (25 mU) served as positive control. Bars represent the mean ± SD from three technical replicates of one experiment. nc, negative control.

Using an antibody raised against deiminated arginine revealed only citrullination of the VSP-tail by the positive control. Although, recombinant ADI was added in excess compared to the human PAD, no citrullination was detected at all.

The catalytic activity of native ADI in parasite lysates to convert free arginine into citrulline was detected. However, the amount of ADI in this lysates was limited. Despite concentrating a large number of trophozoites, addition of native enzyme to the PAD activity-ELISA up to 25 mU, similar to the positive control, was not possible. Thus, it is not clear whether there is no PAD activity of the native ADI or if the activity is below the detection limit of the assay. In future experiments the positive control should be diluted to a level similar to the ADI

activity in the lysate. Where, if at all, native ADI had only negligible PAD activity, recombinant ADI however seemed to have none.

4.2.2 Recombinant *G. duodenalis* ADI had immunomodulatory effects on human DC

The host's innate immunity plays an important role in parasite clearance mechanisms. In giardial infection, DC as APC were identified to be critical for host defense (Kamda and Singer, 2009; Kamda et al., 2012). Due to projection of cellular extensions between epithelial cells into the lumen of the gut, DC can come into close contact to the parasite. The functional properties of these innate immune cells depend on the environment in which they are activated. Thus, it was hypothesized that ADI released by *G. duodenalis* trophozoites changes the DC surrounding milieu by consumption of arginine. If such a pathogen-mediated arginine depletion affects DC function and in consequence alters the subsequent stimulation of the adaptive immune response, e.g. the activation of T cells, is unknown so far.
The following experiments should investigate whether the phenotype of human moDC, especially regarding cell surface markers and cytokine secretion, is influenced by recombinant *G. duodenalis* ADI activity *in vitro*.

4.2.2.1 Preparation of human moDC

To model conditions in the intestine and investigate potential immunomodulatory effects of ADI activity on DC function, human moDC were prepared. Therefore, CD14-positive cells were isolated from human buffy coat by density gradient centrifugation and subsequent magnetic-activated cell sorting. Typically, cells were thereby enriched to ≥90% CD14-positive cells as determined by flow cytometry. Afterwards, these cells were differentiated with human recombinant GM-CSF and IL-4 to obtain moDC (Fig. 9). After 6 days, immature DC were harvested and the cell population was characterized by analyzing an aliquot by flow cytometry. Staining of surface markers revealed consistence with DC phenotype that means low levels of CD14 and CD86 and high levels of HLA-DR, whereas CD25 and CD83 were not expressed (data not shown).

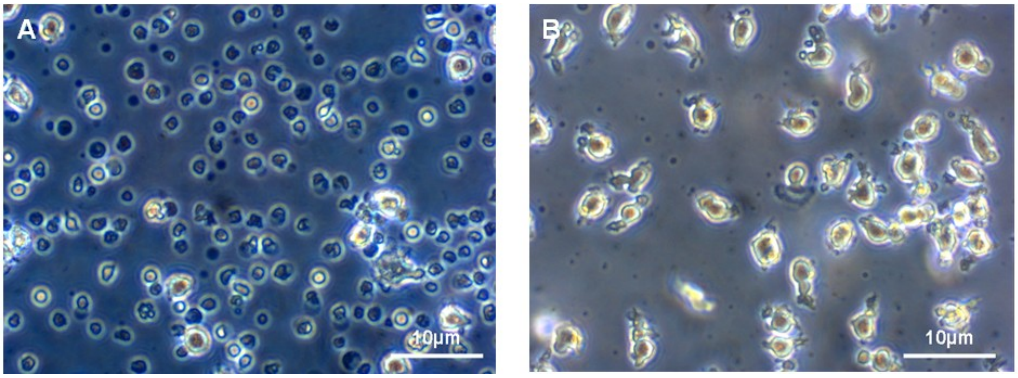

Figure 9: LM-micrograph of human moDC
(A) Nonstimulated human CD14-positive cells isolated from human buffy coat did not show DC phenotype after six days of cultivation. (B) In contrast, same cells differentiated into immature moDC in six days when treated with 1000 U/ml human rGM-CSF and 10 ng/ml human rIL-4.

4.2.2.2 Definition of experimental conditions for arginine depletion by recombinant, enzymatically active ADI during DC activation *in vitro*

The amino acid arginine is known to play important roles during immune responses. For example, arginine affects T cell function (Zea et al., 2004) and is used by NOS as substrate to generate anti-microbial NO. Depletion of arginine is known to be a strategy of pathogens to evade the host's immune defense. Thus, as part of their virulence mechanism, pathogens successfully compete with the host for arginine e.g. by enzymes like arginases (Bronte and Zanovello, 2005; Das et al., 2010).

To investigate whether *G. duodenalis* ADI as potential virulence factor changes the response of DC by arginine depletion, the effect of ADI activity on the amount of arginine that may be available to the parasite during an infection was estimated and the experimental conditions to study the consequences of ADI activity on activated moDC *in vitro* were defined. The average daily intake of arginine by humans has been estimated to be 5 g, which corresponds to 28 mmol (Böger, 2007). It has been reported that an infected person sheds up to 10^9 *G. duodenalis* organisms per day (Danciger and Lopez, 1975). The ADI activity per million trophozoites was determined to be equivalent to approx. 0.02 U by preparing lysates from the laboratory strain WB-C6 and determining the ADI activity (Tab. 16). Therefore, at least 20 U of enzyme may be produced per day of infection. One U corresponds to 1 µmol arginine metabolized per minute, hence > 28 mmol could potentially be turned over in one day. Thus, infection with *Giardia* has the potential to substantially deplete the arginine in the gastrointestinal tract. To achieve arginine depletion by recombinant ADI in a standard 24-h

DC stimulation assay that enables to study the consequences of arginine depletion on DC, enzymatically active enzyme should be added gradually. Theoretically, 4 µg (corresponding to 30 mU and representing the equivalent of the enzymatic activity of two to three trophozoites per DC present in the study) of active recombinant ADI converts all of the free arginine in 43 min (culture volumes of 1 ml RPMI containing 1.15 mM arginine), 10-fold less enzyme in approximately 7 h and 100-fold less enzyme in nearly 72 h, assuming constant activity over time (Fig. 10A). To study dose dependence in the following DC activation experiments, these serial dilutions of active enzyme were used as well as the catalytically inactive mutant form to control for possible effects unrelated to enzyme activity.

The theoretically calculated consumption of arginine by ADI was verified experimentally. Therefore, harvested immature DC were counted and 5 x 10^5 cells/well were seeded in 12-well tissue culture plates. Cells were stimulated with 1 µg/ml or 10 ng/ml LPS and exposed to the mentioned concentrations of ADI and equal amounts of the mutant enzyme. After 24 h supernatants were collected and citrulline formation was determined by a colorimetric assay. The results are shown in Fig. 10B. The predicted, calculated effect of recombinant ADI on arginine turnover was almost absolutely confirmed experimentally. Enzyme concentrations of 4 µg or 0.4 µg led to a citrulline formation of 0.87 mM ± 0.22 (n = 7) and 0.84 mM ± 0.21 (n = 7) respectively and therefore to arginine depletion at the end of the 24-h assay period. As expected, activity of 40 ng ADI, the amount of enzyme that required 72 h to turnover all arginine, formed roughly 30% of the maximal level reached by both other enzyme concentrations. Thus, under these experimental conditions the majority of the enzyme retained pro-longed activity.

Addition of ADI_{C424A} at all of the concentrations tested did not result in any specific citrulline formation (Fig. 10B and data not shown).

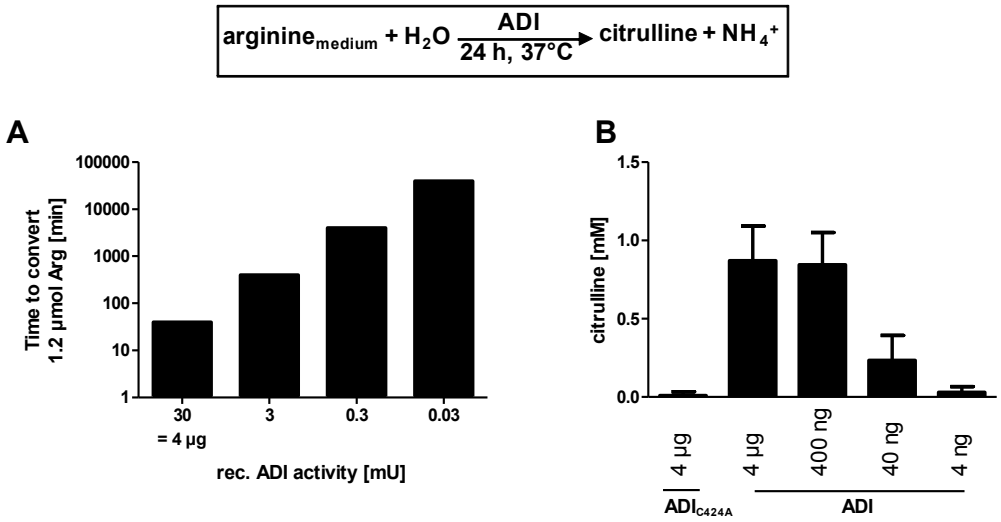

Figure 10: Recombinant ADI converts medium arginine
(A) Theoretic calculation of time being necessary to convert the entire arginine from 1 ml DC growth medium by recombinant ADI. (B) For experimental verification, immature moDC (5 x 10^5 per well of a 12-well tissue culture plate) were treated with a gradual dilution of 4 µg (equal to 30 mU) recombinant ADI or, as a control, corresponding levels of catalytically inactive ADI_{C424A} (only largest amount is shown) and were exposed to LPS (here 1µg/ml). Citrulline content in supernatants was determined as a measure of the cumulative ADI activity and arginine depletion over the 24-h assay time. Bars represent the mean ± SD from experiments with DC prepared from seven different donors.

4.2.2.3 Enzymatic arginine depletion by ADI modifies pro- and anti-inflammatory cytokine secretion of LPS-activated moDC

After confirming citrulline formation by ADI, collected supernatants were used to study the consequences of arginine depletion on moDC. Therefore, cytokine concentrations in the supernatants were determined by ELISA. The results are represented in Fig. 11. Activation of cells with 1 µg/ml LPS stimulated roughly a 100-fold and with 10 ng/ml LPS a 50-fold increase in IL-12p40, TNF-α and IL-10 levels in arginine-replete medium compared to those in nonactivated controls (data not shown). In contrast, LPS-stimulated (1 µg/ml) moDC exposed to 4 µg/ml of ADI produced significantly less IL-10 and IL-12p40. These values were 45% ($P < 0.001$, $n = 7$) and 17% ($P < 0.01$, $n = 6$) lower than those of control cells exposed to mutant ADI_{C424A}, respectively. In contrast, TNF-α secretion by ADI-treated and LPS-activated moDC was increased and values were, on average, 74% ($P < 0.01$, $n = 6$) higher than the values of LPS-stimulated, mutant enzyme exposed-control cells (Fig. 11A). MoDC that were stimulated with 10 ng/ml LPS showed for all three cytokines similar results compared to cells being activated with a higher LPS concentration (Fig. 11B). Of note, decreased IL-10 and IL-12p40 levels were also observed with 10-fold less ADI present

whereas increased TNF-α was observed only at the higher enzyme concentration, indicating that the time required by different doses of the enzyme to deplete arginine was relevant. These data show that arginine depletion by ADI modulates the pro- and anti-inflammatory cytokine secretion of LPS-activated moDC and, importantly, that the effects differ, depending on the cytokine analyzed.

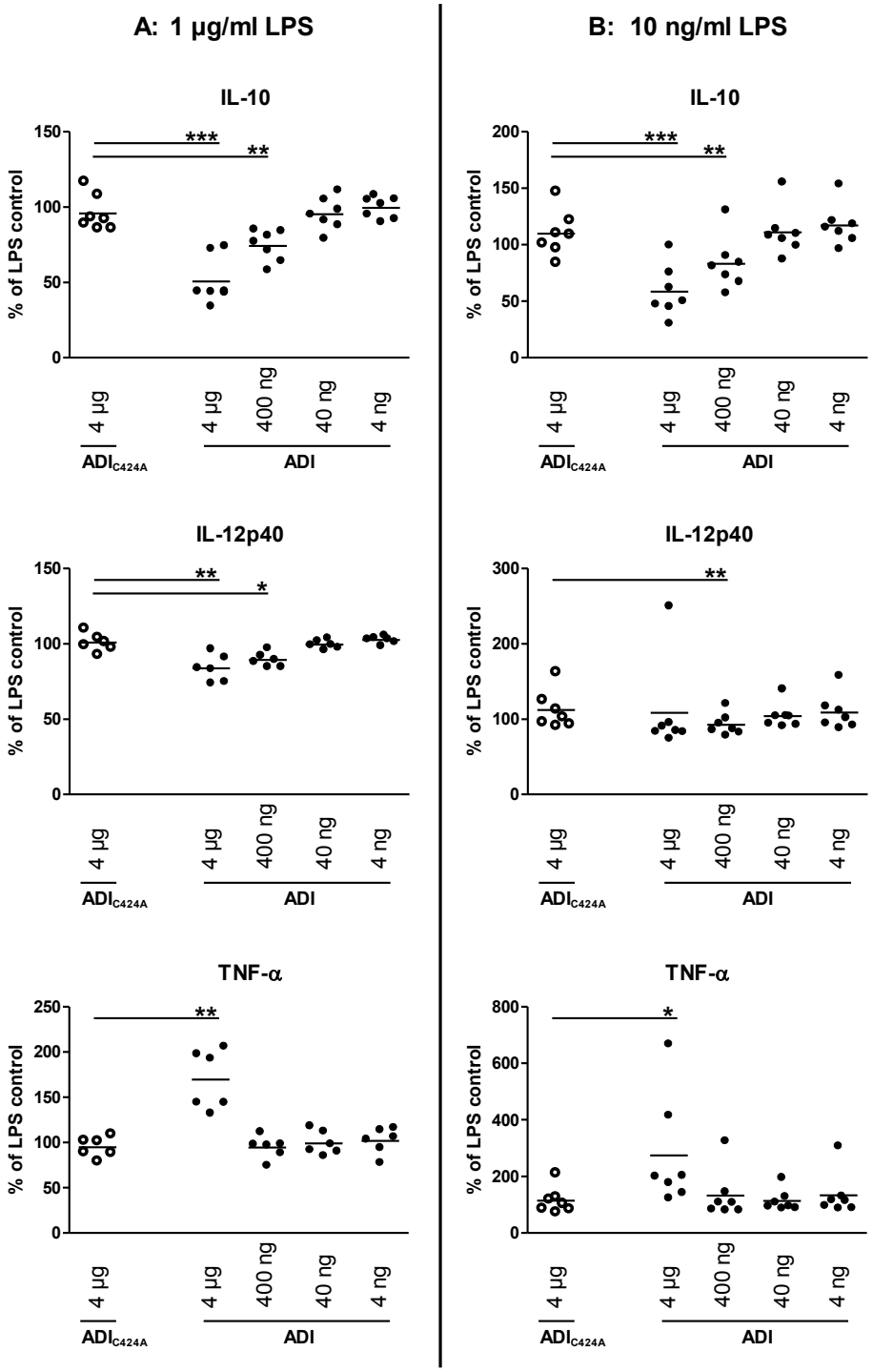

Figure 11: Enzymatic arginine depletion by ADI modulates cytokine secretion of LPS-activated human moDC

Immature moDC (5 x 10^5 per well of a 12-well tissue culture plate) were exposed to the indicated amounts of recombinant ADI or, as a control, corresponding levels of ADI_{C424A} (only the largest amount is shown), and 1 µg/ml (A) or 10 ng/ml (B) LPS was added. After 24 h, DC cytokine secretion into supernatants was assessed by ELISA and is expressed as a percentage of the amount secreted by LPS-stimulated cells not exposed to any ADI protein. Symbols represent values from individual donors, and means are indicated by horizontal lines. Differences between the amounts of cytokines secreted by cells exposed to mutant (control) or active ADI were analyzed by paired (two-tailed) *t* test. *, $P < 0.05$; **, $P < 0.01$; ***, $P < 0.001$.

4.2.2.4 Enzymatic arginine depletion by ADI reduces upregulation of surface CD83 and CD86 levels of LPS-activated moDC

To investigate the influence of arginine depletion by ADI activity on the phenotype of maturing DC, moDC were stimulated with LPS and treated with ADI or the mutant form ADI_{C424A} as described above and were analyzed for selected surface marker protein levels by flow cytometry. Activation of immature moDC with LPS induced upregulation of CD83 and CD86 (Fig. 12A and data not shown) as expected. In contrast, moDC stimulated with 1 µg/ml LPS and treated with arginine-depleting levels of ADI expressed significantly less CD83 and CD86 than did control cells. Surface CD83 was, on average, 22% ($P < 0.05$, $n = 3$) and CD86 was 15% ($P < 0.01$, $n = 4$) lower than on LPS-treated, mutant enzyme-exposed control cells. The effects were again ADI dose dependent (Fig. 12B). These results were confirmed by using 10 ng/ml LPS as stimulus for the moDC (Fig. 12C). The reduced upregulation of surface CD83 and CD86 unlikely reflects a general effect on surface protein levels since HLA-DR abundance on LPS-activated moDC was not affected by ADI (data not shown).

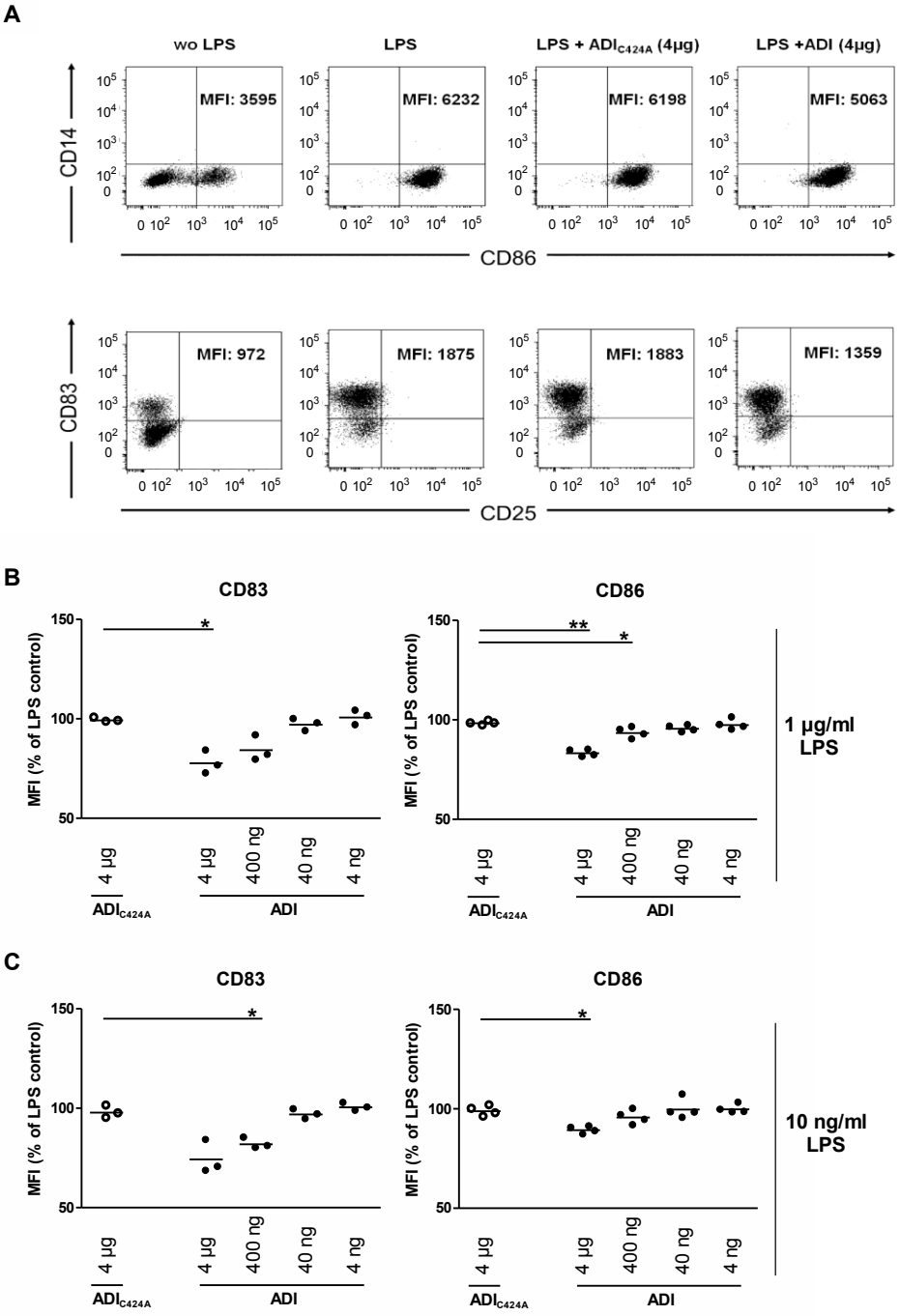

Figure 12: Enzymatic arginine depletion by ADI reduces CD83 and CD86 surface marker levels on LPS-activated moDC

Cells were treated as described in the legend to Fig. 11, and all the cells, except the nonstimulated control cells, were treated with 1 µg/ml (B) or 10 ng/ml (C) LPS. After incubation for 24 h at 37°C, moDC were harvested, stained with cell surface marker-specific antibodies, and analyzed by flow cytometry. (A) Representative dot plots for CD14/CD83 (top) and CD25/CD86 (bottom) expression (here: stimulated with 1µg/ml) with the respective mean fluorescence intensity (MFI) values for CD86- and CD83-positive populations (cells in the lower right and top left quadrants of panel A) are shown. wo, without. (B, C) Relative MFI values as percentages of those of control LPS-stimulated cells for CD83 (n = 3) and CD86 (n = 4) with moDC from different donors are shown. Horizontal lines correspond to mean values, and differences between the respective MFI values on cells exposed to mutant (control) or active ADI were analyzed by paired (two-tailed) t test. *, $P < 0.05$; ** $P < 0.01$. wo, without.

4.2.2.5 ADI immunomodulatory effects on LPS-activated moDC result from both arginine depletion and product formation

Next step was to investigate whether the modulatory effects of ADI on the moDC functional phenotype resulted from arginine depletion and/or the formation of the ADI reaction products citrulline and/or NH_4^+. To investigate possible cause-effect relationships, moDC were generated as described, harvested, and seeded into arginine-free culture medium that was subsequently supplemented with 2 mM or 0.2 mM arginine, citrulline, and/or ammonium chloride, respectively. The supplementation of 2 mM was chosen in accordance to the primary experiment with complete growth medium, whereas 10-fold fewer supplements were added to test whether the resultant effects depend on the amount of reaction products. Cells were treated as before with 4 µg of ADI or ADI_{C424A} and activated with 1µg/ml LPS. After 24 h of incubation, supernatants were collected and citrulline content and cytokine concentration were determined. Determination of citrulline formation in cell culture supernatants confirmed on the one hand functional ADI activity and on the other hand served as control for precise supplementation (Fig. 13). NH_4^+ formation by ADI was also determined in culture supernatants, and levels were comparable to those observed after supplementation with ammonium chloride (data not shown). Furthermore, moDC were harvested and cell surface markers were analyzed.

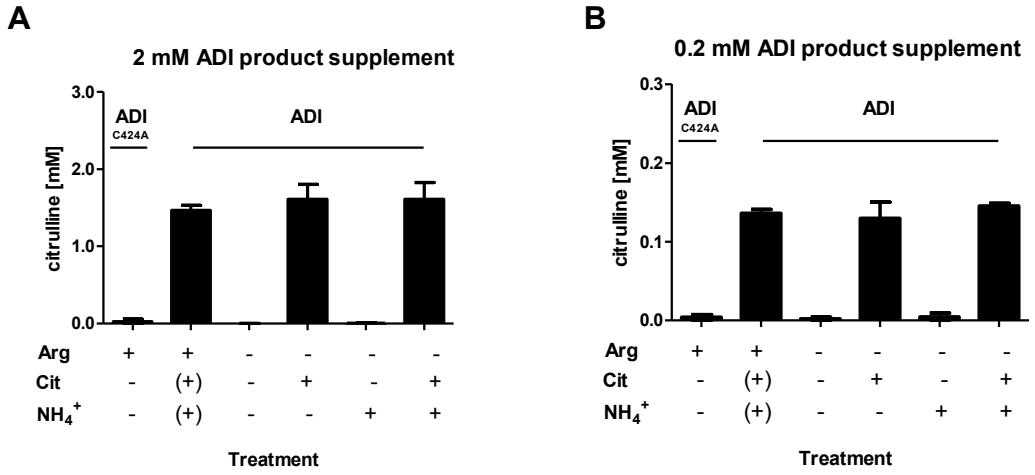

Figure 13: About 75% of supplemented or by recombinant ADI produced citrulline was detectable in cell culture supernatants

After harvest immature moDC were seeded into arginine-free growth medium. The medium was supplemented as indicated with 2 mM (A) or 0.2mM (B) arginine, citrulline and/or ammonium chloride (brackets indicate addition of ADI to arginine-replete medium to reflect formed, not supplemented products). Cells were activated with 1 µg/ml LPS and treated with 4 µg ADI (●) or mutant ADI_{C424A} (○) for control. After 24 h, supernatants were taken and citrulline formation determined by colorimetric assay. Figures show only supernatants of LPS-activated, treated cells. Bars represent the mean ± SD from experiments with DC prepared from three different donors.

IL-10 and TNF-α secretion of cells grown in medium including 2 mM arginine were modulated as described above, i.e. ADI-treated LPS-activated moDC produced less IL-10 and more TNF-α than did control cells. Also the analysis of the surface markers CD83 and CD86 of moDC confirmed the previous obtained phenotype after addition of ADI (Fig. 14A). MoDC stimulated in the absence of arginine showed a small decrease in IL-10 production, but levels remained significantly higher than those of cells treated with ADI in the presence of arginine, where citrulline and NH_4^+ could be formed. The addition of the ADI products, in particular of NH_4^+ in the form of NH_4Cl, reduced IL-10 levels to those observed in the presence of arginine and ADI. Similarly, CD83 and CD86 surface levels were also reduced, although this did not reach statistical significance for the latter marker. In contrast, the increase in TNF-α production was driven mainly by arginine depletion. LPS-activated DC from all of the donors tested showed significantly increased TNF-α production in the absence of arginine ($P < 0.01$; $n = 8$), with cells from some donors reacting particularly strongly, producing nearly three times as much as the respective control DC (data not shown and Fig. 14A). The increase due to arginine depletion was not affected by NH_4^+ but reduced by citrulline, indicating that citrulline could substitute for arginine in this respect (Fig. 14A). By addition of 0.2 mM supplements the described results for addition of 2 mM supplements

could be confirmed but differences did not reach statistical significance (Fig. 14B). Thus, it seems to be that the amount of reaction products that were developed in consequence of ADI activity had an impact on the occurrence of the respective phenotype.

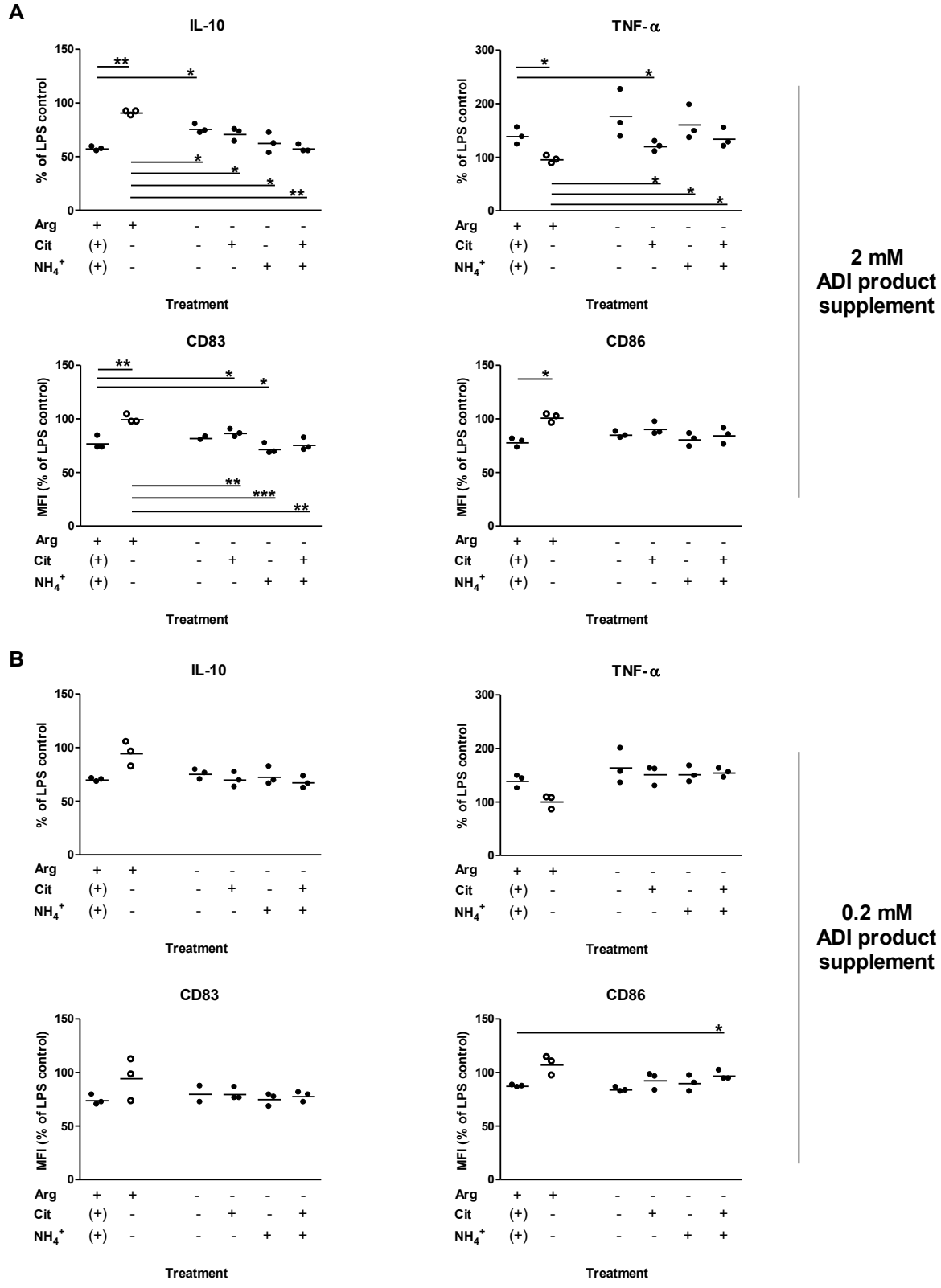

Figure 14: Depletion of arginine and formation of ADI reaction products citrulline and ammonium ions modulate the moDC response to LPS activation

Immature moDC were seeded into arginine-free growth medium. Medium was supplemented as indicated with 2 mM (A) or 0.2 mM (B) arginine (Arg), citrulline (Cit) and/or ammonium chloride (brackets indicate addition of ADI to arginine-replete medium to reflect formed, not supplemented products). Cells were activated with 1µg/ml LPS and treated with 4 µg ADI (●) or mutant ADI_{C424A} (○) as a control. *Continued on next page.*

Values correspond to percentages of the respective parameter determined for cells stimulated with LPS only in arginine-replete medium. After 24 h, supernatants were collected and cytokine concentrations were determined by ELISA. MoDC were harvested and CD83 and CD86 surface markers were analyzed by flow cytometry. Horizontal lines correspond to mean values, and differences between the respective parameter determined with cells exposed to mutant (control) or active ADI were analyzed by paired (two-tailed) *t* test. *, $P < 0.05$; **, $P < 0.01$.

The importance of ammonium ions as reaction product was additionally confirmed by supplementing moDC with NH_4^+ during stimulation in the presence of arginine but in absence of ADI. IL-10 was reduced, but no effect on TNF-α production was noticeable (Fig. 15). Thus, the immunomodulation of moDC by ADI resulted from a combination of distinct effects of arginine depletion and/or citrulline and NH_4^+ product formation.

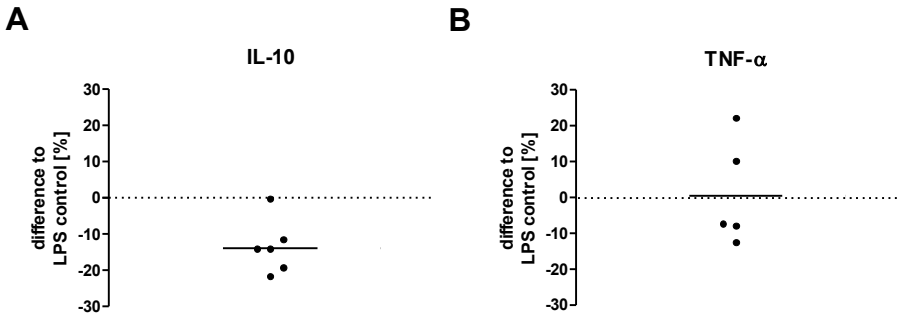

Figure 15: NH_4^+ reduces IL-10 secretion by LPS-stimulated moDC
Immature moDC were prepared and stimulated with LPS as described in the legend to Fig. 14 in medium supplemented with either 2 mM arginine alone (control) or arginine plus NH_4Cl (2mM each). After 24 h, cytokine concentration was determined from supernatants by ELISA. Cytokine concentrations are expressed as percent differences from the cytokine amounts produced by control cells. Each dot represents an independent experiments with moDC prepared from an individual donor. Significance was tested against the null hypothesis that addition of NH_4^+ had no effect by paired (two-tailed) *t* test. *P* values were ($P < 0.01$) for IL-10 levels and nonsignificant ($P > 0.05$) for TNF-α levels.

4.2.2.6 NH_4^+ and urea, the reaction products of ADI and arginases, differ in their effect on cytokine secretion and the surface marker profile of LPS-stimulated moDC

As mentioned before, many pathogens are thought to evade NO-mediated immune clearance through arginine depletion by arginases, which will result in the formation of ornithine and urea (Das et al., 2010). Immunomodulatory effects may thus be different from conditions where deiminases are relevant. Therefore, the immunomodulatory effects of NH_4^+ and urea as well as citrulline and ornithine were compared. LPS-stimulated cells were incubated for 24 h in medium devoid of arginine but supplemented with ammonium chloride, urea, citrulline or

ornithine, and then supernatants were collected for the detection of IL-10 and TNF-α by ELISA (Fig. 16A) and of CD83 and CD86 proteins by flow cytometry (Fig. 16B). Notably, cells stimulated in medium supplemented with urea produced significantly more IL-10 and displayed significantly higher levels of CD83 and CD86 surface proteins than did cells stimulated in the presence of NH_4^+. In contrast and corroborating the findings that TNF-α production was not affected by NH_4^+ (Fig. 15), no differences between cells treated with NH_4^+ and urea were noted with respect to TNF-α release. The comparison of citrulline and ornithine supplementation revealed also no significantly differences, except for CD83 surface proteins, confirming that both reaction products had no effects on moDC phenotype.

To sum up, within this experiment it was shown that NH_4^+ and urea, the reaction products of ADI and arginases, differ in their way to affect cytokine secretion and surface marker profile of LPS-stimulated moDC.

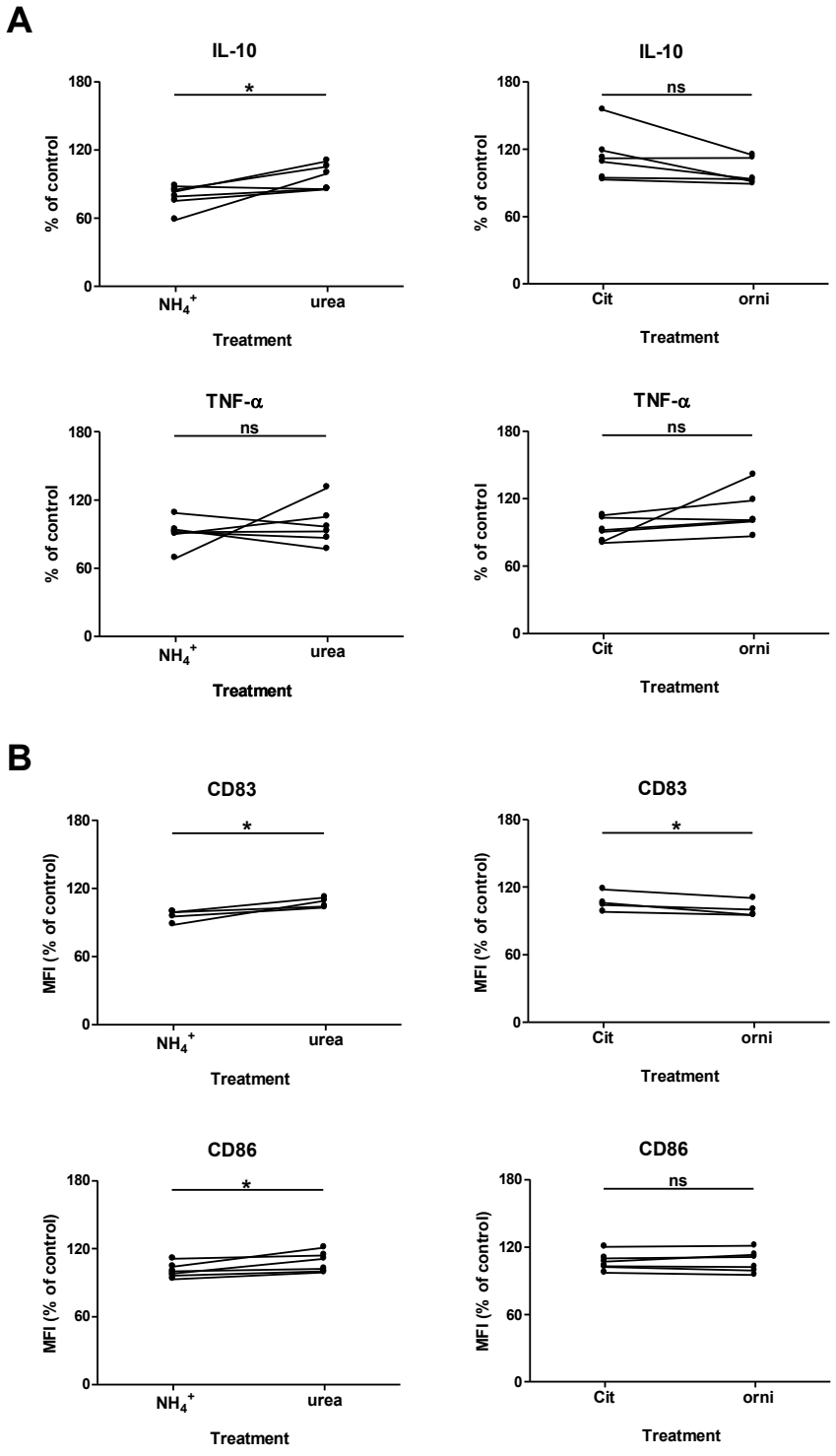

Figure 16: Immunomodulation of LPS-activated moDC undergoing arginine starvation is different between NH_4^+ and urea

MoDC were prepared as described in the legend to Fig. 14 and stimulated in arginine-free medium supplemented either with 2 mM ammonium chloride, urea, ornithine or citrulline. After 24 h, supernatants were collected and cytokine concentrations were determined by ELISA (A). The moDC were harvested, and surface marker proteins were analyzed by flow cytometry (B). Dots represent values from experiments with cells from six (panel A) or four (panel B) individual donors and are expressed as percentages of control values obtained with LPS-activated cells with no supplement. *, $P < 0.05$ (paired [two-tailed] *t* test); ns, nonsignificant.

4.2.2.7 Arginine turnover by ADI results in decreased phosphorylation of the mTOR-signaling pathway target S6K in LPS-activated moDC

Previous studies suggested an inhibitory effect of branched-chain amino acids on the mTOR/S6K signaling pathway, resulting in impaired maturation of moDC and particularly affecting CD83 expression (Kakazu et al., 2007). mTOR is a serine/threonine kinase that is present in two distinct protein complexes, mTORC1 and mTORC2. Activation of mTORC1 leads to the phosphorylation of the proteins S6 kinase (S6K) and the eukaryotic initiation factor 4E (eIF-4E) binding protein 1 (4E-BP1), which are both involved in the regulation of protein translation (Carrera, 2004). Arginine levels have been shown to affect mTOR signaling in several cell types (Ban et al., 2004; Yao et al., 2008). Since ADI by arginine depletion had immunomodulatory effects on moDC, involvement of the mTOR pathway in these cells was investigated. MoDC were seeded in arginine-free medium and then supplemented or not with arginine. The cells were treated with recombinant ADI or catalytically inactive ADI_{C424A} or with the mTOR inhibitor rapamycin as a positive control and were activated with LPS. Cells were incubated for 24 h before determining surface CD83 levels (Fig. 17A). In the presence of arginine, CD83 levels were lower on cells treated with ADI than on cells exposed to mutant enzyme, as shown before. MoDC stimulated in the absence of arginine or in the presence of arginine and rapamycin also showed reduced levels of CD83 protein (Fig. 17A).

To investigate whether reduced CD83 surface levels caused by ADI activity correlated with mTOR signaling, treated cells were harvested 30 min after LPS stimulation to assess mTOR-dependent phosphorylation events. Cells were lysed, and equal amounts of total protein were separated by SDS-PAGE. The abundance of phosphorylated mTOR target protein S6K was then determined by Western blotting (Fig. 17B), and results were quantified. First, Western blot signals obtained for S6K and 4E-BP1 from five independent experiments were related to signals obtain for the reference protein β-actin to ensure that same amounts of the effector molecule were available in all cases (Fig. 17C). Levels of total p70-S6K and 4E-BP1 were not significantly different between the distinct experimental groups.

Second, signals obtained for phosphorylated S6K and 4E-BP1 were related to β-actin signals to identify if the arginine turnover by ADI results in decreased phosphorylation of these both mTOR-signaling pathway targets in LPS-activated moDC. In Fig. 17D results with cells from five independent donors are summarized and these show that suppression S6K phosphorylation in moDC correlated with reduced CD83 surface protein levels, and this

depended on arginine levels. Control cells treated with rapamycin showed the expected suppression of S6K phosphorylation. Contrary to literature (Haidinger et al., 2010), suppression of 4E-BP1 phosphorylation with rapamycin was not observed. A possible explanation is the different experimental setting. Using moDC, phosphorylation of 4E-BP1 might be regulated by an alternative mTOR independent pathway. Adequate interpretation of the experimental results is difficult as they lack a positive control. Nevertheless, by trend, the mTOR/4E-BP1-signaling pathway in moDC did not seem to depend on arginine availability.
These data suggest that arginine levels, similar to what has been shown for branched-chained amino acids (Kakazu et al., 2007), affect mTOR activity in moDC but also indicate a difference between amino acids.

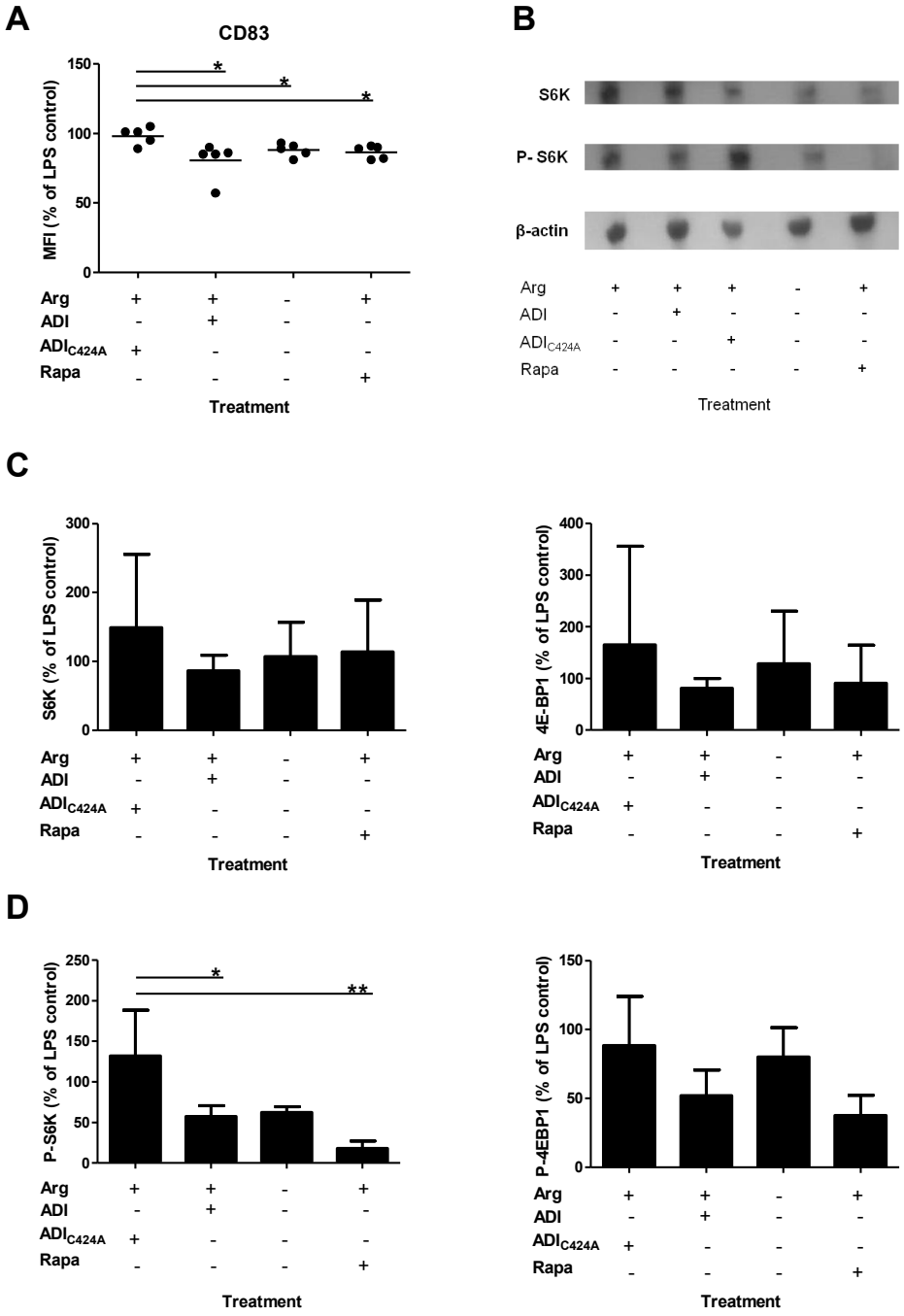

Figure 17: ADI-mediated arginine depletion decreases mTOR signaling in LPS-stimulated moDC

Immature moDC (10^6 in arginine [Arg]-free growth medium) were seeded in into each well of a 12-well tissue culture plate. Arginine-free medium (ΔArg) was supplemented or not with 2 mM arginine, and cells were treated or not with 4 µg of ADI, 4 µg of ADI_{C424A}, or 2 µM rapamycin (Rapa). For activation, 1 µg/ml LPS was added to each sample after 2 h. (A) MoDC CD83 surface marker levels 24 h after stimulation and those of stimulated control cells are compared. Bars represent the mean ± SD of independent experiments with five different donors. *, $P < 0.05$ (paired [two-tailed] *t* test compared with the respective control). In parallel, 30 min after LPS stimulation, cells were harvested, washed, and lysed. A 50-µg sample of cell extract was separated by SDS-PAGE, and p70-S6K,4E-BP1, phospho-p70-S6K, phospho-4E-BP1, and β-actin were detected by immunoblotting. One Western blot is exemplary shown in (B). Immunoblots were quantified by image analysis and p70-S6K or 4E-BP1 (C) and phospho-p70-S6K or phospho-4E-BP1 (D) levels were normalized relative to β-actin and compared to those of stimulated control cells. (C) Levels of total p70-S6K were not significantly different between the different experimental groups. *Continued on next page.*

Bars represent the mean ± SD from five individual experiments with cells from different donors. *, $P < 0.05$; **, $P < 0.01$ (compared with the respective control by paired [two-tailed] *t* test).

4.2.3 Influence of native ADI released by *G. duodenalis* trophozoites on Caco-2 cells

Experiments of Ringqvist et al. (2008) where ADI was shown to be released by *G. duodenalis* WB-C6 trophozoites upon contact with Caco-2 cells supported investigations of human body fluids where the enzyme was noticed to be an immunoreative protein (Palm et el., 2003; Téllez et al., 2003). These findings spotlighted the enzyme to be implicated in virulence of *G. duodenalis* and thus being involved in host-parasite interplay. Further *in vitro* studies have shown that the *G. duodenalis* WB-C6 strain (Eckmann et al., 2000) itself as well as its recombinant ADI (Ringqvist et al., 2008) inhibited NO formation of human IEC by consumption of free arginine. To investigate, whether this phenomenon is strain-dependent and possibly related to its substrate affinities (Fig. 24B), the NO-dependent parasite clearance mechanism of Caco-2 cells was investigated. First, an *in vitro* model was established and release of native ADI by parasites was tested. Second, optimal stimulation conditions for NO production of Caco-2 cells were determined to subsequently investigate the effect of ADI release by *G. duodenalis* trophozoites on the NO production of epithelial cells.

4.2.3.1 Usage of Caco-2 cells as *in vitro* model

So far, no adequate animal model exists to investigate the influence of *Giardia* parasites on host immune responses *in vivo*. Several investigations were performed using an adult mouse model for infection. Colonization of the mouse small intestine was difficult and depended on both, the mouse and the parasite strain. Successful infection of adult mice with *G. duodenalis* strains causing human giardiasis was only possible with the two laboratory strains GS/M-H7 and WB-C6 (Byrd et al., 1994; Solaymani-Mohammadi and Singer, 2011).
However, investigations of other human *G. duodenalis* isolates are essential. As alternative to the *in vivo* mouse model, human Caco-2 cells as an intestinal epithelial tumor cell line were used for *in vitro* studies (Ringqvist et al., 2008; Maia-Brigagão et al., 2012; Stadelmann et al., 2012). *In vitro* cultivated Caco-2 cells grow as confluent monolayer and undergo epithelial differentiation (Grasset et al., 1984) that results in morphological and functional features similar to small intestinal enterocytes (Ferruzza et al., 2012). During differentiation

the formation of tight junctions seals adjacent cells and thus creates intercellular boundaries. These cell-to-cell adhesion structures have protective (e.g prevent diffusion of solutes across the cellular sheet) and functional (e.g maintain cellular polarization) features (Alberts et al., 2002). Tight junction assembly is mediated by junction-associated membrane proteins such as zonula occludens (ZO)-1 (Stevenson et al., 1986). In this study ZO-1 was used as a marker to verify tight junctions because of its structural and signalling roles during cell-cell contact formation (Anderson et al., 1989).

Caco-2 cells were seeded into 12-well tissue culture plates and were cultured until confluence. After further 17-21 days in culture, cells were checked for development of cell-cell contacts by fluorescent staining (Fig. 18).

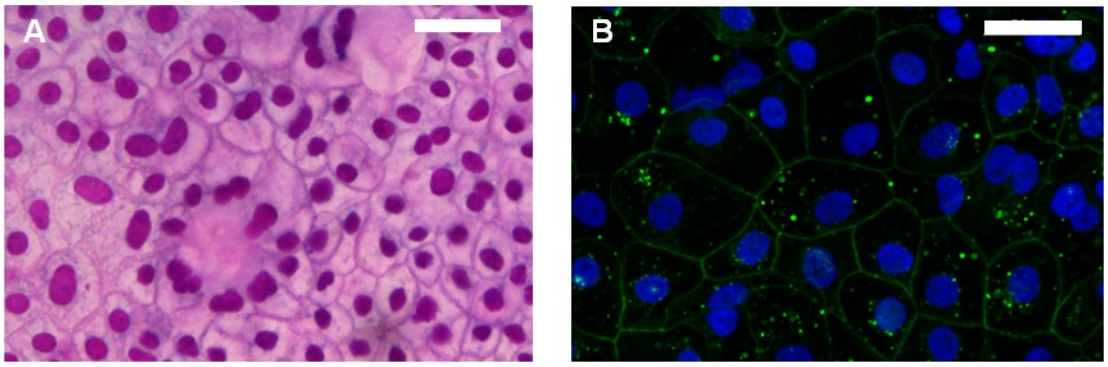

Figure 18: LM-micrograph of differentiated human Caco-2 cells
Caco-2 cells grown for 17-21 days post-confluence were stained either with DiffQuik® (A) to show cell morphology or with fluorescent-conjugated antibody directed against ZO-1 protein (B) to verify differentiation. Scale bar = 50 µm.

Usage of an antibody raised against the ZO-1 protein revealed the formation of tight junctions in the monolayer. Thus, Caco-2 cells served as a useful model in the following experiments.

4.2.3.2 Release of *G. duodenalis* ADI upon contact with Caco-2 cells is strain-independent

To prove the hypothesis that ADI as a potential virulence factor is involved in host-parasite interplay, the observation of Ringqvist et al. (2008) needed to be confirmed. Thus, the release of ADI by *G. duodenalis* WB-C6 trophozoites but additionally the release by other *G. duodenalis* strains upon contact with Caco-2 cells was examined. Therefore, the *Giardia* biobank (4.3.1) provided a good opportunity to test for several clinical isolates that

were also of assemblage A, but had another subgenotype than the laboratory strain WB-C6. For this reason, Caco-2 cells in a tight monolayer were exposed to trophozoites of the different patient isolates and the laboratory strain WB-C6 as well. Three times more parasites than cells were added. Further cultivation allowed a quick attachment of the trophozoites to their host cells. After 45 min, cell-free supernatants were taken and released proteins were analyzed in Western blot (Fig. 19).

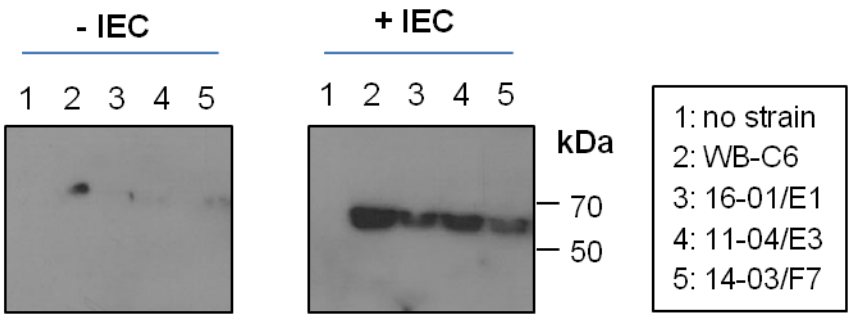

Figure 19: Release of native *G. duodenalis* ADI upon contact with Caco-2 cells
Differentiated Caco-2 cells were infected (MOI of 3) either with trophozoites of strains collected in the *Giardia* biobank or of the laboratory strain WB-C6. After further cultivation for 45 min under aerobic conditions, cell-free supernatants were taken and included proteins precipitated. Total proteins were loaded on SDS-PAGE for Western blot analysis. Native ADI was detected by polyclonal alpaca antiserum raised against the enzyme.

Addition of all strains to Caco-2 cells led to release of native ADI identified as ~ 64 kDa band in immunoblotting. Cell-free supernatants from trophozoites that were seeded in parallel in a 12-well tissue culture plate without IEC showed no or rather a weak signal for ADI in Western blot analysis. That indicated a specific release of the enzyme after host-parasite contact. To clarify whether trophozoites of distinct strains release different amounts of ADI as a kind of virulence mechanism, lysis of the parasite during the experiment needed to be excluded. One possibility was to verify e.g. tubulin, an intracellularly located protein that is import for the arrangement of the cytoskeleton, in Western blot analysis. Unfortunately, it was not possible to distinguish between lysis of Caco-2 cells and parasites as both express eukaryotic tubulin. Alternatively, parasite lysis was verified by fluorescent cell staining. Substance of choice was CFDA-SE that enters the cytoplasm of cells and is cleaved by intracellular esterases to CFSE that reacts with intracellular molecules, forming fluorescent conjugates. Unfortunately, this approach was without any success (data not shown). Focusing on the Western blot analysis and considering the aspect that all samples were treated identical

and entire proteins were loaded on SDS-PAGE, by trend the laboratory strain WB-C6 released more ADI than the other strains.

4.2.3.3 *G. duodenalis* reduced NO formation of stimulated Caco-2 cells is strain-independent

The free radical NO is an important molecule for various biological functions in the body. NO and citrulline are formed by the conversion of arginine and oxygen by the enzymatic activity of NOS. There exist three different isoforms of NOS termed neuronal NOS (nNOS, or NOS1), inducible NOS (iNOS, or NOS2) and endothelial NOS (eNOS, or NOS3). The expression of iNOS is regulated by cytokines, whereas nNOS and eNOS are constitutively expressed and calcium-dependently regulated. NO acts as cellular signaling molecule in the cardiovascular and nervous system, on the other hand it has effector (e.g. antimicrobial and anti-tumor activity) and immunoregulatory functions (e.g. pro- or anti-inflammatory effects) in the immune system (Bogdan, 2001). In the latter, NO is generated by several cells, e.g. macrophages, DC, mast cells as wells as other cells involved in immune response like epithelial cells. Previously, it was shown that addition of recombinant *G. duodenalis* ADI with cytokines to differentiated Caco-2 epithelial cells impaired their NO formation by competing for arginine with iNOS (Ringqvist et al., 2008). Thus, the influence on the NO-dependent parasite clearance mechanism of Caco-2 cells was investigated with the collected *G. duodenalis* parasites, releasing ADI of different assemblage subtypes that differ in their substrate affinity for arginine compared to the laboratory strain WB-C6.

First step was to determine the optimal stimulation conditions for Caco-2 cells to produce NO. Therefore, differentiated Caco-2 cells (seeded in a 12-well tissue culture plate) were treated with various cytokine mixtures including human TNF-α, IFN-γ and IL-1β in different concentrations. After 24 h, supernatants were collected and NO formation was determined as total nitrite within a colorimetric assay. The strongest stimulation and therefore the highest NO formation was reached with a concentration of 50 ng/well TNF-α, 25 ng/well IL-1β and 50 ng (330 U)/well IFN-γ (data not shown). The next experiment was to determine the NO formation over time under the optimal cytokine concentrations. Therefore, Caco-2 cells were stimulated, cell-free supernatants were taken after certain time points and total nitrite was measured. Approximately 6 h after induction of iNOS, NO production was detectable and approximately 28 h after induction NO production reached its maximum (Fig. 20). In parallel

cultivated, nonstimulated Caco-2 cells showed no NO formation at all. For following experiments it was decided to take supernatants 28 h after induction.

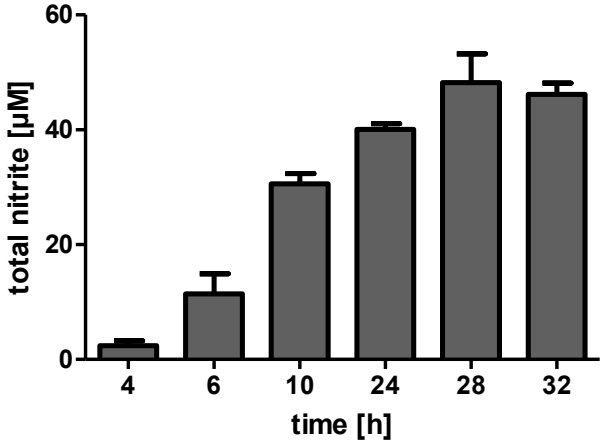

Figure 20: NO formation over time after stimulation of Caco-2 cells
Differentiated Caco-2 cells, that were initially seeded into a 12-well tissue culture plate, were stimulated or not with 25 ng IL1-β/well, 50 ng TNF-α/well and 50 ng IFN-γ/well. After certain time point's cell-free supernatants were taken and total nitrite was measured in a colorimetric assay. Nonstimulated cells were not able to produce NO in detectable amounts. One representative experiment out of two is shown. Each bar represents the mean ± SD of three technical replicates.

Under defined experimental conditions, the influence of substrate affinity on NO production was investigated for the native ADI of the laboratory strain WB-C6 and the clinical isolates collected in the *Giardia* biobank. Because of time deficit, it was only possible to perform this experiment once with three technical replicates. Caco-2 epithelial cells were stimulated or not with cytokines as described and were in parallel infected with three times more (MOI of 3) or three times less (MOI of 0.33) trophozoites of the various *G. duodenalis* strains. Cell-free supernatants were collected and total nitrite concentration was determined. It was observed that *Giardia* infection without cytokine stimulation did not result in NO formation by Caco-2 cells. Under stimulating conditions, the addition of the laboratory strain WB-C6 in both MOIs showed impaired NO production in Caco-2 cells, as described in the literature (Eckmann et al., 2000). Same results were also obtained by infecting of IEC with other *G. duodenalis* strains. Interestingly, by using an MOI of 3 it was observed that by trend the isolates collected in the *Giardia* biobank and the laboratory strain WB-C6 differed in their ability to reduce NO. This might be due to differences in the substrate affinity. In contrast, for an MOI of 0.33 this phenomenon could not be observed any longer (Fig. 21).

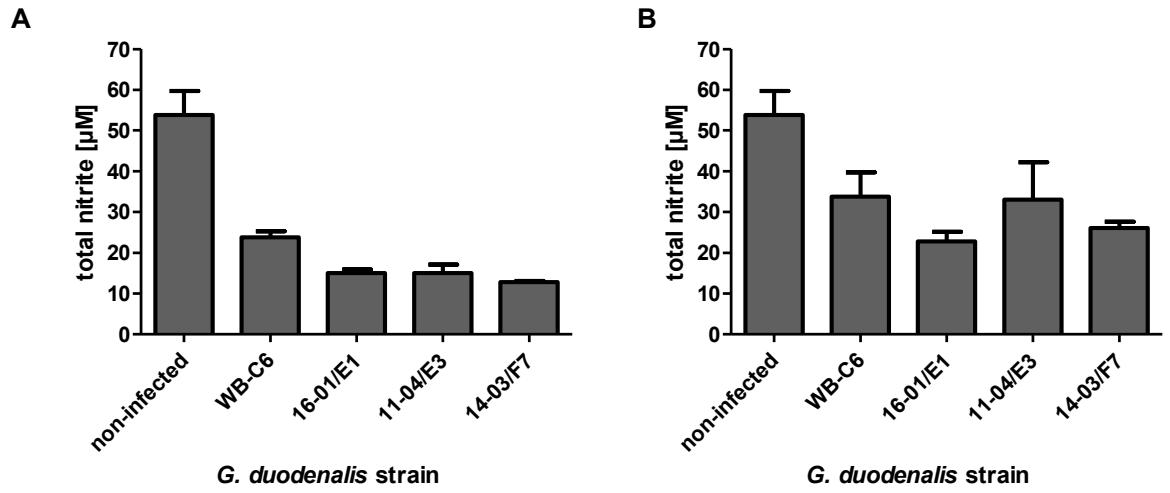

Figure 21: NO formation of stimulated Caco-2 cells in presence of *G. duodenalis* trophozoites

Differentiated Caco-2 cells (seeded in a 12-well tissue culture plate) were infected with (A) three times more trophozoites of the laboratory strain WB-C6 or different patient isolates or (B) three times less parasites than cells. In parallel, cells were stimulated or not with 25 ng IL1-β/well, 50 ng TNF-α/well and 50 ng IFN-γ/well. After 28 h cell-free supernatants were taken and total nitrite was measured in a colorimetric assay. Nonstimulated cells were not able to produce NO in detectable amounts. Each bar represents the mean ± SD of three technical replicates.

4.3 Functional analysis of native and recombinant ADI of different *G. duodenalis* strains

G. duodenalis is divided into different assemblages, where assemblage A and B are known to be pathogenic for humans. Until now, it remains unclear why progression of *Giardia* infection differs from patient to patient and if this is related to the different genotypes. To explore the pathogenesis of human giardial infections, investigations of factors involved in pathogen's virulence are important.

Among environmental isolates, virulence factors can vary in their nucleotide sequence. Such genomic variations can lead to amino acid exchanges that influence the tertiary and quaternary structure of the protein or its posttranslational modification. In case of enzymes, these modifications can lead to a partial or complete loss of its activity, especially when the active center is affected.

Due to *G. duodenalis* genome sequencing of the different genotypes A, B and E, first hints exist that amino acid sequence variants of ADI occur. To which extent these variations influence the enzymatic activity is still unclear. In the following the hypothesis that *G. duodenalis* ADI as a potential virulence factor has differences in its enzyme activity profile that are related to diversity in its gene sequence was investigated. Therefore, it was necessary to characterize and compare both the recombinant and the native enzyme.

4.3.1 Establishment of a *Giardia* biobank as source for functional analyses

Basis for upcoming experiments was the availability of *G. duodenalis* strains isolated from human biological samples. Therefore, the *Giardia* biobank established by the working group served as resource. It stored biomaterial in combination with medical information (e.g. patient's health status, therapeutic response) to create a tool for functional epidemiology of *G. duodenalis* infections. To generate this biobank, *Giardia* positive human fecal samples were collected in cooperation with the Charité Berlin (Institute for Tropical Medicine). In a routinely executed working procedure (technicians work), cysts were isolated and used to prepare genomic DNA for subsequent genotyping *via* sequencing and for excystation and limiting dilution. The limiting dilution was necessary to prevent mixtures of different *G. duodenalis* strains that can occur within biological samples and thus to obtain clonal trophozoite cell lines (Fig. 22) that could be used to for the functional assays.

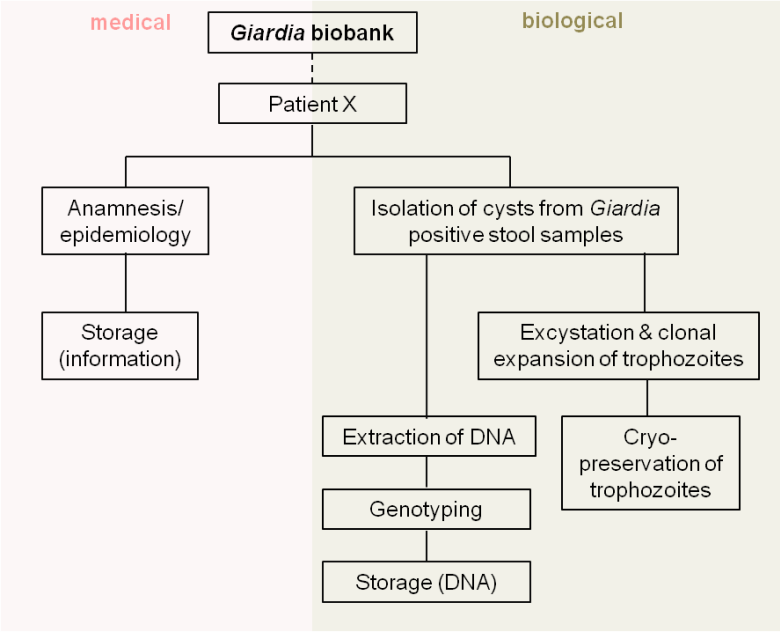

Figure 22: Overview about the structure of the *Giardia* biobank

The isolation of cysts and subsequent generation of viable clonal trophozoite cell lines was difficult. Despite cyst DNA was genotyped in 78% of the cases as assemblage B, only trophozoites of assemblage A survived indicating that culture conditions preferentially supported growth of parasites from this genotype. Also the cultivation of another

laboratory *G. duodenalis* strain (GS/M-H7), known to belong to the genotype B, remained without any success. Finally, four clinical isolates named in the following 16-01/E1, 11-04/E3, 14-03/F7 and 115-01/H2 were available for the planned functional analysis. All of them belong to the subassemblage AII and were compared to the laboratory strain WB-C6 that belongs to the subassemblage AI (Tab. 7).

4.3.2 Characterization of native and recombinant ADI of different (sub)genotypes

After the availability of different *G. duodenalis* isolates was assured by the *Giardia* biobank, beside recombinant ADI of assemblage A also recombinant forms of assemblage B and E were prepared. Through *G. duodenalis* genome sequencing, the nucleotide and amino acid sequence of these ADI genotypes are available on databases like NCBI or *Giardia*DB. Thus, it was possible to produce recombinant ADI of assemblage B and E without amplifying both genes from genomic DNA. Instead, by an external service, both genes were synthesized in a donor vector equivalent that allowed further processing with the StarGate® cloning system after delivery. After transformation into the expression strain DH5αZ1, both recombinant proteins were purified, as described for ADI and ADI_{C424A}, by affinity chromatography. Afterwards, successful purification was verified by SDS-PAGE (Fig. 23). Both enzymes were identical in size and purity like the purified recombinant ADI and ADI_{C424A}.

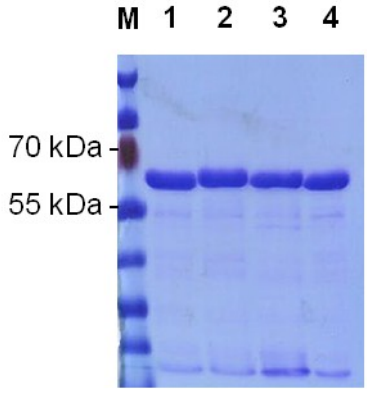

Figure 23: SDS-PAGE of purified recombinant ADI proteins of different assemblages
Successful affinity purification of 5 µg recombinant ADI assemblage A (lane 1), ADI assemblage B (lane 2), ADI assemblage E (lane 3) and mutant form of ADI assemblage A (lane 4) was verified in SDS-PAGE after Coomassie staining. M: Marker.

In parallel, the expression of native ADI by the laboratory strain WB-C6 and the clinical isolates (16-01/E1, 11-04/E3, 14-03/F7 and 115-01/H2) being collected in the *Giardia* biobank was investigated in Western blot analysis. Thereby, similar amounts of ADI at ~ 64 kDa were identified in all lysates (data not shown). So far, there is no information about (different) posttranslational modifications like phosphorylations of the various ADI subgenotypes. This needs to be answered in continuative experiments.

For further functional analysis, it was tested whether the native ADI is also enzymatically active within the *G. duodenalis* lysates like the purified, recombinant one. Due to the fact that trophozoites were counted before preparing the *G. duodenalis* lysates, the specific activity, expressed as U per trophozoites, of ADI was determined for all strains (Tab. 16). Finally, the enzymatic activity of *G. duodenalis* ADI was confirmed to be almost identical in all prepared lysates which were then used for further characterization.

Table 16: Verification of specific ADI activity in lysates of different *G. duodenalis* strains
For subsequent ADI activity determination, three independent lysates for each parasitic strain were prepared. U is defined as µmol substrate/min at 37°C in Hepes buffer.

***G. duodenalis* strain**	**Specific activity (U/10^6 trophozoites)**
WB-C6	0.016 ± 0.003
16-01/E1	0.006 ± 0.002
11-04/E3	0.010 ± 0.007
14-03/F7	0.008 ± 0.003
115-01/H2	0.012 ± 0.003

4.3.2.1 Determination of K_m values from native and recombinant ADI

The activity profile of enzymes involved in pathogen's virulence can differ between strains. To find further hints for ADI to be involved in *G. duodenalis* virulence, the enzyme kinetic of different genotype variants was characterized. A simple model for the analysis of enzyme kinetics is the Michaelis-Menten theory. It assumes that in an enzymatic reaction substrate and enzyme form an enzyme-substrate complex. The substrate is then catalytically converted and the complex disaggregates into a free product and the enzyme. Enzyme-catalyzed reactions are saturable and show a hyperbolic curve progression. This saturation curve is formed due to the fact that at low substrate concentrations the active centers of the enzymes are predominantly available for substrate binding. Thus, the reaction rate can increase linearly with the substrate concentration. However, at high substrate concentrations nearly all of the

free enzyme binding sites are occupied. The reaction rate approximates its theoretical maximum (V_{max}) given by the enzyme and does not longer increase. To determine the substrate affinity of an enzyme in an enzymatic reaction, the Michaelis constant (K_m) is calculated. The K_m value is defined as substrate concentration at which the reaction rate is half maximal (V_{max}). The K_m value is independent from the enzyme concentration whereas the maximal reaction velocity proportionally depends on it. A higher K_m value reflects a higher substrate concentration necessary to reach $V_{max}/2$. Thus, the higher the K_m value, the lower is the affinity of an enzyme to a certain substrate. In enzyme kinetics, the K_m value is obtained by using constant reaction conditions but varying the substrate concentration and subsequent direct-linear plotting of substrate concentration against reaction rate (Müller-Esterl, 2004). In this study, first the K_m value of native ADI from different *G. duodenalis* strains was determined. Therefore, prepared lysates were directly used in the enzyme kinetic assay and subsequently the K_m value was computed with GraphPAD software. Representatively, one graph is shown in Fig. 24A. The comparison between native ADI of different *G. duodenalis* strains revealed variations in the K_m values among the subgenotypes. The ADI of lysates prepared from the laboratory strain WB-C6 (that belongs to assemblage AI) showed with 0.25 mM ± 0.06 an at least three times lower K_m value compared to the ADI of all other clinical isolates (that are of assemblage AII), i.e. the ADI of the laboratory strain WB-C6 had the highest affinity for arginine as substrate (Fig. 24B).

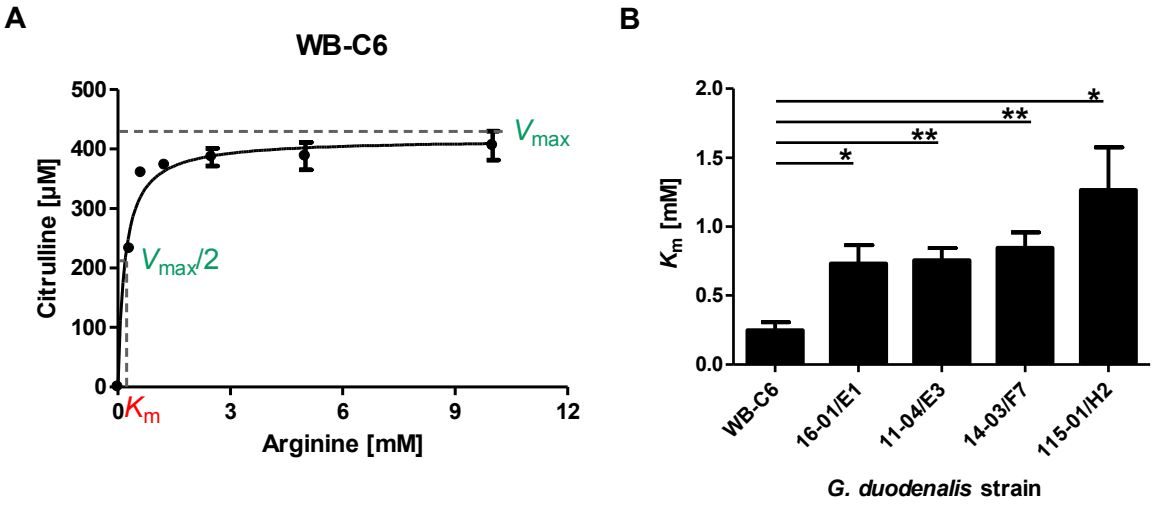

Figure 24: Comparison of K_m values from native ADI of different *G. duodenalis* strains
(A) To determinate the K_m value of native ADI, lysates of different parasitic strains were incubated with increasing concentration of arginine as substrate. To calculate the Michaelis constant, the rate of citrulline formation was plotted against the various substrate concentrations, here shown for lysates of the laboratory strain WB-C6. (B) summarizes the obtained K_m values for all native ADIs. Data for each strain represent mean ± SD of three independent experiments (paired (two-tailed) *t* test with *, $P < 0.05$; **, $P < 0.01$).

Next, the K_m value of recombinant ADI of different assemblages was determined. For this purpose, purified enzymes as well as lysates of bacteria overexpressing the recombinant ADI variants were used in the enzyme kinetic assay. Interestingly, the K_m value of the recombinant ADI of assemblage A was two times higher compared to the native ADI of the laboratory strain WB-C6, although both were identical in their amino acid sequence. Nevertheless, the computation of the K_m values revealed differences in substrate affinity between the different recombinant ADI assemblages (Fig. 25). The ADI of assemblage A and E had a higher affinity than the enzyme of assemblage B. This is in accordance to the fact that assemblage A and E are more closely related in their amino acid identity.

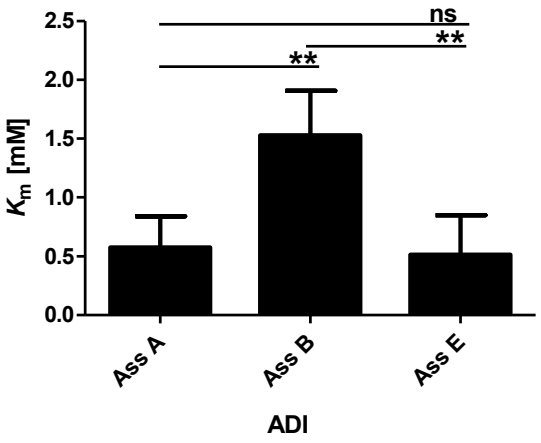

Figure 25: Comparison of K_m values from recombinant ADI of different assemblages
For determination of the K_m value of recombinant ADI from different genotypes (assemblage A, B and E), likewise both purified enzyme and lysates of DH5αZ1 cells overexpressing the enzymes were incubated with increasing concentration of arginine as substrate. Calculation of the Michaelis constant was identical to that described in Fig. 24. Data for each strain represent mean ± SD of six independent experiments (paired (two-tailed) *t* test with **, $P < 0.01$). Ass: assemblage.

4.3.2.2 Analysis of the amino acids sequence from native and recombinant ADI

The next step was to investigate if the noticed differences in substrate affinity of recombinant and native ADIs are related to the diversity in their amino acid sequence and in consequence to a diversity in their protein structure. So far, no crystal structure of the *G. duodenalis* ADI has been determined. However, there exist homologues of the enzyme in other organism like bacteria that have been crystallized and thus could be used as template for *in silico* three-dimensional protein structure prediction. Thereby, the target protein is screened within a

liberty for an adequate template protein of know structure to perform a sequence alignment for subsequent modeling (Bordoli et al., 2009). The Web-based program 'SWISS-MODEL' (http://swissmodel.expasy.org/) enables such a comparative method and was therefore applied for protein modeling of *G. duodenalis* ADI (Guex and Peitsch, 1997; Schwede et al., 2003; Arnold et al., 2006). The protein model of *G. duodenalis* ADI (assemblage A) was generated on the basis of the structure known for ADI of *Pseudomonas aeruginosa* (Galkin et al., 2005) and is shown in Fig. 26.

Figure 26: 3D model of G. *duodenalis* ADI (assemblage A) by SWISS-MODEL
The homology model was built as single chain and its reliability was visualized by a color gradient from blue (representing more reliable regions) to red (representing potentially unreliable regions).

Protein modeling predicted a complex folding structure of ADI (assemblage A) with several α-helices and β-sheets. Unfortunately, the target and template sequences were highly diverse. Thus, model quality for all three assemblages was indicated as poor. As alternative, to compare protein structures of different G. *duodenalis* ADI variants, a secondary structure prediction with the online server "PSIPRED" choosing PSIPRED v3.3 as prediction method (Jones, 1999) was performed. The analysis is based on a multiple sequencing profile for the target sequence by PSI-Blast (McGuffin et al., 2000). In comparison to multiple sequence alignment in standard protein-protein BLAST, PSI-BLAST has the advantage to find more distantly related sequences and therefore is more sensitive (Altschul et al., 1997). The

secondary structure prediction for the different assemblages of ADI (Fig. 27) revealed a high frequency of secondary structure elements confirming the results of the previous performed three-dimensional protein modeling. Interestingly, due to their differences in the amino acid sequence, the overall number and position of α-helices and β-sheets varied between the assemblages. If and which structure alterations of ADI influence its enzymatic activity is not known so far and thus should be investigated in further experiments.

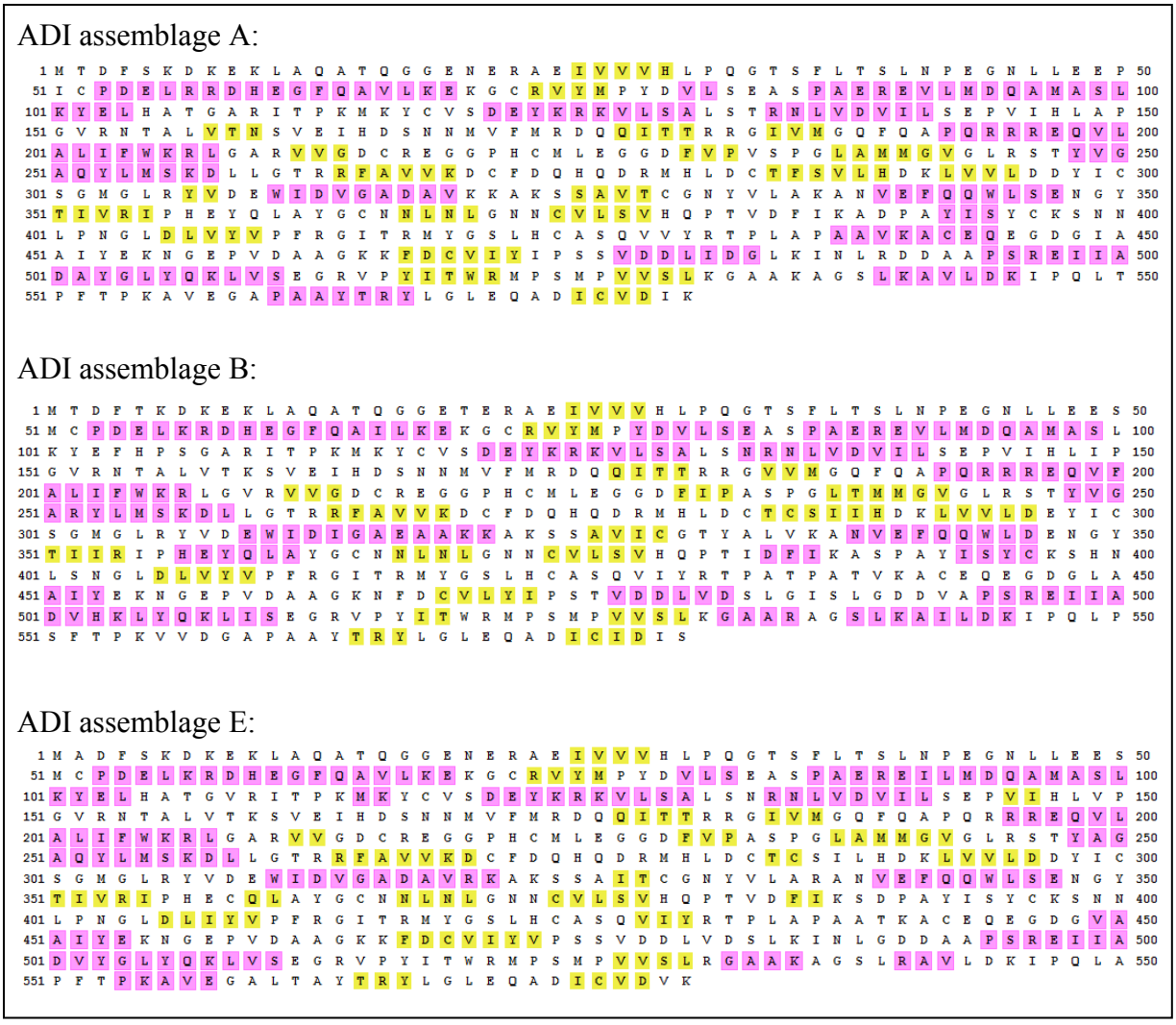

Figure 27: Secondary structure prediction of G. *duodenalis* ADI variants by PSIPRED
Feature predictions are highlighted onto the sequence as follows: yellow = sheet, pink = helix, noncolored = coil.

Next step was to investigate whether there were differences in the amino acids sequence of ADI between patient isolates and the laboratory strain WB-C6 that might be responsible for the variation in substrate affinity. To determine the sequence variability of ADI in strains of

different subgenotypes, the *ArcA* gene was amplified from genomic G. *duodenalis* DNA, sequenced and translated to generate a multiple protein sequence alignment using ClustalW that is shown in Fig. 28. It was noticeable that there exist several amino acid alterations between the subgenotypes AI and AII of ADI that could explain the obtained differences in the K_m values. But also differences in the ADI amino acid sequence within the subgenotype class AII was observed by comparing results obtained for the 115-01/H2 strain with the other clinical isolates at amino acid position 448.

It is of interest whether the exchange of amino acids in the ADI primary structure can influence potential posttranslational modification, e.g. phosphorylation, and therefore can directly or indirectly change its activity. Thus, the web programs NetPhos 2.0 Server (http://www.cbs.dtu.dk/services/NetPhos/) was used to predict for serine, threonine and tyrosine phosphorylation sites (Blom et al., 1999) in G. *duodenalis* WB-C6 ADI. The obtained phosphorylation prediction sites were then compared to the amino acid changes in the ADI sequence of the clinical isolates that belong to the subgenotype AII. This comparison revealed that amino acids potentially important for phosphorylation of the enzyme were not exchanged. However, in case of serine that was predicted to be phosphorylated at amino acid position 495, an amino acid in the direct surrounding is altered in the subgenotype AII (data not shown). Furthermore, the comparison of predicted phosphorylation site between the known protein sequences of ADI assemblage A, B and E that are published in databases show clearly differences in their posttranslational modification pattern (data not shown). If this in consequence leads to changes in functional characteristics of the enzyme is not clear, and should be further investigated.

To sum up, the analysis of the amino acids sequence from native and recombinant ADI give first hints that its differences in substrate affinity could rely on amino acid sequence variants within different (sub)genotypes. However, a definite link of patient's symptoms to functional differences and amino acid variations in ADI is so far not evident.

```
16-01/E1        MTDFSKDKEKLAQATQGGENERAEIVVVHLPQGTSFLTSLNPEGNLLEEPICPDELRRDH 60
115-01/H2       MTDFSKDKEKLAQATQGGENERAEIVVVHLPQGTSFLTSLNPEGNLLEEPICPDELRRDH 60
WB-C6           MTDFSKDKEKLAQATQGGENERAEIVVVHLPQGTSFLTSLNPEGNLLEEPICPDELRRDH 60
                ************************************************************

16-01/E1        EGFQAVLKEKGCRVYMPYDVLSEASPAEREVLMDQAMASLKYELHATGARITPKMKYCVS 120
115-01/H2       EGFQAVLKEKGCRVYMPYDVLSEASPAEREVLMDQAMASLKYELHATGARITPKMKYCVS 120
WB-C6           EGFQAVLKEKGCRVYMPYDVLSEASPAEREVLMDQAMASLKYELHATGARITPKMKYCVS 120
                ************************************************************

16-01/E1        DEYKRKVLSALSTRNLVDVILSEPVIHLAPGVRNTALVTNSVEIHDGNNMVFMRDQQITT 180
115-01/H2       DEYKRKVLSALSTRNLVDVILSEPVIHLAPGVRNTALVTNSVEIHDGNNMVFMRDQQITT 180
WB-C6           DEYKRKVLSALSTRNLVDVILSEPVIHLAPGVRNTALVTNSVEIHDSNNMVFMRDQQITT 180
                ********************************************** *************

16-01/E1        RRGIVMGQFQAPQRRREQVLALIFWKRLGARVVGDCREGGPHCMLEGGDFVPVSPGLAMM 240
115-01/H2       RRGIVMGQFQAPQRRREQVLALIFWKRLGARVVGDCREGGPHCMLEGGDFVPVSPGLAMM 240
WB-C6           RRGIVMGQFQAPQRRREQVLALIFWKRLGARVVGDCREGGPHCMLEGGDFVPVSPGLAMM 240
                ************************************************************

16-01/E1        GVGLRSTYVGAQYLMSKDLLGTRRFAVVKDCFDQHQDRMHLDCTFSVLHDKLVVLDDYIC 300
115-01/H2       GVGLRSTYVGAQYLMSKDLLGTRRFAVVKDCFDQHQDRMHLDCTFSVLHDKLVVLDDYIC 300
WB-C6           GVGLRSTYVGAQYLMSKDLLGTRRFAVVKDCFDQHQDRMHLDCTFSVLHDKLVVLDDYIC 300
                ************************************************************

16-01/E1        SGMGLRYVDEWIDVGADAVKKAKSSAVTCGNYVLAKANVEFQQWLSENGYTIVRIPHEYQ 360
115-01/H2       SGMGLRYVDEWIDVGADAVKKAKSSAVTCGNYVLAKANVEFQQWLSENGYTIVRIPHEYQ 360
WB-C6           SGMGLRYVDEWIDVGADAVKKAKSSAVTCGNYVLAKANVEFQQWLSENGYTIVRIPHEYQ 360
                ************************************************************

16-01/E1        LAYGCNNLNLGNNCVLSVHQPTVDFIKADPAYISYCKSNNLPNGLDLVYVPFRGITRMYG 420
115-01/H2       LAYGCNNLNLGNNCVLSVHQPTVDFIKADPAYISYCKSNNLPNGLDLVYVPFRGITRMYG 420
WB-C6           LAYGCNNLNLGNNCVLSVHQPTVDFIKADPAYISYCKSNNLPNGLDLVYVPFRGITRMYG 420
                ************************************************************

16-01/E1        SLHCASQVVYRTPLAPAAVKACEQEGDGVAAIYEKNGEPVDAAGKKFDCVIYIPSSVDDL 480
115-01/H2       SLHCASQVVYRTPLAPAAVKACEQEGDEVAAIYEKNGEPVDAAGKKFDCVIYIPSSVDDL 480
WB-C6           SLHCASQVVYRTPLAPAAVKACEQEGDGIAAIYEKNGEPVDAAGKKFDCVIYIPSSVDDL 480
                ************************** ******************************

16-01/E1        IDGLKINLRDDAALSREIIADAYGLYQKLVSEGRVPYITWRMPSMPVVSLKGAAKAGSLK 540
115-01/H2       IDGLKINLRDDAALSREIIADAYGLYQKLVSEGRVPYITWRMPSMPVVSLKGAAKAGSLK 540
WB-C6           IDGLKINLRDDAAPSREIIADAYGLYQKLVSEGRVPYITWRMPSMPVVSLKGAAKAGSLK 540
                ************ ************************************************

16-01/E1        AVLDKIPQLTPFTPKAVEGAPAAYTRYLGLEQADICVDIK 580
115-01/H2       AVLDKIPQLTPFTPKAVEGAPAAYTRYLGLEQADICVDIK 580
WB-C6           AVLDKIPQLTPFTPKAVEGAPAAYTRYLGLEQADICVDIK 580
                ****************************************
```

Figure 28: Amino acid alignment of native ADI variants from different G. *duodenalis* strains

The amino acid differences in the ADI sequences of clinical isolates and the laboratory strain WB-C6 were highlighted in yellow. Because of having an identical sequence, 16-01/E1 is shown representatively for 11-04/E3 and 14-03/F7.

5 Discussion

Giardiasis is one of the most prevalent parasitic diseases worldwide. Its causative agent *G. duodenalis* infects human and other mammals that in consequence can suffer from intestinal malabsorption and (chronic) diarrhea. Giardial infections influence humans in two ways: directly by being a major public health concern in developing and developed countries, and indirectly by constituting an economical problem e.g. when livestock, like cattle, are affected.

So far, no vaccine against human giardiasis is available. In the past, it was tried to immunize domestic animals with commercial available or self-prepared veterinary vaccines. Subsequent experimental infections of kittens showed that vaccination does not prevent infection but reduces intensity of symptoms and secretion of cysts (Olson et al., 1996). However, this partial success of vaccination was rebutted for other animals like calves (Uehlinger et al., 2007). To cure *G. duodenalis* infections several drugs are administered. Unfortunately, in humans treatment failures, e.g. due to development of resistance, occur. Additionally, patients often have a bad compliance caused by several side effects like acid regurgitation and nausea (Upcroft and Upcroft, 1993; Lalle, 2010). Thus, the development of new treatment or prevention strategies is indispensable. One possibility to find new drug targets is the identification of virulence factors. To date, certain *Giardia*-induced mechanisms that enable the parasite to handle or evade the host's immune systems are described. Furthermore, also factors that are potentially involved in parasite virulence, like the *G. duodenalis* ADI, were noticed. For the treatment of giardiasis the *G. duodenalis* ADI is an interesting parasite-specific target for the design of new drugs because its expression is limited to the parasite, it catalyzes the first step in the parasite's energy metabolism and it seems to be involved in host-parasite interplay (Ankarklev et al., 2010; Rópolo and Touz, 2010).

The aim of this study was to find distinct hints that confirm the role of *G. duodenalis* ADI as a virulence factor. Therefore, the enzyme's genetic diversity and its role in host-parasite interaction were analyzed. The impact of recombinant *G. duodenalis* ADI on DC initiating host's adaptive immune response was investigated. Furthermore, the influence of viable parasites expressing native *G. duodenalis* ADI on epithelial cells that serving as guardians of the mucosal immunity was studied. By sequencing and enzyme kinetics of both, native and recombinant *G. duodenalis* ADI, a potential link between substrate affinity and genotypic diversity was investigated.

5.1 *G. duodenalis* ADI is involved in host-pathogen interplay

One strategy of several pathogens to evade immune effector mechanisms is to deplete arginine with microbial enzymes. As part of their virulence mechanisms, these enzymes often compete with the host enzymes for the same substrate leading to a limited immunological response. An intensively studied example is the arginine-depleting enzyme arginase that is expressed by pathogens to compete for arginine with the host's NOS to prevent the formation of anti-microbial NO (Bronte and Zanovello, 2005; Das et al., 2010). Another arginine-metabolizing enzyme, the ADI, has been implicated in virulence of several other microbes like *Streptococcus, Mycoplasma* and *Listeria* (Gong et al., 1999; Benga et al., 2004; Ryan et al., 2009; Fulde et al., 2011). Which impact the enzymatic activity of *G. duodenalis* ADI, that means the consumption of arginine to form citrulline and ammonia, has on host defense mechanism is less understood and thus was investigated. The results of this study shall be discussed in the following.

5.1.1 Interaction between *G. duodenalis* ADI and human moDC

5.1.1.1 Usage of human moDC as host cells

As linker between innate and adaptive immune response, DC are important in pathogen clearance mechanism. As described, they are able to control the gut lumen with their dendrites and thereby can come into close contact with parasites like *Giardia* during an infection. To date, only two studies with murine cells have been published that investigated the interaction of *Giardia* parasites with DC (Kamda and Singer, 2009; Kamda et al., 2012). These studies revealed that DC are critical for clearance of *Giardia* infections in mice and that the parasite has the ability to modulate their function.

Prior studying the interaction of *Giardia* with DC, several experimental conditions were pondered for the following reasons. To generate a surrounding that is related those in human infections and to ensure that enough cells were available for the planned experiments, it was decided to generate and use DC from human moDC. This moDC were stimulated with different concentrations of LPS, because treatment with recombinant enzyme alone did not lead to DC activation. Interestingly, also a previous study has shown that *Giardia* extracts or live trophozoites were found to weakly activate mouse DC (Kamda and Singer, 2009). For investigation of host-parasite interplay, DC were treated with recombinant enzyme instead of

live *Giardia* trophozoites. This was done for several reasons. First, moDC grow in suspension and thus do not form a monolayer where *Giardia* trophozoites can attach, second both cell types have different oxygen requirements, and third it is not clear whether trophozoites release and to which extent *G. duodenalis* ADI in absence of IEC. An alternative would be the usage of *G. duodenalis* lysates as it was done by Kamda and Singer (2009). However, in this case it cannot be excluded that other factors than ADI lead to a resultant DC phenotype or if these factors influence the ADI function.

5.1.1.2 Consequences of moDC treatment with *G. duodenalis* ADI

G. duodenalis ADI was shown to modulate cell surface markers and cytokine response of *in vitro* activated human moDC. In the past, studies illustrated that especially cytokines are necessary in host defense against *Giardia* (Bienz et al., 2003; Zhou et al., 2003; Zhou et al., 2007). In this report, determination of several pro- and anti-inflammatory cytokine revealed a cytokine-specific influence of ADI that resulted in an impaired secretion of IL-10 and IL-12p40 and increased levels of TNF-α compared to untreated DC. The release of cytokines is a complex immunological network where single components depend on each other, e.g. it is known that anti-inflammatory IL-10 suppresses the production of pro-inflammatory TNF-α (Armstrong et al., 1996; Williams et al., 2004). Thus, the observed increased TNF-α release might be a consequence of impaired IL-10 release. Children suffering from symptomatic giardiasis were shown to have increased mucosal levels of pro-inflammatory cytokines including TNF-α, which decreased after anti-parasitic treatment and resolution of symptoms while local levels of IL-10 increased after treatment (Maciorkowska et al., 2005). This is in agreement with the *in vitro* findings of this study and may indicate that ADI activity impairing IL-10 and enhancing TNF-α secretion by mucosal DC could underlay the *in situ* observation in samples from these children. The relative abundance of IL-10 and TNF-α is recognized as a critical parameter in intestinal diseases in mice (Kontoyiannis et al., 2001) and humans (Glocker et al., 2011; Ordás et al., 2012). Another report, correlating with the results of this study, identified increased serum levels of TNF-α in Turkish children infected with *G. duodenalis*. After treatment with MTZ, patients became free of parasites and cytokine level returned to normal state (Bayraktar et al., 2005). Additionally, Kamda and Singer (2009) recognized small amount of TNF-α after stimulation of mouse bone marrow-derived DC with live *Giardia* trophozoites and *Giardia* extracts.

After release of ADI, which function does the increasing TNF-α secretion and the arginine depletion and formation of ammonia and citrulline have for the parasite? Arginine-dependent response modulation would be consistent with observations on the pathophysiology of human giardiasis. Atrophy of villi has been detected microscopically in intestinal biopsies of chronically infected patients, and symptomatic disease has been correlated with a dysfunction of the epithelial barrier (Troeger et al., 2007) but the process leading to this is not yet understood. These sequelae can, however, also be observed when a human intestinal epithelial cell line is treated with TNF-α (Schmitz et al., 1999). TNF-α may thus have pathogenic properties in this context. Studies in mice showed that peak level *Giardia* parasite loads were around 10-fold higher in animals devoid of TNF-α (Zhou et al., 2007) hence it was proposed that it has a protective function in giardiasis. However, in the same study transepithelial resistance was reduced to the same extent despite a much lower parasite burden in TNF-α responsive mice. An explanation consistent with the results from human epithelial cell line exposed to TNF-α (Schmitz et al., 1999) could be that reduced epithelial integrity during giardiasis is due to parasite factors and TNF-α, the latter exerting a dual (protective and pathogenic) role. Interestingly, beside ADI also OCT (the next enzyme in the ADH pathway) is released by the parasite in contact with intestinal cells *in vitro* (Ringqvist et al., 2008) and was detected, like ADI, to be an immunodominant antigens during infection (Palm et el., 2003; Téllez et al., 2005). This indicates that significant amounts of both enzymes are found extracellular and therefore free citrulline generated by ADI may even be further metabolized to ornithine by OCT. It is tempting to speculate that this may exacerbate TNF-α production because the negative feedback of citrulline (which was observed in this study) on this parameter would be reduced. Thus, release of ADH compounds could have evolved in part due to selective pressure by the host's immune response.

Another observation of this study was that the expression of the surface molecules CD86 and CD83 was impaired after treatment of LPS-activated moDC with ADI. The reduction of CD86 was also seen by Kamda and Singer (2009) after treatment of LPS-stimulated murine bone marrow-derived DC with *Giardia* extract. If the parasite, in addition to ADI, possess several other immunomodulatory factors is unclear and further studies are needed to identify their molecular nature. Nevertheless, it is conceivable that the parasite actively changes DC function to negatively influence the activation of the host's adaptive immune response. Intact cell-cell interplay between APC and T cells is indispensable, especially during giardial infection where T cells were indicated to be involved in parasite elimination.

5.1.1.3 Reasons for immunomodulation of moDC by *G. duodenalis* ADI

Although DC are important for adaptive immunity against microbial infections, the effect of pathogen-mediated arginine depletion on their function is not clear yet. It is known, that arginine-dependent virulence mechanisms of pathogens rely on enzymes such as arginases or deiminases that deplete arginine but also generate reaction products at the same time. Of note, these products differ between these classes of enzymes that generate ornithine and urea or citrulline and ammonia, respectively. Commonly, changes of immune cell responses due to different arginine levels have been studied by comparing responses in the presence or absence of arginine. However, this does not reflect the situation when arginine is depleted by an enzymatic reaction as it can be the case during infections. Yet, the combined effect of arginine depletion by an enzymatic reaction and the ensuing product formation on immune cells has largely been ignored. Thus, after monitoring the immunomodulatory effects on *in vitro* activated human moDC after treatment with recombinant ADI, it was tested whether arginine depletion and/or the generated reaction products citrulline and NH_4^+ are responsible for the obtained phenotype. It was recognized in this study, that DC modulation of cell surface markers and cytokine response required parasite enzyme activity and the effects depend on both, depletion of arginine and the ADI reaction products, in particular NH_4^+. This was the first time showing an immunomodulatory effect of arginine depletion and NH_4^+ formation on the response of DC other than on NO formation known from other pathogens like *Helicobacter pylori* (Gobert et al., 2001) and *Leishmania spp.* (Gaur et al., 2007) that rely on the action of arginases.

As mentioned before, both arginases and ADI have been associated with pathogen virulence. Both deplete arginine but their reaction products ornithine/urea and citrulline/NH_4^+ differ. In this work it was noticed that NH_4^+ but not urea exacerbated the inhibition of IL-10 production and surface marker upregulation compared with arginine depletion alone. These findings suggest a difference between the products of arginases and deiminases with respect to their potency of modulating human moDC cytokine secretion and surface marker expression. More widely, it can be hypothesized that pathogens have evolved diverse arginine-dependent immunomodulation mechanisms. Of note, ADI homologues have been implicated in the virulence of *Streptococci* isolates (Fulde et al., 2011) affecting intracellular survival of the bacteria (Benga et al., 2004) and inhibiting proliferation of PBMC *in vitro* (Degnan et al., 1998). It will be interesting to investigate whether ADI in the case of these bacterial infections has similar extended immunomodulatory activity as described here for *G. duodenalis* ADI.

In this study, the reduction of surface located CD83 correlated with an inhibition of the mTOR pathway since phosphorylation of the mTOR S6K target protein was decreased after treatment of DC with *G. duodenalis* ADI. Precedence for a clinically relevant role of amino acids in modulating immune responses exists (Evoy et al., 1998; Calder, 2006). Thereby, for example arginine is not only necessary for generation of NO but it plays also other important roles during immune response. Lack of arginine was shown to inhibit T-cell function (Zea et al., 2004), and arginine levels affect signaling *via* the mTOR pathway as reported for other cells (Ban et al., 2004; Yao et al., 2008). So far, the role of arginine for mTOR signaling in DC is not known. However, for DC it has been shown that branched-chain amino acids affect maturation, and it has been proposed that this modulation is a consequence of inhibition of the mTOR pathway (Kakazu et al., 2007). The results of this study are consistent with this hypothesis but extend the concept to arginine. Of note, NH_4^+ has recently been reported to modulate mTOR activity in yeast cells (Santos et al., 2012). This suggests that reaction products formed by arginine-depleting enzymes could further affect mTOR signaling. However, additional signaling pathways are likely to be involved in mediating the distinct effects of arginine depletion alone and NH_4^+ formation. The latter has recently also been invoked in the T cell inhibition mediated by *Salmonella* L-asparaginase II (Kullas et al., 2012). Further studies are required to understand this comprehensively.

To sum up, it was shown that enzymatic activity of *G. duodenalis* ADI modulates surface markers and cytokine response of *in vitro* activated human moDC. It is suggested that the resultant impaired IL-10 and enhanced TNF-α secretion plays a central role in pathogenesis and that the reduced upregulation of surface CD83 and CD86 molecules, partially caused due to inhibition of the mTOR signaling pathway, can influence the adaptive immune response. These alterations of DC function were identified to depend on both, depletion of arginine and the ADI reaction products, in particular NH_4^+. That arginine depletion may indeed occur *in situ* by release of ADI was calculated here and thus the ability to modulate DC function could provide a selective advantage to the parasite. Furthermore, the comparison of NH_4^+ and urea revealed distinct immunomodulatory activities for these products of deiminases and arginases, respectively. These data implicate that arginine-metabolizing enzymes of pathogens are more widely involved in immunomodulation of DC and suggest distinct roles for the reaction products of different enzyme classes in this process. This observation can contribute to the general understanding of arginine-dependent virulence mechanisms of pathogens.

5.1.2 Interaction between *G. duodenalis* ADI and Caco-2 cells

Structures and functions of mucosal immunity are complex. So far, the communication between *Giardia* as parasite and IEC as well as DC as host cells is less understood.

Evidences for the interaction of host and parasite were revealed in this study. It was observed that *G. duodenalis* was more aerotolerant in the presence of Caco-2 cells. This phenomenon was also recognized by Roxström-Lindquist et al. (2005) and was found during co-cultivation of tissue culture cells with other anaerobic bacteria (Claesson and Gotthardsson, 1988; Hosogi and Duncan, 2005). Additionally, Roxström-Lindquist et al. (2005) showed an induced secretion of CCL20, a chemokine being important for DC recruitment, by IEC after *in vitro* treatment of the cells with the parasite. Same results were obtained after contact of IEC with trophozoite-free medium from a *Giardia* culture indicating that secreted parasitic factor(s) are involved in upregulation of the chemokine response. That secreted *Giardia* factors can influence IEC function was given by Lee et al. (2012) showing that excretory-secretory products of the parasite are able to induce IL-8 production in HT-29 cells. As described, a known parasitic factor of *G. duodenalis* that is released *in vivo* and *in vitro* in the intestine is its ADI (Ringqvist et al., 2008). Microarray analysis of the parasitic transcriptional response to host cell contact revealed a transient upregulation of ADI mRNA levels within 1.5 h (Ringqvist et al., 2011). The observation that release occurs already within 15 min after contact of the parasite with Caco-2 cells (Ringqvist et al., 2008) was confirmed in this study. Furthermore, host induced release of ADI was identified to occur independent from the subassemblage by all investigated *G. duodenalis* strains and thus indicating its general role in host-parasite interaction. Commonly, eukaryotic secretory proteins are translocated by the endoplasmic reticulum (ER)-Golgi pathway to the cell surface and are released there into the extracellular space (Nickel, 2003). *G. duodenalis* lacks an intact ER/Golgi system and its ADI does not contain a classical signal peptide being necessary for this route. In future, it needs to be investigated whether the release of the enzyme is mediated by unconventional protein export, e.g. by formation of exosomes, as known for other proteins (Nickel, 2003).

Release of ADI is also known from other microbes like *Streptococcus* (Christopher et al., 2010), but its function in context with giardiasis is not understood yet. It is supposed that the resultant arginine depletion and formation of reaction products by enzymatic active *G. duodenalis* ADI influences the immunological function of IEC and thus is involved in disease mechanism. Reduced NO production in consequence of arginine depletion by pathogenic upregulation of host arginases was observed in several infectious diseases (Lahiri

et al., 2008; Lewis et al., 2010; Andrade et al., 2012). Also other arginine-depleting enzymes as the recombinant *Mycoplasma* ADI were shown to negatively affected the NO formation in macrophages *in vitro* (Noh et al., 2002). *In vitro* investigations of *G. duodenalis* WB-C6 (Eckmann et al., 2000) as well as its recombinant ADI (Ringqvist et al., 2008) revealed inhibition of NO formation of human IEC by consumption of free arginine. Additionally, this study identified that *G. duodenalis* strains of another subgenotype than the laboratory strain WB-C6 were able to reduce NO to a similar extent. As NO is known to disturb differentiation and growth of *Giardia* (Eckmann et al., 2000), it seems to be that arginine consumption by ADI to prevent its formation by the host is an alternative to the upregulation of host arginases and used as general defense mechanism by the parasite.

Beside reduction of NO formation, arginine depletion by *G. duodenalis* ADI led to reduced proliferation of human IEC lines *in vitro* (Stadelmann et al., 2012). This ability of ADI to inhibit growth was also shown for *Mycoplasma*-infected cells, e.g. tumor cell lines, indicating a complex role of the enzyme in disease mechanisms (Miyazaki et al., 1990; Takaku et al., 1992). To further investigate the multiple function of ADI in giardiasis, the communication between IEC and DC during giardial infection should not be disregarded. Microarray analysis revealed an upregulation of the TNF-α receptor on IEC after contact with *Giardia* trophozoites *in vitro* indicating an activation of intestinal epithelium to respond to TNF-α (Roxström-Lindquist et al., 2005). In this study, an upregulation of TNF-α secretion was recognized by ADI-treated moDC *in vitro*. Although Li et al. (2006) described NOS-1 to be involved in the elimination of giardial infection in mice, this and other studies (Eckmann et al., 2000) showed that infection of human IEC cultures with *G. duodenalis* inhibits epithelial NO production under TNF-α stimulation. A linkage between TNF-α and NO was represented in *Giardia* independent study where rats were stimulated intraperitoneally with LPS. NO was upregulated in the duodenum by increasing levels of TNF-α. Interestingly, some of these rats developed diarrhea (Arya et al., 2000). This, in turn, could be a consequence of the increasing NO level as NO is discussed to be linked to secretion of water in the intestine (Mourad et al., 1999; Kukuruzovic et al., 2002).

Here, it is suggested that there exists a linkage between DC response to *G. duodenalis* ADI and IEC function in giardiasis. This should be further investigated in an adequate *in vitro* or *in vivo* model where several cell types can be treated with *G. duodenalis* ADI in parallel.

5.1.3 Interaction between *G. duodenalis* ADI and host proteins

Enzymes of mammals like human PADs are able to citrullinate intrapeptidic arginine in proteins. That kind of posttranslational modification can lead to an altered biological function of the affected protein or disrupt its interaction with other molecules. This was shown in the immunological context by Proost et al. (2008) where PAD purified from rabbit skeletal muscle citrullinated the chemokine CXCL8 and in consequence altered the neutrophil extravasation during inflammation. ADI-mediated citrullination of e.g. receptors of host immune cells would give *Giardia* the ability to immunomodulate and thus to escape the host immune response. Such a dual function of the enzyme to deiminate free and intrapeptidic arginine is known from the pathogen *Porphyromonas gingivalis* that causes periodontitis (Shirai et al., 2006; Rodríguez et al., 2009). Although no pad homologous genes have been found in the *Giardia* genome, Touz et al. (2008) revealed a PAD activity for *G. duodenalis* ADI. Although using the same reaction conditions, this result could not be confirmed in this study. That the parasite's ADI cannot citrullinate intrapeptidic arginine was also shown by Li et al. (2009) and thus the results described here were in agreement with their *in vitro* test. The main difference and a possible explanation for the contrary results is that Touz et al. (2008) used ADI purified from *G. duodenalis* trophozoites in contrast to the here used purified *G. duodenalis* ADI expressed recombinantly in *E. coli*. *In vivo* overexpression in eukaryotes allowed potential posttranslational modification of the native ADI that might impact its function, whereas expression in bacteria did not. It remains unclear whether the observed PAD activity does really exist and, if so, whether it has physiologically relevance.

5.2 *G. duodenalis* ADI has assemblage-associated genotypic and functional differences

One characteristic feature of human giardial infection is its variable outcome among patients. It is discussed whether clinical symptoms are correlated to the assemblage type of the parasite. Several investigations describe infections with assemblage A parasites to be more severe than those with assemblage B parasites (Haque et al., 2005; Sahagún et al, 2008). Other studies showed assemblage B parasites to be more pathogenic (Homan and Mank, 2001; Mohammed Mahdy et al., 2009). Controversially, Kohli et al. (2008) demonstrated both assemblage types to cause similar illness. Same results but with trends to certain symptoms, e.g. that assemblage AII was more often associated with abdominal pain, nausea and vomiting (Sarkari et al., 2012) or fever (Breathnach et al., 2010) and flatulence was linked to

assemblage B (Lebbad et al., 2011), were noticed by others. Additionally, experiments with *Giardia*-infected gerbils (Bénéré et al., 2012) and IEC (Koh et al., 2013) confirmed assemblage-specific differences in pathogenicity.

Comparative genomic analyses were used to identify virulence factors for other pathogens (Sahl et al., 2013; Tang et al., 2013). Gene sequence alignment of *G. duodenalis* ADI revealed assemblage-specific differences being characteristically for a virulence factor. In detail, a nucleotide identity of 81% between A-B, 89% between A-E and 80% between B-E and an amino acid identity of 89% between A-B, 94% between A-E and 89% between B-E was determined. If *G. duodenalis* ADI, as potential virulence factors, has sequence-variability that leads to functional differences was investigated. Therefore, recombinant ADI (assemblage A, B and E) and the native enzyme (different subtypes of assemblage A) were genotypically and functionally characterized in this study.

ADI is expressed by several microorganisms and was identified to be highly specific for arginine as substrate in the 1960s (Kihara and Snell, 1957; Petrack et al., 1957). Here, biochemical characterization of recombinant *G. duodenalis* ADI (assemblage A) revealed a K_m value of 0.58 mM for arginine. In a similar range, Li et al. (2009) described a K_m value of 0.16 mM. The deviation can be explained by usage of different buffer and reaction conditions (pH, temperature). The determined K_m value for *G. duodenalis* ADI was comparable to those observed for ADI of other microbes like *Pseudomonas plecoglossicida* with $K_m = 0.7$ mM arginine (Zhu et al., 2010) or *Burkholderia mallei* with $K_m = 0.09$ mM arginine (Li et al., 2008). Comparison of native and recombinant *G. duodenalis* ADI (both WB-C6; assemblage AI) revealed a twofold difference in the K_m value at the same reaction conditions. This might be due to (different) factors included in the used *Giardia* or *E. coli* lysate influencing the enzyme directly or indirectly. Furthermore, a threefold difference in substrate affinity between recombinant enzymes of assemblage A and E to B was detected. As assemblage A and E ADI are closer related in their amino acid sequence, a correlation between genotype and enzyme activity is indicated. The comparison of K_m value of native ADI expressed by different *G. duodenalis* isolates revealed a subassemblage-specific difference in substrate affinity as well. That amino acid exchange in proteins results in changes of the K_m value was shown for other microorganisms like *Mycoplasma hominis* where ADI mutation leads to a shift from 0.24 mM to 0.71 mM (Wei et al., 2007). In *Pseudomonas aeruginosa* the substrate affinity to arginine changed from 0.14 mM of the wild-type enzyme to 1.1-38 mM in mutant ADI's (Lu et al., 2006).

It is assumed that the differences in K_m values are correlated to the ADI sequence variations of the certain *G. duodenalis* strains. *G. duodenalis* ADI belongs to the guanidino group-modifying enzyme superfamily, which conserves a Cys-, His-, and Asp-based catalytic core (Li et al., 2009). Further details of its three dimensional structure are less understood. It is important to investigate to which extent the amino acid differences between the individual (sub)assemblages influence the active site of the enzyme. Therefore, amino acid substitution in both, the native *G. duodenalis* ADI (transgenic parasites) and the recombinant enzyme should be performed.

Posttranslational modifications are known to influence protein structure and function. For example, alteration of enzyme activity was shown in studies of Mesojednik and Legisa (2005) where activity of degraded 6-phosphofructo-1-kinase of *Aspergillus niger* was restored after induction of phosphorylation. Possible posttranslational modifications of *G. duodenalis* ADI are unclear. A previously described (Touz et al., 2008) higher-molecular-mass 85-kDa form of native *G. duodenalis* ADI, caused by sumoylation, could not be confirmed in this study. This does not exclude posttranslational modification of the parasite's ADI at all. For this reason, it should be tested whether amino acids differences in ADI (sub)assemblages changes posttranslational modification patterns of the enzyme which in turn could influence its activity.

5.3 Future perspectives

This work revealed two major hints for ADI to be a (molecularly defined) virulence and pathogenicity factor of *G. duodenalis* and thus potentially disease-causing or at least involved in the establishment of the infection. First, recombinant *G. duodenalis* ADI as well as *G. duodenalis* ADI variants of clinical isolates (including the laboratory strain WB-C6) were identified to have substrate affinity differences probably caused through sequence variation. It is speculated, that the ADI activity might be related in this context to different disease outcome. Second, *G. duodenalis* ADI was identified to be immunomodulating. It was observed that as consequence of enzyme activity surface markers and cytokine response of *in vitro*-activated human moDC was changed. This depended on both, depletion of arginine and the ADI reaction products, in particular NH_4^+. By investigating the *in vitro* consequences of arginine depletion, it was recognized that the mTOR pathway is implicated in the molecular signaling process and leads in part to the modulation of DC response. Furthermore,

a modulating effect on the response of IEC was observed *in vitro* as well. *G. duodenalis* trophozoites of different clinical isolates reduced the NO formation of Caco-2 cells, probably due to the consumption of arginine by the parasite's ADI. Together with the observation that immunomodulation and arginine-metabolizing enzymes were also noticed to be implicated in pathogen's virulence and immune evasion mechanisms in a broad range of other infections, the hypothesis of *G. duodenalis* ADI to be a virulence factor was strengthened.

The relevance of these *in vitro* findings for the understanding of the pathogenesis of giardiasis must remain speculative at the moment. It can only be suggested that the modification of DC and IEC function by its ADI provides a selective advantage for the parasite to evade the host immune response. To clarify if this is also true in human infections, further studies are required. Thereby, the communication between different immune cells as response to a giardial infection should be considered. For example, it would be interesting to investigate how T cells and IEC were affected by *G. duodenalis* ADI-modified DC *in vivo*.

To study host-parasite interplay in giardial infections, *in vivo* animal models are necessary, but difficult to establish as e.g. infection of mice is limited to certain *G. duodenalis* strains (Solaymani-Mohammadi and Singer, 2011). Thus, an adequate *in vitro* model that is closer related to the *in vivo* situation should be established. An option might be the usage of intestine-like structures. Such organoids have been established from primary human intestinal tissue (Sato et al., 2011) and human induced pluripotent stem cells (Spence et al., 2011). These 3D structures do not reproduce the *in vivo* situation completely e.g. due to lacking immune cells, but give a well-differentiated intestinal epithelial tissue for *in vitro* investigations (Klotz et al., 2012). To further analyze the role of ADI in giardial infections, organoids can be treated with either recombinant or native enzyme. The latter can be used as purified enzyme from *G. duodenalis* trophozoites (of different assemblages) transiently overexpressing ADI or by directly adding these trophozoites. As negative control, an ADI knockdown in *Giardia* parasites should be generated (e.g. by antisense technique). As ADI is possibly essential for the parasite's survival due to its role in ATP metabolism, a functional knockout of the enzyme should be avoided. The possibility to genetically manipulate the parasite was shown by Touz et al. (2008) who already overexpressed ADI in *G. duodenalis*.

In continuing experiments, an alternative to trophozoites overexpressing ADI would be the use of cell culture supernatants from *Giardia*-treated Caco-2 cells containing the released native enzyme. However, the presence of other enzymes that were described to be released (e.g. enolase) by the parasite (Ringqvist et al., 2008) can be prejudicially. Another method

would be to infect mice with *G. duodenalis* trophozoites and to immunoprecipitate native ADI from the intestine by using the generated anti-*Gd* ADI antiserum. Thereby, the possibility that mice cannot be infected with all *G. duodenalis* strains has to be considered.
Furthermore, for functional epidemiology it is necessary to augment the number of available *G. duodenalis* isolates of symptomatic and asymptomatic patients within the *Giardia* biobank. The more ADI variants can be by characterized on basis of epidemiological data, the higher the chance to identify a potential link between enzyme function and clinical pathology.

Further investigation will show whether *G. duodenalis* ADI is a virulence factor and thus a potential new target for treatment strategies and drug design. If so, developing of *G. duodenalis* ADI inhibitors or supplementation of arginine, as shown for other parasitic infections (Castro et al., 2012), might be approaches to cure giardiasis.

6 References

Adam RD. 2001. Biology of *Giardia lamblia*. *Clin Microbiol Rev.* 14(3):447-75.

Aggarwal A, Nash TE. 1988. Antigenic variation of *Giardia lamblia in vivo*. *Infect Immun*. 56(6):1420-3.

Alberts B, Johnson A, Lewis J, Raff M, Roberts K, Walter P. 2002. Molecular Biology of the Cell. 4th edition. New York: *Garland Science*; Cell Junctions.

Aley SB, Zimmerman M, Hetsko M, Selsted ME, Gillin FD. 1994. Killing of *Giardia lamblia* by cryptdins and cationic neutrophil peptides. *Infect Immun*. 62(12):5397-403.

Altschul SF, Madden TL, Schäffer AA, Zhang J, Zhang Z, Miller W, Lipman DJ. 1997. Gapped BLAST and PSI-BLAST: a new generation of protein database search programs. *Nucleic Acids Res*. 25(17):3389-402.

Amar CF, Dear PH, Pedraza-Díaz S, Looker N, Linnane E, McLauchlin J. 2002. Sensitive PCR-restriction fragment length polymorphism assay for detection and genotyping of *Giardia duodenalis* in human feces. *J Clin Microbiol*. 40(2):446-52.

Anderson JM, Van Itallie CM, Peterson MD, Stevenson BR, Carew EA, Mooseker MS. 1989. ZO-1 mRNA and protein expression during tight junction assembly in Caco-2 cells. *J Cell Biol*. 109(3):1047-56.

Andrade MR, Amaral EP, Ribeiro SC, Almeida FM, Peres TV, Lanes V, D'Império-Lima MR, Lasunskaia EB. 2012. Pathogenic *Mycobacterium bovis* strains differ in their ability to modulate the proinflammatory activation phenotype of macrophages. *BMC Microbiol*. 12:166.

Ankarklev J, Jerlström-Hultqvist J, Ringqvist E, Troell K, Svärd SG. 2010. Behind the smile: cell biology and disease mechanisms of *Giardia* species. *Nat Rev Microbiol*. 8(6):413-22.

Armstrong L, Jordan N, Millar A. 1996. Interleukin 10 (IL-10) regulation of tumour necrosis factor alpha (TNF-alpha) from human alveolar macrophages and peripheral blood monocytes. *Thorax*. 51(2):143-9.

Arnold K, Bordoli L, Kopp J, Schwede T. 2006. The SWISS-MODEL workspace: a web-based environment for protein structure homology modelling. *Bioinformatics*. 22(2):195-201.

Arya R, Grossie VB Jr, Weisbrodt NW, Lai M, Mailman D, Moody F. 2000. Temporal expression of tumor necrosis factor-alpha and nitric oxide synthase 2 in rat small intestine after endotoxin. *Dig Dis Sci*. 45(4):744-9.

Ballweber LR, Xiao L, Bowman DD, Kahn G, Cama VA. 2010. Giardiasis in dogs and cats: update on epidemiology and public health significance. *Trends Parasitol*. 26(4):180-9.

Ban H, Shigemitsu K, Yamatsuji T, Haisa M, Nakajo T, Takaoka M, Nobuhisa T, Gunduz M, Tanaka N, Naomoto Y. 2004. Arginine and Leucine regulate p70 S6 kinase and 4E-BP1 in intestinal epithelial cells. *Int J Mol Med*. 13(4):537-43.

Banchereau J, Briere F, Caux C, Davoust J, Lebecque S, Liu YJ, Pulendran B, Palucka K. 2000. Immunobiology of dendritic cells. *Annu Rev Immunol*. 18:767-811.

Bayraktar MR, Mehmet N, Durmaz R. 2005. Serum cytokine changes in Turkish children infected with *Giardia lamblia* with and without allergy: Effect of metronidazole treatment. *Acta Trop*. 95(2):116-22.

Belosevic M, Faubert GM, MacLean JD. 1989. Disaccharidase activity in the small intestine of gerbils (*Meriones unguiculatus*) during primary and challenge infections with *Giardia lamblia*. *Gut*. 30(9):1213-9.

Bénéré E, Van Assche T, Van Ginneken C, Peulen O, Cos P, Maes L. 2012. Intestinal growth and pathology of *Giardia duodenalis* assemblage subtype A(I), A(II), B and E in the gerbil model. *Parasitology*. 139(4):424-33.

Benga L, Goethe R, Rohde M, Valentin-Weigand P. 2004. Non-encapsulated strains reveal novel insights in invasion and survival of *Streptococcus suis* in epithelial cells. *Cell Microbiol*. 6(9):867-81.

Benyacoub J, Pérez PF, Rochat F, Saudan KY, Reuteler G, Antille N, Humen M, De Antoni GL, Cavadini C, Blum S, Schiffrin EJ. 2005. *Enterococcus faecium* SF68 enhances the immune response to *Giardia intestinalis* in mice. *J Nutr*. 135(5):1171-6.

Berkman DS, Lescano AG, Gilman RH, Lopez SL, Black MM. 2002. Effects of stunting, diarrhoeal disease, and parasitic infection during infancy on cognition in late childhood: a follow-up study. *Lancet*. 359(9306):564-71.

Bernander R, Palm JE, Svärd SG. 2001. Genome ploidy in different stages of the *Giardia lamblia* life cycle. *Cell Microbiol*. 3(1):55-62.

Bicker KL, Thompson PR. 2013. The protein arginine deiminases: Structure, function, inhibition, and disease. *Biopolymers*. 99(2):155-63.

Bienz M, Dai WJ, Welle M, Gottstein B, Müller N. 2003. Interleukin-6-deficient mice are highly susceptible to *Giardia lamblia* infection but exhibit normal intestinal immunoglobulin A responses against the parasite. *Infect Immun*. 71(3):1569-73.

Blom N, Gammeltoft S, Brunak S. 1999. Sequence and structure-based prediction of eukaryotic protein phosphorylation sites. *J Mol Biol*. 294(5):1351-62.

Bogdan C. 2001. Nitric oxide and the immune response. *Nat Immunol*. 2(10):907-16.

Bordoli L, Kiefer F, Arnold K, Benkert P, Battey J, Schwede T. 2009. Protein structure homology modeling using SWISS-MODEL workspace. *Nat Protoc*. 4(1):1-13.

Boreham PF, Upcroft JA, Upcroft P. 1990. Changing approaches to the study of *Giardia* epidemiology: 1681-2000. *Int J Parasitol*. 20(4):479-87.

Botero-Garcés JH, García-Montoya GM, Grisales-Patiño D, Aguirre-Acevedo DC, Alvarez-Uribe MC. 2009. *Giardia intestinalis* and nutritional status in children participating in the complementary nutrition program, Antioquia, Colombia, May to October 2006. *Rev Inst Med Trop Sao Paulo*. 51(3):155-62.

Böger RH. 2007. The pharmacodynamics of L-arginine. *J Nutr*. 137(6 Suppl 2):1650S-55S.

Breathnach AS, McHugh TD, Butcher PD. 2010. Prevalence and clinical correlations of genetic subtypes of *Giardia lamblia* in an urban setting. *Epidemiol Infect*. 138(10):1459-67.

Bronte V, Zanovello P. 2005. Regulation of immune responses by L-arginine metabolism. *Nat Rev Immunol*. 5(8):641-54.

Buret A, Hardin JA, Olson ME, Gall DG. 1992. Pathophysiology of small intestinal malabsorption in gerbils infected with *Giardia lamblia*. *Gastroenterology*. 103(2):506-13.

Buret A, Gall DG, Olson ME. 1991. Growth, activities of enzymes in the small intestine, and ultrastructure of microvillous border in gerbils infected with *Giardia duodenalis*. *Parasitol Res*. 77(2):109-14.

Byrd LG, Conrad JT, Nash TE. 1994. *Giardia lamblia* infections in adult mice. *Infect Immun*. 62(8):3583-5.

Cacciò SM, De Giacomo M, Pozio E. 2002. Sequence analysis of the beta-giardin gene and development of a polymerase chain reaction-restriction fragment length polymorphism assay to genotype *Giardia duodenalis* cysts from human faecal samples. *Int J Parasitol*. 32(8):1023-30.

Cacciò SM, Ryan U. 2008. Molecular epidemiology of giardiasis. *Mol Biochem Parasitol*. 160(2):75-80.

Calder PC. 2006. Branched-chain amino acids and immunity. *J Nutr*. 136(1 Suppl):288S-93S.

Carlson DW, Finger DR. 2004. Beaver fever arthritis. *J Clin Rheumatol*. 10(2):86-8.

Carranza PG, Feltes G, Ropolo A, Quintana SM, Touz MC, Luján HD. 2002. Simultaneous expression of different variant-specific surface proteins in single *Giardia lamblia* trophozoites during encystation. *Infect Immun*. 70(9):5265-8.

Carrera AC. 2004. TOR signaling in mammals. *J Cell Sci*. 117(Pt 20):4615-6.

Castro IC, Oliveira BB, Slowikowski JJ, Coutinho BP, Siqueira FJ, Costa LB, Sevilleja JE, Almeida CA, Lima AA, Warren CA, Oriá RB, Guerrant RL. 2012. Arginine decreases *Cryptosporidium parvum* infection in undernourished suckling mice involving nitric oxide synthase and arginase. *Nutrition*. 28(6):678-85.

CDC. 2010. Giardiasis surveillance-United States, 2006-2008. *Morb Mortal Wkly Rep*. 59(SS06):15-25.

CDC. 2013. http://www.cdc.gov/parasites/giardia/

Chieppa M, Rescigno M, Huang AY, Germain RN. 2006. Dynamic imaging of dendritic cell extension into the small bowel lumen in response to epithelial cell TLR engagement. *J Exp Med*. 203(13):2841-52.

Chin AC, Teoh DA, Scott KG, Meddings JB, Macnaughton WK, Buret AG. 2002. Strain-dependent induction of enterocyte apoptosis by *Giardia lamblia* disrupts epithelial barrier function in a caspase-3-dependent manner. *Infect Immun*. 70(7):3673-80.

Christopher AB, Arndt A, Cugini C, Davey ME. 2010. A streptococcal effector protein that inhibits *Porphyromonas gingivalis* biofilm development. *Microbiology*. 156(Pt 11):3469-77.

Claesson BE, Gotthardsson IH. 1988. A tissue culture model for study of growth promotion and antimicrobial susceptibility in *Bacteroides fragilis*. *J Antimicrob Chemother*. 21(1):17-26.

Cross AS. 2008. What is a virulence factor? *Crit Care*. 12(6):196.

Danciger M, Lopez M. 1975. Numbers of *Giardia* in the feces of infected children. *Am J Trop Med Hyg*. 24(2):237-42.

Das P, Lahiri A, Lahiri A, Chakravortty D. 2010. Modulation of the arginase pathway in the context of microbial pathogenesis: a metabolic enzyme moonlighting as an immune modulator. *PLoS Pathog*. 6(6):e1000899.

Dawson SC. 2010. An insider's guide to the microtubule cytoskeleton of *Giardia*. *Cell Microbiol*. 12(5):588-98.

Dawson SC, House SA. 2010. Life with eight flagella: flagellar assembly and division in *Giardia*. *Curr Opin Microbiol*. 13(4):480-90.

Degnan BA, Palmer JM, Robson T, Jones CE, Fischer M, Glanville M, Mellor GD, Diamond AG, Kehoe MA, Goodacre JA. 1998. Inhibition of human peripheral blood mononuclear cell proliferation by *Streptococcus pyogenes* cell extract is associated with arginine deiminase activity. *Infect Immun*. 66(7):3050-8.

Eckmann L. 2003. Mucosal defences against *Giardia*. *Parasite Immunol*. 25(5):259-70.

Eckmann L, Laurent F, Langford TD, Hetsko ML, Smith JR, Kagnoff MF, Gillin FD. 2000. Nitric oxide production by human intestinal epithelial cells and competition for arginine as potential determinants of host defense against the lumen-dwelling pathogen *Giardia lamblia*. *J Immunol*. 164(3):1478-87.

Elmendorf HG, Dawson SC, McCaffery JM. 2003. The cytoskeleton of *Giardia lamblia*. *Int J Parasitol*. 33(1):3-28.

Engler C, Kandzia R, Marillonnet S. 2008. A one pot, one step, precision cloning method with high throughput capability. *PLoS One*. 3(11):e3647.

Engvall E, Perlmann P. 1971. Enzyme-linked immunosorbent assay (ELISA). Quantitative assay of immunoglobulin G. *Immunochemistry*. 8(9):871-4.

Erlandsen SL, Macechko PT, van Keulen H, Jarroll EL. 1996. Formation of the *Giardia* cyst wall: studies on extracellular assembly using immunogold labeling and high resolution field emission SEM. *J Eukaryot Microbiol*. 43(5):416-29.

Escobedo AA, Cimerman S. 2007. Giardiasis: a pharmacotherapy review. *Expert Opin Pharmacother*. 8(12):1885-902.

Evoy D, Lieberman MD, Fahey TJ 3rd, Daly JM. 1998. Immunonutrition: the role of arginine. *Nutrition*. 14(7-8):611-7.

Farthing MJ. 1993. Diarrhoeal disease: current concepts and future challenges. Pathogenesis of giardiasis. *Trans R Soc Trop Med Hyg*. 87 Suppl 3:17-21.

Farthing MJ. 1997. The molecular pathogenesis of giardiasis. *J Pediatr Gastroenterol Nutr*. 24(1):79-88.

Ferreira RC, Forsyth LE, Richman PI, Wells C, Spencer J, MacDonald TT. 1990. Changes in the rate of crypt epithelial cell proliferation and mucosal morphology induced by a T-cell-mediated response in human small intestine. *Gastroenterology*. 98(5 Pt 1):1255-63.

Ferruzza S, Rossi C, Scarino ML, Sambuy Y. 2012. A protocol for differentiation of human intestinal Caco-2 cells in asymmetric serum-containing medium. *Toxicol In Vitro*. 26(8):1252-5.

Flanagan PA. 1992. *Giardia*-diagnosis, clinical course and epidemiology. A review. *Epidemiol Infect*. 109(1):1-22.

Fogh J, Wright WC, Loveless JD. 1977. Absence of HeLa cell contamination in 169 cell lines derived from human tumors. *J Natl Cancer Inst*. 58(2):209-14.

Franzén O, Jerlström-Hultqvist J, Castro E, Sherwood E, Ankarklev J, Reiner DS, Palm D, Andersson JO, Andersson B, Svärd SG. 2009. Draft genome sequencing of *Giardia intestinalis* assemblage B isolate GS: is human giardiasis caused by two different species? *PLoS Pathog*. 5(8):e1000560.

Fulde M, Willenborg J, de Greeff A, Benga L, Smith HE, Valentin-Weigand P, Goethe R. 2011. ArgR is an essential local transcriptional regulator of the arcABC operon in *Streptococcus suis* and is crucial for biological fitness in an acidic environment. *Microbiology*. 157(Pt 2):572-82.

Galkin A, Lu X, Dunaway-Mariano D, Herzberg O. 2005. Crystal structures representing the Michaelis complex and the thiouronium reaction intermediate of *Pseudomonas aeruginosa* arginine deiminase. *J Biol Chem*. 280(40):34080-7.

Gardner TB, Hill DR. 2001. Treatment of giardiasis. *Clin Microbiol Rev*. 14(1):114-28.

Gaur U, Roberts SC, Dalvi RP, Corraliza I, Ullman B, Wilson ME. 2007. An effect of parasite-encoded arginase on the outcome of murine cutaneous leishmaniasis. *J Immunol*. 179(12):8446-53.

Gerwig GJ, van Kuik JA, Leeflang BR, Kamerling JP, Vliegenthart JF, Karr CD, Jarroll EL. 2002. The *Giardia intestinalis* filamentous cyst wall contains a novel beta(1-3)-N-acetyl-D-galactosamine polymer: a structural and conformational study. *Glycobiology*. 12(8):499-505.

Geurden T, Levecke B, Cacció SM, Visser A, De Groote G, Casaert S, Vercruysse J, Claerebout E. 2009. Multilocus genotyping of *Cryptosporidium* and *Giardia* in non-outbreak related cases of diarrhoea in human patients in Belgium. *Parasitology*. 136(10):1161-8.

Gillin FD, Reiner DS, McCaffery JM. 1996. Cell biology of the primitive eukaryote *Giardia lamblia*. *Annu Rev Microbiol*. 50:679-705.

Gillon J, Al Thamery D, Ferguson A. 1982. Features of small intestinal pathology (epithelial cell kinetics, intraepithelial lymphocytes, disaccharidases) in a primary *Giardia muris* infection. *Gut*. 23(6):498-506.

Gilman RH, Marquis GS, Miranda E, Vestegui M, Martinez H. 1988. Rapid reinfection by *Giardia lamblia* after treatment in a hyperendemic Third World community. *Lancet*. 1(8581):343-5.

Glocker EO, Kotlarz D, Klein C, Shah N, Grimbacher B. 2011. IL-10 and IL-10 receptor defects in humans. *Ann N Y Acad Sci*. 1246:102-7.

Gobert AP, McGee DJ, Akhtar M, Mendz GL, Newton JC, Cheng Y, Mobley HL, Wilson KT. 2001. *Helicobacter pylori* arginase inhibits nitric oxide production by eukaryotic cells: a strategy for bacterial survival. *Proc Natl Acad Sci U S A*. 98(24):13844-9.

Gong H, Zölzer F, von Recklinghausen G, Rössler J, Breit S, Havers W, Fotsis T, Schweigerer L. 1999. Arginine deiminase inhibits cell proliferation by arresting cell cycle and inducing apoptosis. *Biochem Biophys Res Commun*. 261(1):10-4.

Goyal N, Shukla G. 2013. Probiotic *Lactobacillus rhamnosus* GG modulates the mucosal immune response in *Giardia intestinalis*-infected BALB/c mice. *Dig Dis Sci*. 58(5):1218-25.

Grasset E, Pinto M, Dussaulx E, Zweibaum A, Desjeux JF. 1984. Epithelial properties of human colonic carcinoma cell line Caco-2: electrical parameters. *Am J Physiol*. 247(3 Pt 1):C260-7.

Guex N, Peitsch MC. 1997. SWISS-MODEL and the Swiss-PdbViewer: an environment for comparative protein modeling. *Electrophoresis*. 18(15):2714-23.

Haidinger M, Poglitsch M, Geyeregger R, Kasturi S, Zeyda M, Zlabinger GJ, Pulendran B, Hörl WH, Säemann MD, Weichhart T. 2010. A versatile role of mammalian target of rapamycin in human dendritic cell function and differentiation. *J Immunol*. 185(7):3919-31.

Hanevik K, Dizdar V, Langeland N, Hausken T. 2009. Development of functional gastrointestinal disorders after *Giardia lamblia* infection. *BMC Gastroenterol*. 9:27.

Hanevik K, Kristoffersen EK, Sørnes S, Mørch K, Næss H, Rivenes AC, Bødtker JE, Hausken T, Langeland N. 2012. Immunophenotyping in post-giardiasis functional gastrointestinal disease and chronic fatigue syndrome. *BMC Infect Dis*. 12(1):258.

Haque R, Roy S, Kabir M, Stroup SE, Mondal D, Houpt ER. 2005. *Giardia* assemblage A infection and diarrhea in Bangladesh. *J Infect Dis*. 192(12):2171-3.

Hardin JA, Buret AG, Olson ME, Kimm MH, Gall DG. 1997. Mast cell hyperplasia and increased macromolecular uptake in an animal model of giardiasis. *J Parasitol*. 83(5):908-12.

Hetsko ML, McCaffery JM, Svärd SG, Meng TC, Que X, Gillin FD. 1998. Cellular and transcriptional changes during excystation of *Giardia lamblia in vitro*. *Exp Parasitol*. 88(3):172-83.

Holmgren J, Czerkinsky C. 2005. Mucosal immunity and vaccines. *Nat Med*. 11(4 Suppl):S45-53.

Homan WL, Mank TG. 2001. Human giardiasis: genotype linked differences in clinical symptomatology. *Int J Parasitol*. 31(8):822-6.

Hosogi Y, Duncan MJ. 2005. Gene expression in *Porphyromonas gingivalis* after contact with human epithelial cells. *Infect Immun*. 73(4):2327-35.

Humen MA, De Antoni GL, Benyacoub J, Costas ME, Cardozo MI, Kozubsky L, Saudan KY, Boenzli-Bruand A, Blum S, Schiffrin EJ, Pérez PF. 2005. *Lactobacillus johnsonii* La1 antagonizes *Giardia intestinalis in vivo*. *Infect Immun*. 73(2):1265-9.

Jerlström-Hultqvist J, Ankarklev J, Svärd SG. 2010. Is human giardiasis caused by two different *Giardia* species? *Gut Microbes*. 1(6):379-82.

Jones DT. 1999. Protein secondary structure prediction based on position-specific scoring matrices. *J Mol Biol*. 292(2):195-202.

Kabnick KS, Peattie DA. 1990. *In situ* analyses reveal that the two nuclei of *Giardia lamblia* are equivalent. *J Cell Sci*. 95(Pt 3):353-60.

Kakazu E, Kanno N, Ueno Y, Shimosegawa T. 2007. Extracellular branched-chain amino acids, especially valine, regulate maturation and function of monocyte-derived dendritic cells. *J Immunol*. 179(10):7137-46.

Kamda JD, Nash TE, Singer SM. 2012. *Giardia duodenalis*: dendritic cell defects in IL-6 deficient mice contribute to susceptibility to intestinal infection. *Exp Parasitol*. 130(3):288-91.

Kamda JD, Singer SM. 2009. Phosphoinositide 3-kinase-dependent inhibition of dendritic cell interleukin-12 production by *Giardia lamblia*. *Infect Immun*. 77(2):685-93.

Keister DB. 1983. Axenic culture of *Giardia lamblia* in TYI-S-33 medium supplemented with bile. *Trans R Soc Trop Med Hyg*. 77(4):487-8.

Kihara H, Snell EE. 1957. The enzymatic cleavage of canavanine to O-ureidohomoserine and ammonia. *J Biol Chem*. 226(1):485-95.

Klotz C, Aebischer T, Seeber F. 2012. Stem cell-derived cell cultures and organoids for protozoan parasite propagation and studying host-parasite interaction. *Int J Med Microbiol*. 302(4-5):203-9.

Knipp M, Vasák M. 2000. A colorimetric 96-well microtiter plate assay for the determination of enzymatically formed citrulline. *Anal Biochem*. 286(2):257-64.

Knodler LA, Schofield PJ, Edwards MR. 1995. L-arginine transport and metabolism in *Giardia intestinalis* support its position as a transition between the prokaryotic and eukaryotic kingdoms. *Microbiology*. 141(Pt 9):2063-70.

Knodler LA, Sekyere EO, Stewart TS, Schofield PJ, Edwards MR. 1998. Cloning and expression of a prokaryotic enzyme, arginine deiminase, from a primitive eukaryote *Giardia intestinalis*. *J Biol Chem*. 273(8):4470-7.

Koh WH, Geurden T, Paget T, O'Handley R, Steuart RF, Thompson RC, Buret AG. 2013. *Giardia duodenalis* assemblage-specific induction of apoptosis and tight junction disruption in human intestinal epithelial cells: effects of mixed infections. *J Parasitol*. 99(2):353-8.

Kohli A, Bushen OY, Pinkerton RC, Houpt E, Newman RD, Sears CL, Lima AA, Guerrant RL. 2008. *Giardia duodenalis* assemblage, clinical presentation and markers of intestinal inflammation in Brazilian children. *Trans R Soc Trop Med Hyg*. 102(7):718-25.

Kontoyiannis D, Kotlyarov A, Carballo E, Alexopoulou L, Blackshear PJ, Gaestel M, Davis R, Flavell R, Kollias G. 2001. Interleukin-10 targets p38 MAPK to modulate ARE-dependent TNF mRNA translation and limit intestinal pathology. *EMBO J*. 20(14):3760-70.

Kukuruzovic R, Robins-Browne RM, Anstey NM, Brewster DR. 2002. Enteric pathogens, intestinal permeability and nitric oxide production in acute gastroenteritis. *Pediatr Infect Dis J*. 21(8):730-9.

Kullas AL, McClelland M, Yang HJ, Tam JW, Torres A, Porwollik S, Mena P, McPhee JB, Bogomolnaya L, Andrews-Polymenis H, van der Velden AW. 2012. L-Asparaginase II produced by *Salmonella typhimurium* inhibits T cell responses and mediates virulence. *Cell host & microbe*. 12:791-798.

Laemmli UK. 1970. Cleavage of structural proteins during the assembly of the head of bacteriophage T4. *Nature*. 227(5259):680-5.

Lahiri A, Das P, Chakravortty D. 2008. Arginase modulates *Salmonella* induced nitric oxide production in RAW264.7 macrophages and is required for *Salmonella* pathogenesis in mice model of infection. *Microbes Infect*. 10(10-11):1166-74.

Lalle M. 2010. Giardiasis in the post genomic era: treatment, drug resistance and novel therapeutic perspectives. *Infect Disord Drug Targets*. 10(4):283-94.

Lane S, Lloyd D. 2002. Current trends in research into the waterborne parasite *Giardia*. *Crit Rev Microbiol*. 28(2):123-47.

Langford TD, Housley MP, Boes M, Chen J, Kagnoff MF, Gillin FD, Eckmann L. 2002. Central importance of immunoglobulin A in host defense against *Giardia spp*. *Infect Immun*. 70(1):11-8.

Lasek-Nesselquist E, Welch DM, Sogin ML. 2010. The identification of a new *Giardia duodenalis* assemblage in marine vertebrates and a preliminary analysis of *G. duodenalis* population biology in marine systems. *Int J Parasitol*. 40(9):1063-74.

Lebbad M, Mattsson JG, Christensson B, Ljungström B, Backhans A, Andersson JO, Svärd SG. 2010. From mouse to moose: multilocus genotyping of *Giardia* isolates from various animal species. *Vet Parasitol*. 168(3-4):231-9.

Lebbad M, Petersson I, Karlsson L, Botero-Kleiven S, Andersson JO, Svenungsson B, Svärd SG. 2011. Multilocus genotyping of human *Giardia* isolates suggests limited zoonotic transmission and association between assemblage B and flatulence in children. *PLoS Negl Trop Dis*. 5(8):e1262.

Lee HY, Hyung S, Lee NY, Yong TS, Han SH, Park SJ. 2012. Excretory-secretory products of *Giardia lamblia* induce interleukin-8 production in human colonic cells *via* activation of p38, ERK1/2, NF-κB and AP-1. *Parasite Immunol*. 34(4):183-98.

Leitch GJ, Udezulu IA, He Q, Visvesvara GS. 1993. Effects of protein malnutrition on experimental giardiasis in the Mongolian gerbil. *Scand J Gastroenterol*. 28(10):885-93.

Levecke B, Geldhof P, Claerebout E, Dorny P, Vercammen F, Cacciò SM, Vercruysse J, Geurden T. 2009. Molecular characterisation of *Giardia duodenalis* in captive non-human primates reveals mixed assemblage A and B infections and novel polymorphisms. *Int J Parasitol*. 39(14):1595-601.

Lewis ND, Asim M, Barry DP, Singh K, de Sablet T, Boucher JL, Gobert AP, Chaturvedi R, Wilson KT. 2010. Arginase II restricts host defense to *Helicobacter pylori* by attenuating inducible nitric oxide synthase translation in macrophages. *J Immunol*. 184(5):2572-82.

Li Z, Kulakova L, Li L, Galkin A, Zhao Z, Nash TE, Mariano PS, Herzberg O, Dunaway-Mariano D. 2009. Mechanisms of catalysis and inhibition operative in the arginine deiminase from the human pathogen *Giardia lamblia*. *Bioorg Chem*. 37(5):149-61.

Li L, Li Z, Wang C, Xu D, Mariano PS, Guo H, Dunaway-Mariano D. 2008. The electrostatic driving force for nucleophilic catalysis in L-arginine deiminase: a combined experimental and theoretical study. *Biochemistry*. 47(16):4721-32.

Li E, Zhou P, Petrin Z, Singer SM. 2004. Mast cell-dependent control of *Giardia lamblia* infections in mice. *Infect Immun*. 72(11): 6642–49.

Li E, Zhou P, Singer SM. 2006. Neuronal nitric oxide synthase is necessary for elimination of *Giardia lamblia* infections in mice. *J Immunol*. 176(1):516-21.

Lorentz K, Koch H. 1971. Determination of ornithinecarbamoyl-transferase by the Fearon reaction. I. Determination of citrulline. *Z Klin Chem Klin Biochem*. 9(3):215-9.

Lu X, Galkin A, Herzberg O, Dunaway-Mariano D. 2004. Arginine deiminase uses an active-site cysteine in nucleophilic catalysis of L-arginine hydrolysis. *J Am Chem Soc*. 126(17):5374-5.

Lu X, Li L, Wu R, Feng X, Li Z, Yang H, Wang C, Guo H, Galkin A, Herzberg O, Mariano PS, Martin BM, Dunaway-Mariano D. 2006. Kinetic analysis of *Pseudomonas aeruginosa* arginine deiminase mutants and alternate substrates provides insight into structural determinants of function. *Biochemistry*. 45(4):1162-72.

Maciorkowska E, Kaczmarski M, Kemona A. 2005. The role of cytokines in giardiasis in children. *Med Wieku Rozwoj*. 9(4):665-73.

Maia-Brigagão C, Morgado-Díaz JA, De Souza W. 2012. *Giardia* disrupts the arrangement of tight, adherens and desmosomal junction proteins of intestinal cells. *Parasitol Int*. 61(2):280-7.

McDowall RM, Peregrine AS, Leonard EK, Lacombe C, Lake M, Rebelo AR, Cai HY. 2011. Evaluation of the zoonotic potential of *Giardia duodenalis* in fecal samples from dogs and cats in Ontario. *Can Vet J*. 52(12):1329-33.

McGhee JR, Fujihashi K. 2012. Inside the mucosal immune system. *PLoS Biol*. 10(9):e1001397.

McGuckin MA, Lindén SK, Sutton P, Florin TH. 2011. Mucin dynamics and enteric pathogens. *Nat Rev Microbiol*. 9(4):265-78.

McGuffin LJ, Bryson K, Jones DT. 2000. The PSIPRED protein structure prediction server. *Bioinformatics*. 16(4):404-5.

Mesojednik S, Legisa M. 2005. Posttranslational modification of 6-phosphofructo-1-kinase in *Aspergillus niger*. *Appl Environ Microbiol*. 71(3):1425-32.

Miyazaki K, Takaku H, Umeda M, Fujita T, Huang WD, Kimura T, Yamashita J, Horio T. 1990. Potent growth inhibition of human tumor cells in culture by arginine deiminase purified from a culture medium of a *Mycoplasma*-infected cell line. *Cancer Res*. 50(15):4522-7.

Mohammed Mahdy AK, Surin J, Wan KL, Mohd-Adnan A, Al-Mekhlafi MS, Lim YA. 2009. *Giardia intestinalis* genotypes: Risk factors and correlation with clinical symptoms. *Acta Trop. Oct*. 112(1):67-70.

Monis PT, Andrews RH, Mayrhofer G, Ey PL. 2003. Genetic diversity within the morphological species *Giardia intestinalis* and its relationship to host origin. *Infect Genet Evol*. 3(1):29-38.

Monis PT, Caccio SM, Thompson RC. 2009. Variation in *Giardia*: towards a taxonomic revision of the genus. *Trends Parasitol*. 25(2):93-100.

Morrison HG, McArthur AG, Gillin FD, Aley SB, Adam RD, Olsen GJ, Best AA, Cande WZ, Chen F, Cipriano MJ, Davids BJ, Dawson SC, Elmendorf HG, Hehl AB, Holder ME, Huse SM, Kim UU, Lasek-Nesselquist E, Manning G, Nigam A, Nixon JE, Palm D, Passamaneck NE, Prabhu A, Reich CI, Reiner DS, Samuelson J, Svard SG, Sogin ML. 2007. Genomic minimalism in the early diverging intestinal parasite *Giardia lamblia*. *Science*. 317(5846):1921-6.

Mourad FH, Turvill JL, Farthing MJ. 1999. Role of nitric oxide in intestinal water and electrolyte transport. *Gut*. 44(2):143-7.

Müller J, Ley S, Felger I, Hemphill A, Müller N. 2008. Identification of differentially expressed genes in a *Giardia lamblia* WB C6 clone resistant to nitazoxanide and metronidazole. *J Antimicrob Chemother*. 62(1):72-82.

Müller-Esterl W. 2004. Biochemie-Eine Einführung für Mediziner und Naturwissenschaftler. *Spektrum Akademischer Verlag*.172-5.

Münz C, Steinman RM, Fujii S. 2005. Dendritic cell maturation by innate lymphocytes: coordinated stimulation of innate and adaptive immunity. *J Exp Med*. 202(2):203-7.

Nagler-Anderson C. 2001. Man the barrier! Strategic defences in the intestinal mucosa. *Nat Rev Immunol*. 1(1):59-67.

Nash TE. 2002. Surface antigenic variation in *Giardia lamblia*. *Mol Microbiol*. 45(3):585-90.

Nash TE, Aggarwal A, Adam RD, Conrad JT, Merritt JW Jr. 1988. Antigenic variation in *Giardia lamblia*. *J Immunol*. 141(2):636-41.

Nash TE, Herrington DA, Losonsky GA, Levine MM. 1987. Experimental human infections with *Giardia lamblia*. *J Infect Dis*. 156(6):974-84.

Nash TE, McCutchan T, Keister D, Dame JB, Conrad JD, Gillin FD. 1985. Restriction-endonuclease analysis of DNA from 15 *Giardia* isolates obtained from humans and animals. *J Infect Dis*. 152(1):64-73.

Nash TE, Merritt JW Jr, Conrad JT. 1991. Isolate and epitope variability in susceptibility of *Giardia lamblia* to intestinal proteases. *Infect Immun*. 59(4):1334-40.

Nickel W. 2003. The mystery of nonclassical protein secretion. A current view on cargo proteins and potential export routes. *Eur J Biochem*. 270(10):2109-19.

Nkrumah B, Nguah SB. 2011. *Giardia lamblia*: a major parasitic cause of childhood diarrhoea in patients attending a district hospital in Ghana. *Parasit Vectors*. 4:163.

Noh EJ, Kang SW, Shin YJ, Kim DC, Park IS, Kim MY, Chun BG, Min BH. 2002. Characterization of mycoplasma arginine deiminase expressed in *E. coli* and its inhibitory regulation of nitric oxide synthesis. *Mol Cells*. 13(1):137-43.

Oberhuber G, Kastner N, Stolte M. 1997. Giardiasis: a histologic analysis of 567 cases. *Scand J Gastroenterol*. 32(1):48-51.

Olivares JL, Fernández R, Fleta J, Ruiz MY, Clavel A. 2002. Vitamin B12 and folic acid in children with intestinal parasitic infection. *J Am Coll Nutr*. 21(2):109-13.

Olson ME, Morck DW, Ceri H. 1996. The efficacy of a *Giardia lamblia* vaccine in kittens. *Can J Vet Res*. 60(4):249-56.

Ordás I, Mould DR, Feagan BG, Sandborn WJ. 2012. Anti-TNF monoclonal antibodies in inflammatory bowel disease: pharmacokinetics-based dosing paradigms. *Clin Pharmacol Ther*. 91(4):635-46.

Palm JE, Weiland ME, Griffiths WJ, Ljungström I, Svärd SG. 2003. Identification of immunoreactive proteins during acute human giardiasis. *J Infect Dis*. 187(12):1849-59.

Panaro MA, Cianciulli A, Mitolo V, Mitolo CI, Acquafredda A, Brandonisio O, Cavallo P. 2007. Caspase-dependent apoptosis of the HCT-8 epithelial cell line induced by the parasite *Giardia intestinalis*. *FEMS Immunol Med Microbiol*. 51(2):302-9.

Petrack B, Sullivan L, Ratner S. 1957. Behavior of purified arginine desiminase from *S. faecalis*. *Arch Biochem Biophys*. 69:186-97.

Porter EM, Bevins CL, Ghosh D, Ganz T. 2002. The multifaceted Paneth cell. *Cell Mol Life Sci*. 59(1):156-70.

Proost P, Loos T, Mortier A, Schutyser E, Gouwy M, Noppen S, Dillen C, Ronsse I, Conings R, Struyf S, Opdenakker G, Maudgal PC, Van Damme J. 2008. Citrullination of CXCL8 by peptidylarginine deiminase alters receptor usage, prevents proteolysis, and dampens tissue inflammation. *J Exp Med*. 205(9):2085-97.

Prucca CG, Rivero FD, Luján HD. 2011. Regulation of antigenic variation in *Giardia lamblia*. *Annu Rev Microbiol*. 65:611-30.

Pulendran B, Palucka K, Banchereau J. 2001. Sensing pathogens and tuning immune responses. *Science*. 293(5528):253-6.

Regoes A, Zourmpanou D, León-Avila G, van der Giezen M, Tovar J, Hehl AB. 2005. Protein import, replication, and inheritance of a vestigial mitochondrion. *J Biol Chem*. 280(34):30557-63.

Reiner DS, Ankarklev J, Troell K, Palm D, Bernander R, Gillin FD, Andersson JO, Svärd SG. 2008. Synchronisation of *Giardia lamblia*: identification of cell cycle stage-specific genes and a differentiation restriction point. *Int J Parasitol*. 38(8-9):935-44.

Rescigno M, Urbano M, Valzasina B, Francolini M, Rotta G, Bonasio R, Granucci F, Kraehenbuhl JP, Ricciardi-Castagnoli P. 2001. Dendritic cells express tight junction proteins and penetrate gut epithelial monolayers to sample bacteria. *Nat Immunol*. 2(4):361-7.

Ringqvist E, Avesson L, Söderbom F, Svärd SG. 2011. Transcriptional changes in *Giardia* during host-parasite interactions. *Int J Parasitol*. 41(3-4):277-85.

Ringqvist E, Palm JE, Skarin H, Hehl AB, Weiland M, Davids BJ, Reiner DS, Griffiths WJ, Eckmann L, Gillin FD, Svärd SG. 2008. Release of metabolic enzymes by *Giardia* in response to interaction with intestinal epithelial cells. *Mol Biochem Parasitol*. 159(2):85-91.

RKI. 2011. Infektionsepidemiologisches Jahrbuch meldepflichtiger Krankheiten für 2010.

RKI. 2012. Infektionsepidemiologisches Jahrbuch meldepflichtiger Krankheiten für 2011.

Rodríguez SB, Stitt BL, Ash DE. 2009. Expression of peptidylarginine deiminase from *Porphyromonas gingivalis* in *Escherichia coli*: enzyme purification and characterization. *Arch Biochem Biophys*. 488(1):14-22.

Rópolo AS, Saura A, Carranza PG, Lujan HD. 2005. Identification of variant-specific surface proteins in *Giardia muris* trophozoites. *Infect Immun*. 73(8):5208-11.

Rópolo AS, Touz MC. 2010. A lesson in survival, by *Giardia lamblia*. *ScientificWorldJournal*. 10:2019-31.

Roskens H, Erlandsen SL. 2002. Inhibition of *in vitro* attachment of *Giardia* trophozoites by mucin. *J Parasitol*. 88(5):869-73.

Rousset M. 1986. The human colon carcinoma cell lines HT-29 and Caco-2: two *in vitro* models for the study of intestinal differentiation. *Biochimie*. 68(9):1035-40.

Roxström-Lindquist K, Palm D, Reiner D, Ringqvist E, Svärd SG. 2006. *Giardia* immunity-an update. *Trends Parasitol*. 22(1):26-31.

Roxström-Lindquist K, Ringqvist E, Palm D, Svärd S. 2005. *Giardia lamblia*-induced changes in gene expression in differentiated Caco-2 human intestinal epithelial cells. *Infect Immun*. 73(12):8204-8.

Ryan S, Begley M, Gahan CG, Hill C. 2009. Molecular characterization of the arginine deiminase system in *Listeria monocytogenes*: regulation and role in acid tolerance. *Environ Microbiol*. 11(2):432-45.

Sahagún J, Clavel A, Goñi P, Seral C, Llorente MT, Castillo FJ, Capilla S, Arias A, Gómez-Lus R. 2008. Correlation between the presence of symptoms and the *Giardia duodenalis* genotype. *Eur J Clin Microbiol Infect Dis*. 27(1):81-3.

Sahl JW, Gillece JD, Schupp JM, Waddell VG, Driebe EM, Engelthaler DM, Keim P. 2013. Evolution of a pathogen: a comparative genomics analysis identifies a genetic pathway to pathogenesis in *Acinetobacter*. *PLoS One*. 8(1):e54287.

Sambrook J, Fritsch EF, Maniatis T. 1989. Molecular cloning: a laboratory manual. 2nd edition. New York: *Cold Spring Harbor Laboratory Press*.

Sanchez-Pernaute O, Filkova M, Gabucio A, Klein M, Maciejewska-Rodrigues H, Ospelt C, Brentano F, Michel BA, Gay RE, Herrero-Beaumont G, Gay S, Neidhart M, Juengel A. 2012. Citrullination enhances the pro-inflammatory response to fibrin in rheumatoid arthritis synovial fibroblasts. *Ann Rheum Dis*. ahead of print.

Santos J, Sousa MJ, Leão C. 2012. Ammonium is toxic for aging yeast cells, inducing death and shortening of the chronological lifespan. *PLoS One*. 7(5):e37090.

Sarkari B, Ashrafmansori A, Hatam GR, Motazedian MH, Asgari Q, Mohammadpour I. 2012. Genotyping of *Giardia lamblia* isolates from human in southern Iran. *Trop Biomed*. 29(3):366-71.

Sato T, Stange DE, Ferrante M, Vries RG, Van Es JH, Van den Brink S, Van Houdt WJ, Pronk A, Van Gorp J, Siersema PD, Clevers H. 2011. Long-term expansion of epithelial organoids from human colon, adenoma, adenocarcinoma, and Barrett's epithelium. *Gastroenterology*. 141(5):1762-72.

Savioli L, Smith H, Thompson A. 2006. *Giardia* and *Cryptosporidium* join the 'Neglected Diseases Initiative'. *Trends Parasitol*. 22(5):203-8.

Schmitz H, Fromm M, Bentzel CJ, Scholz P, Detjen K, Mankertz J, Bode H, Epple HJ, Riecken EO, Schulzke JD. 1999. Tumor necrosis factor-alpha (TNFalpha) regulates the epithelial barrier in the human intestinal cell line HT-29/B6. *J Cell Sci*. 112(Pt 1):137-46.

Schofield PJ, Costello M, Edwards MR, O'Sullivan WJ. 1990. The arginine dihydrolase pathway is present in *Giardia intestinalis*. *Int J Parasitol*. 20(5):697-9.

Schofield PJ, Edwards MR, Matthews J, Wilson JR. 1992. The pathway of arginine catabolism in *Giardia intestinalis*. *Mol Biochem Parasitol*. 51(1):29-36.

Schwede T, Kopp J, Guex N, Peitsch MC. 2003. SWISS-MODEL: An automated protein homology-modeling server. *Nucleic Acids Res*. 31(13):3381-5.

Scott KG, Logan MR, Klammer GM, Teoh DA, Buret AG. 2000. Jejunal brush border microvillous alterations in *Giardia muris*-infected mice: role of T lymphocytes and interleukin-6. *Infect Immun*. 68(6):3412-8.

Scott KG, Yu LC, Buret AG. 2004. Role of CD8+ and CD4+ T lymphocytes in jejunal mucosal injury during murine giardiasis. *Infect Immun*. 72(6):3536-42.

Shirai H, Mokrab Y, Mizuguchi K. 2006. The guanidino-group modifying enzymes: structural basis for their diversity and commonality. *Proteins*. 64(4):1010-23.

Singer SM, Nash TE. 2000. T-cell-dependent control of acute *Giardia lamblia* infections in mice. *Infect Immun*. 68(1):170-5.

Smith PD, Gillin FD, Spira WM, Nash TE. 1982. Chronic giardiasis: studies on drug sensitivity, toxin production, and host immune response. *Gastroenterology*. 83(4):797-803.

Solaymani-Mohammadi S, Genkinger JM, Loffredo CA, Singer SM. 2010. A meta-analysis of the effectiveness of albendazole compared with metronidazole as treatments for infections with *Giardia duodenalis*. *PLoS Negl Trop Dis*. 4(5):e682.

Solaymani-Mohammadi S, Singer SM. 2011. Host immunity and pathogen strain contribute to intestinal disaccharidase impairment following gut infection. *J Immunol*. 187(7):3769-75.

Spence JR, Mayhew CN, Rankin SA, Kuhar MF, Vallance JE, Tolle K, Hoskins EE, Kalinichenko VV, Wells SI, Zorn AM, Shroyer NF, Wells JM. 2011. Directed differentiation of human pluripotent stem cells into intestinal tissue *in vitro*. *Nature*. 470(7332):105-9.

Sprong H, Cacciò SM, van der Giessen JW; ZOOPNET network and partners. 2009. Identification of zoonotic genotypes of *Giardia duodenalis*. *PLoS Negl Trop Dis*. 3(12):e558.

Stadelmann B, Merino MC, Persson L, Svärd SG. 2012. Arginine consumption by the intestinal parasite *Giardia intestinalis* reduces proliferation of intestinal epithelial cells. *PLoS One*. 7(9):e45325.

Stevenson BR, Siliciano JD, Mooseker MS, Goodenough DA. 1986. Identification of ZO-1: a high molecular weight polypeptide associated with the tight junction (zonula occludens) in a variety of epithelia. *J Cell Biol*. 103(3):755-66.

Sulaiman IM, Fayer R, Bern C, Gilman RH, Trout JM, Schantz PM, Das P, Lal AA, Xiao L. 2003. Triosephosphate isomerase gene characterization and potential zoonotic transmission of *Giardia duodenalis*. *Emerg Infect Dis*. 9(11):1444-52.

Sun CH, McCaffery JM, Reiner DS, Gillin FD. 2003. Mining the *Giardia lamblia* genome for new cyst wall proteins. *J Biol Chem*. 278(24):21701-8.

Svärd SG, Hagblom P, Palm JE. 2003. *Giardia lamblia*- a model organism for eukaryotic cell differentiation. *FEMS Microbiol Lett*. 218(1):3-7.

Svärd SG, Meng TC, Hetsko ML, McCaffery JM, Gillin FD. 1998. Differentiation-associated surface antigen variation in the ancient eukaryote *Giardia lamblia*. *Mol Microbiol*. 30(5):979-89.

Takaku H, Takase M, Abe S, Hayashi H, Miyazaki K. 1992. *In vivo* anti-tumor activity of arginine deiminase purified from *Mycoplasma arginini*. *Int J Cancer*. 51(2):244-9.

Tang F, Bossers A, Harders F, Lu C, Smith H. 2013. Comparative genomic analysis of twelve *Streptococcus suis* (pro)phages. *Genomics*. 101(6):336-44.

Téllez A, Palm D, Weiland M, Alemán J, Winiecka-Krusnell J, Linder E, Svärd S. 2005. Secretory antibodies against *Giardia intestinalis* in lactating Nicaraguan women. *Parasite Immunol*. 27(5):163-9.

Téllez A, Winiecka-Krusnell J, Paniagua M, Linder E. 2003. Antibodies in mother's milk protect children against giardiasis. *Scand J Infect Dis*. 35(5):322-5.

The Medical Letter. 2010. Drugs for Parasitic Infections. 2nd edition.

Thompson RC. 2000. Giardiasis as a re-emerging infectious disease and its zoonotic potential. *Int J Parasitol*. 30(12-13):1259-67.

Touz MC, Rópolo AS, Rivero MR, Vranych CV, Conrad JT, Svard SG, Nash TE. 2008. Arginine deiminase has multiple regulatory roles in the biology of *Giardia lamblia*. *J Cell Sci*. 121(Pt 17):2930-8.

Towbin H, Staehelin T, Gordon J. 1992. Electrophoretic transfer of proteins from polyacrylamide gels to nitrocellulose sheets: procedure and some applications. 1979. *Biotechnology*. 24:145-9.

Troeger H, Epple HJ, Schneider T, Wahnschaffe U, Ullrich R, Burchard GD, Jelinek T, Zeitz M, Fromm M, Schulzke JD. 2007. Effect of chronic *Giardia lamblia* infection on epithelial transport and barrier function in human duodenum. *Gut*. 56(3):328-35.

Tůmová P, Hofstetrová K, Nohýnková E, Hovorka O, Král J. 2007. Cytogenetic evidence for diversity of two nuclei within a single diplomonad cell of *Giardia*. *Chromosoma*. 116(1):65-78.

Turchany JM, Aley SB, Gillin FD. 1995. Giardicidal activity of lactoferrin and N-terminal peptides. *Infect Immun*. 63(11):4550-2.

Uehlinger FD, O'Handley RM, Greenwood SJ, Guselle NJ, Gabor LJ, Van Velsen CM, Steuart RF, Barkema HW. 2007. Efficacy of vaccination in preventing giardiasis in calves. *Vet Parasitol*. 146(1-2):182-8.

Upcroft JA, Upcroft P. 1993. Drug resistance and *Giardia*. *Parasitol Today*. 9(5):187-90.

Van Steendam K, Tilleman K, De Ceuleneer M, De Keyser F, Elewaut D, Deforce D. 2010. Citrullinated vimentin as an important antigen in immune complexes from synovial fluid of rheumatoid arthritis patients with antibodies against citrullinated proteins. *Arthritis Res Ther*. 12(4):R132.

Venkatesan P, Finch RG, Wakelin D. 1997. A comparison of mucosal inflammatory responses to *Giardia muris* in resistant B10 and susceptible BALB/c mice. *Parasite Immunol*. 19(3):137-43.

von Allmen N, Bienz M, Hemphill A, Müller N. 2004. Experimental infections of neonatal mice with cysts of *Giardia lamblia* clone GS/M-83-H7 are associated with an antigenic reset of the parasite. *Infect Immun*. 72(8):4763-71.

Wei Y, Zhou H, Sun Y, He Y, Luo Y. 2007. Insight into the catalytic mechanism of arginine deiminase: functional studies on the crucial sites. *Proteins*. 66(3):740-50.

WHO. 1979. Parasitic zoonoses. Report of a WHO expert committee with the participation of FAO. (http://whqlibdoc.who.int/trs/WHO_TRS_637.pdf).

Williams LM, Ricchetti G, Sarma U, Smallie T, Foxwell BM. 2004. Interleukin-10 suppression of myeloid cell activation-a continuing puzzle. *Immunology*. 113(3):281-92.

Wood NJ. 2011. Infection: *Giardia lamblia* is associated with an increased risk of both IBS and chronic fatigue that persists for at least 3 years. *Nat Rev Gastroenterol Hepatol*. 8(11):597.

Yao K, Yin YL, Chu W, Liu Z, Deng D, Li T, Huang R, Zhang J, Tan B, Wang W, Wu G. 2008. Dietary arginine supplementation increases mTOR signaling activity in skeletal muscle of neonatal pigs. *J Nutr*. 138(5):867-72.

Yomogida S, Hua J, Sakamoto K, Nagaoka I. 2008. Glucosamine suppresses interleukin-8 production and ICAM-1 expression by TNF-alpha-stimulated human colonic epithelial HT-29 cells. *Int J Mol Med*. 22(2):205-11.

Yu LZ, Birky CW Jr, Adam RD. 2002. The two nuclei of *Giardia* each have complete copies of the genome and are partitioned equationally at cytokinesis. *Eukaryot Cell*. 1(2):191-9.

Zea AH, Rodriguez PC, Culotta KS, Hernandez CP, DeSalvo J, Ochoa JB, Park HJ, Zabaleta J, Ochoa AC. 2004. L-Arginine modulates CD3zeta expression and T cell function in activated human T lymphocytes. *Cell Immunol*. 232(1-2):21-31.

Zhou P, Li E, Shea-Donohue T, Singer SM. 2007. Tumour necrosis factor alpha contributes to protection against *Giardia lamblia* infection in mice. *Parasite Immunol*. 29(7):367-74.

Zhou P, Li E, Zhu N, Robertson J, Nash T, Singer SM. 2003. Role of interleukin-6 in the control of acute and chronic *Giardia lamblia* infections in mice. *Infect Immun*. 71(3):1566-8.

Zhu L, Tee KL, Roccatano D, Sonmez B, Ni Y, Sun ZH, Schwaneberg U. 2010. Directed evolution of an antitumor drug (arginine deiminase PpADI) for increased activity at physiological pH. *Chembiochem*. 11(5):691-7.

7 Supplementary material

7.1 Selbstständigkeitserklärung

Hiermit bestätige ich, Stefanie Marek (geb. Banik), die Kenntnisnahme über die dem angestrebten Verfahren zugrunde liegende Promotionsordnung.

Gemäß § 7 Absatz 3 der Promotionsordnung erkläre ich an Eides statt, dass ich die vorliegende Dissertation mit dem Titel „*Giardia duodenalis* arginine deiminase and its role in host-parasite interplay" selbstständig verfasst und keine anderen als die angegebenen Quellen und Hilfsmittel verwendet habe.

Des Weiteren versichere ich, dass diese Dissertation nie Gegenstand eines früheren Promotionsverfahrens gewesen ist oder als ungenügend beurteilt wurde.

Unter meiner Anleitung und Betreuung hat Anna-Luise Kluge ihre Bachelorarbeit „Herstellung und Charakterisierung von rekombinanten *Giardia duodenalis* Arginin-Deiminase-Proteinen verschiedener Genotypen" in der Arbeitsgruppe von Herrn Dr. rer. nat. Aebischer (FG 16, Robert Koch-Institut) angefertigt. Ein Teil der daraus resultierenden Rohdaten wurden in meiner Dissertation verwendet.

7.2 Publikation und Tagungsbeiträge

Publikation:

Banik S, Renner Viveros P, Seeber F, Klotz C, Ignatius R, Aebischer T. 2013. *Giardia duodenalis* arginine deiminase modulates the phenotype and cytokine secretion of human dendritic cells by depletion of arginine and formation of ammonia. *Infect Immun*. 81(7):2309-17.

Tagungsbeiträge:

A) Poster

- Nationales Symposium für Zoonosenforschung (Berlin 2010 und 2011):

  "Fundamental investigations for functional epidemiology of *Giardia duodenalis* infections"

- 63. DGHM Jahrestagung (Essen 2011) und DGP-Jahrestagung (Heidelberg 2012):

  "*Giardia duodenalis* arginine deiminase- exploring its function for host-parasite interplay "

- 64. DGHM Jahrestagung (Hamburg 2012):

  "*Giardia duodenalis* arginine deiminase has immunomodulatory effects on human dendritic cells"

B) Vorträge

- Statusworkshop der DGHM-Fachgruppe "Eukaryontische Krankheitserreger" (Düsseldorf 2011, Berlin 2012):

  "*Giardia duodenalis* arginine deiminase: Exploring its function for host-parasite interplay"